



AFOSR-TR 81-0461

**LEVEL**

II

12

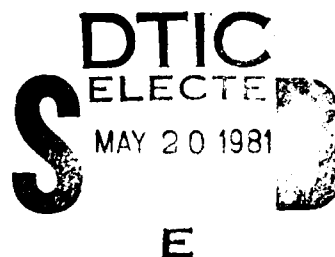
**PARAMETRIC INVESTIGATION  
OF  
RADOME ANALYSIS METHODS:**

**COMPUTER-AIDED RADOME ANALYSIS USING  
THE HUYGENS-FRESNEL PRINCIPLE AND  
LORENTZ RECIPROCITY**

AD A099183

By

G. K. Huddleston, H. L. Bassett, & J. M. Newton



Prepared for

**AIR FORCE OFFICE OF SCIENTIFIC RESEARCH (AFSC)  
BOLLING AIR FORCE BASE, D. C. 20332**

**FINAL TECHNICAL REPORT, VOLUME III OF IV  
GRANT AFOSR-77-3469  
30 September 1977 - 31 December 1980**

February 1981

**GEORGIA INSTITUTE OF TECHNOLOGY**  
SCHOOL OF ELECTRICAL ENGINEERING &  
Engineering Experiment Station  
Atlanta, Georgia 30332

1981



DTIC FILE COPY

Approved for public release;  
distribution unlimited.

The views and conclusions contained in this document are those of the authors and should not be interpreted as necessarily representing the official policies or endorsements, either expressed or implied, of the Air Force Office of Scientific Research or the U. S. Government.

UNCLASSIFIED

SECURITY CLASSIFICATION OF THIS PAGE (When Data Entered)

REPORT DOCUMENTATION PAGE		READ INSTRUCTIONS BEFORE COMPLETING FORM
1. REPORT NUMBER <b>AFOSR-TR-81-046T</b>	2. GOVT ACCESSION NO. <b>AD-A099283</b>	3. RECIPIENT'S CATALOG NUMBER
4. TITLE (and Subtitle) PARAMETRIC INVESTIGATION OF RADOME ANALYSIS METHODS: COMPUTER-AIDED RADOME ANALYSIS USING THE HUYGENS-FRESNEL PRINCIPLE AND LORENTZ RECIPROCITY		5. TYPE OF REPORT & PERIOD COVERED Final Technical Report, Vol. 3 of 4 30 September 1977-31 Dec. 1980
7. AUTHOR(s) G. K. Huddleston, H. L. Bassett, & J. M. Newton		6. PERFORMING ORG. REPORT NUMBER
9. PERFORMING ORGANIZATION NAME AND ADDRESS Georgia Institute of Technology School of Electrical Engineering & Engineering Experiment Station Atlanta, Georgia 30332		8. CONTRACT OR GRANT NUMBER(s) AFOSR-77-3469
11. CONTROLLING OFFICE NAME AND ADDRESS Air Force Office of Scientific Research /NF Physics Directorate Bolling Air Force Base, D. C. 20332		10. PROGRAM ELEMENT, PROJECT, TASK AREA & WORK UNIT NUMBERS 61102F 2301/A6
14. MONITORING AGENCY NAME & ADDRESS (if different from Controlling Office)		12. REPORT DATE February 1981
		13. NUMBER OF PAGES 133
		15. SECURITY CLASS. (of this report) UNCLASSIFIED
		15a. DECLASSIFICATION DOWNGRADING SCHEDULE
16. DISTRIBUTION STATEMENT (of this Report)  Approved for public release; distribution unlimited.		
17. DISTRIBUTION STATEMENT (of the abstract entered in Block 20, if different from Report)		
18. SUPPLEMENTARY NOTES		
19. KEY WORDS (Continue on reverse side if necessary and identify by block number) Radome Analysis Huygens-Principle Lorentz Reciprocity Surface Integration		
20. ABSTRACT (Continue on reverse side if necessary and identify by block number) -A Fortran computer program is described for computing the effects of a tan- gent ogive radome on the receiving patterns and Loeresight directions of a mono- pulse antenna. A receiving formulation with the inside surface of the radome being the surface of integration is used. Aperture integration is used to com- pute the near fields of the antenna. The main program and seven subroutines are well documented.		



TABLE OF CONTENTS

	<u>PAGE</u>
<u>CHAPTER 1</u>	
Introduction and Summary. . . . .	1
<u>CHAPTER 2</u>	
PROGRAM SIIRACP . . . . .	7
<u>CHAPTER 3</u>	
SUBROUTINE RECM . . . . .	55
<u>CHAPTER 4</u>	
SUBROUTINE TRECNF . . . . .	75
<u>CHAPTER 5</u>	
SUBROUTINE APINT. . . . .	91
<u>CHAPTER 6</u>	
SUBROUTINE DIPOLES. . . . .	95
<u>CHAPTER 7</u>	
SUBROUTINE WALL . . . . .	123
<u>CHAPTER 8</u>	
SUBROUTINE CAXCB. . . . .	124

LIST OF ILLUSTRATIONS

<u>FIGURE</u>		<u>PAGE</u>
1-1.	Theoretical Basis of Radome Analysis	3
1-2.	Illustration of Radome Analysis Method Using Inside Radome Surface as Surface of Integration in Reciprocity Integral . . . . .	5
2-1.	Tangent Ogive Radome Geometry. . . . .	9
2-2.	Coordinate Systems Used in Radome Analysis . . . . .	11
2-3.	Coordinate System for Far Field Patterns . . . . .	14
3-1.	Radome Geometry for Defining Elemental Surface Area in $\theta$ Direction . . . . .	60
3-2.	Definition of Elemental Surface Area in $\phi$ Direction. . .	62
4-1.	Approximation of Circular Aperture by Rectangular Grid of Sample Points . . . . .	78
4-2.	Geometry of Flat Plate Antenna . . . . .	80
6-1.	Geometry of Rectangular Aperture Antenna Approximated by Elementary Dipoles. . . . .	97

LIST OF TABLES

<u>TABLE</u>	<u>PAGE</u>
2-1. Input Data for SIIRACP . . . . .	41
4-1. Values of Non-Zero Elements in Circular Aperture (ICHAN=1, ICASE=1 or 2). . . . .	81
4-2. Symmetrical Amplitude Distribution for Flat Plate Antenna.	83
6-1. Elementary Dipole Fields of Z-Directed Currents. . . . .	99
6-2. Rectangular Field Components of Elementary Dipoles . . . .	102
6-3. Fields of Elementary x-Directed and y-Directed Dipoles . .	104
6-4. Fields Computed by Subroutine DIPOLES Along z-Axis for 4" x 4" Uniform Aperture ( $\lambda=1.18"$ ) . . . . .	108
6-5. Fields Computed by Subroutine DIPOLES Along x-Axis at z=8 inches . . . . .	112
6-6. Fields Computed by Subroutine DIPOLES Along x-Axis at z=24 inches. . . . .	115
6-7. Fields Computed by Subroutine DIPOLES Along x-Axis at z=48 inches. . . . .	119

## Chapter 1

### INTRODUCTION AND SUMMARY

#### 1-1. Introduction

This Volume III of this final technical report of four volumes documents a surface integration radome analysis computer program written in Fortran IV for use on the Cyber 70/74 computing system at Georgia Institute of Technology and the IBM 3033 computing system at Johns Hopkins University Applied Physics Laboratory. The program was developed at Georgia Institute of Technology over the past three years under grant AFOSR-77-3469 and documented herein under the cognizance of R. C. Mallaleiu (APL Contract 60153).

The analysis package described was used during the research to analyze the antennas and radomes as described in Volumes I and IV. Its documentation was done in conjunction with an on-going radome technology program at JHU/APL. It is intended to serve as part of a technology base for the radome technical community.

This report is organized by chapters, where each chapter describes the main program or one subprogram not already described in Reference 1 (Ray Tracing Formulation). The main program (Chapter 2) described herein differs only slightly from that in Reference 1. Only six new subroutines are required for the surface integration formulation as described in Chapters 3-8. References cited in each chapter are listed therein. Each chapter is terminated with the program listing.

This software is currently being used in a parametric investigation of radome analysis methods, and additional information concerning its speed and accuracy is presented in Volume I [2].



## 1-2. Description of the Analysis

The basis of analysis is illustrated in Figure 1-1. The inner surface of the radome  $S_1$  is chosen as one surface of integration in the Lorentz reciprocity integral (upper left in figure). A surface  $S_2$  enclosing the antenna and extending into its interior, as illustrated, comprises the second surface. Together,  $S_1 + S_2$  enclose the source-free Volume  $V$  indicated; hence, the Lorentz surface integral is identically zero and the integral over  $S_1$  equals the negative of the integral over  $S_2$ .

Consider the surface  $S_2$  more closely. The surface integral over  $S_2$  is zero except over that part of  $S_2$  which is placed across the waveguiding structure that connects the Source "a" to the radiating (flared) part of the antenna. Call this surface  $S'_2$ . If there can be defined a single dominant mode in the waveguide when Source "a" is activated, then voltage and current  $V_a, I_a$  can be defined at this terminal plane [4]. When Source "b" is activated, voltage and current  $V_b, I_b$  at  $S'_2$  can also be defined; in fact,  $V_b$  is the "received voltage". The received current  $I_b$  is related to  $V_b$  by a linear impedance relationship

$$V_b = I_b Z_a \quad (1)$$

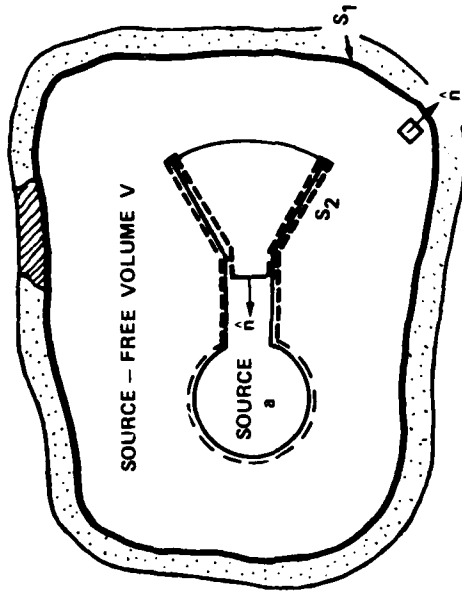
where  $Z_a$  is the impedance seen at  $S'_2$  looking toward Source "a" (sinusoidal steady state assumed; time variations of the form  $e^{j\omega t}$  understood and suppressed). Also,  $I_a$  and  $V_a$  are related by

$$V_a = I_a Z_1 \quad (2)$$

$$\oint_{S_1+S_2} (\underline{E}_a \times \underline{H}_b - \underline{E}_b \times \underline{H}_a) \cdot \hat{n} da = 0$$

SOURCE b

$$\begin{aligned} \int_{S_1} (\underline{E}_a \times \underline{H}_b - \underline{E}_b \times \underline{H}_a) \cdot \hat{n} da \\ = - \int_{S_2} (\underline{E}_a \times \underline{H}_b - \underline{E}_b \times \underline{H}_a) \cdot \hat{n} da \\ = V_a I_b + V_b I_a \end{aligned}$$



$$\underline{E}(x, y, z) = 1/4\pi \int_S [-j\omega\mu\psi(\hat{n} \times \underline{H}) + (\hat{n} \times \underline{E}) \times \nabla\psi + (\hat{n} \cdot \underline{E})\nabla\psi] dS$$

$$\underline{H}(x, y, z) = 1/4\pi \int_S [j\omega\epsilon(\hat{n} \times \underline{E}) \cdot \psi + (\hat{n} \times \underline{H}) \times \nabla\psi + (\hat{n} \cdot \underline{H})\nabla\psi] dS$$

FIGURE 1-1. THEORETICAL BASIS OF RADOME ANALYSIS.

where  $Z_1$  is the impedance seen at  $S'_2$  looking to the right in Figure 1-1. Combining these results yields the desired expression for the received voltage  $V_b$ ; viz.,

$$V_b = V_{REC} = \frac{Z_1 Z_a}{V_a (Z_1 + Z_a)} \int_{S_1} (\underline{E}_a \times \underline{H}_b - \underline{E}_b \times \underline{H}_a) \cdot \hat{n} da \quad (3)$$

Note that the unit normal is directed positively outward from volume  $V$  as dictated by Gauss' theorem.

When Source "b" in Figure 1-1 is removed a great distance from the antenna/radome structure, the fields of "b" approach those of an electromagnetic plane wave (target return). The practical analysis approach then takes the form shown in Figure 1-2. The inner radome surface is divided into a number of contiguous elemental areas  $\Delta A$ , each of which is represented by a sample point  $P'$  at its center. The fields  $\underline{E}_T, \underline{H}_T$  at  $P'$  are assumed to be those present there in the absence of the radome and are found by aperture integration, the theoretical basis of which is the Huygens-Fresnel principle [5] as stated by the lower integrals in Figure 1-1. The fields  $\underline{E}_R, \underline{H}_R$  at  $P'$  are found by applying the normal voltage transmission coefficients [6] to the plane wave incident on the outside at point  $P$ . The received voltage is found by summing all the contributions as indicated in Equation (3).

The method of analysis indicated by Equation (3) is exact; however, certain approximations are necessarily introduced in its implementation. The fields  $\underline{E}_T, \underline{H}_T$  should correctly include reflections from the inner radome surface. The use of the flat panel transmission coefficients to transform the incident plane wave at  $P$  to  $P'$  is an approximate method based on the theory of geometrical optics (zero wavelength) and whose

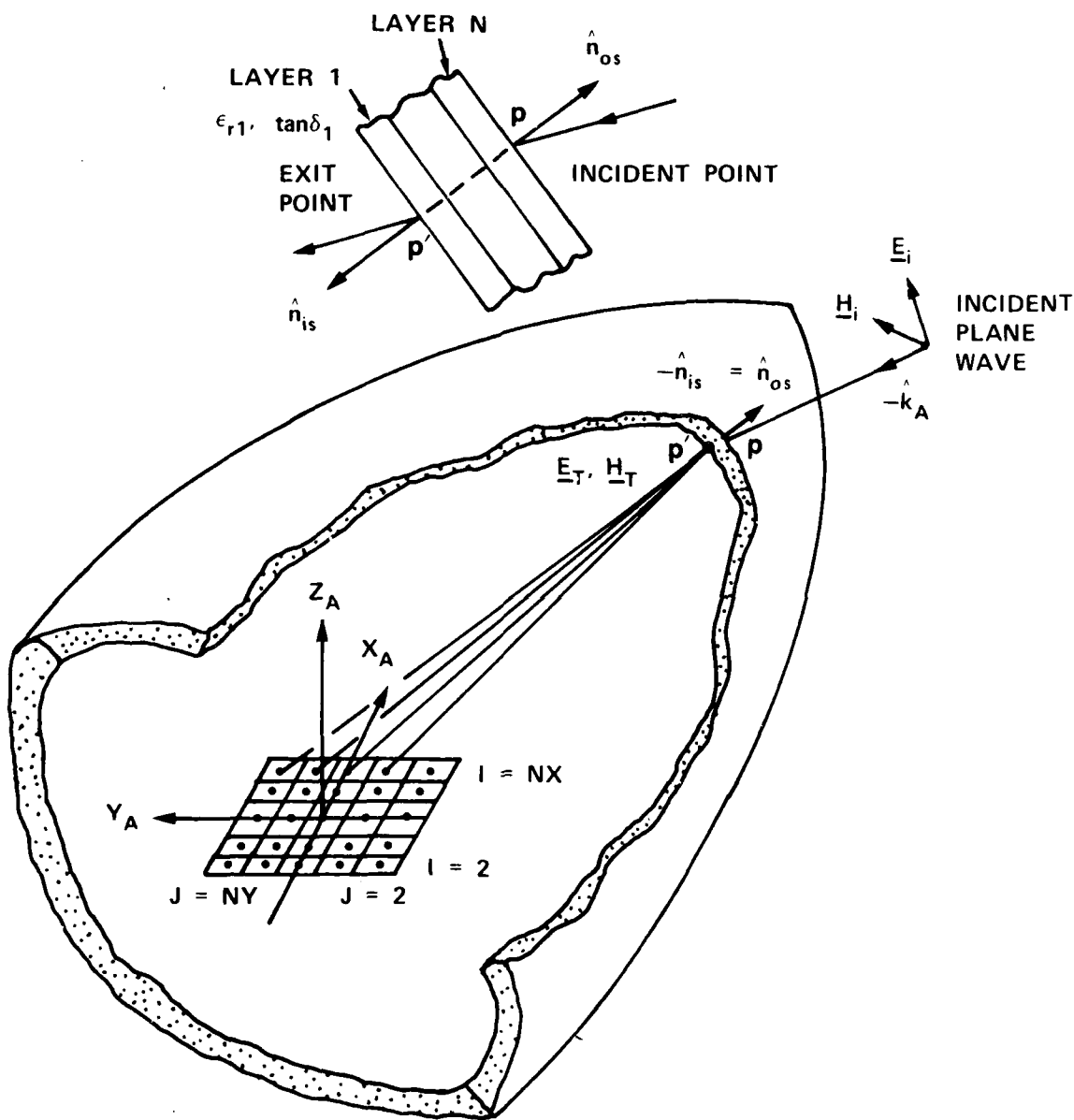


FIGURE 1-2. ILLUSTRATION OF RADOME ANALYSIS METHOD USING INSIDE RADOME SURFACE AS SURFACE OF INTEGRATION IN RECIPROCITY INTEGRAL.

accuracy depends upon the radius of curvature of the radome wall. The accuracy of the method also depends on the size of the samples used to represent the radiating aperture as well as the radome surface. The computational speed of the analysis most certainly depends on the number of these samples.

1-3. References

1. G. K. Huddleston, H. L. Bassett, & J. M. Newton, "Parametric Investigation of Radome Analysis Methods: Computer-aided Radome Analysis Using Geometrical Optics and Lorentz Reciprocity", Final Technical Report, Volume II of IV, Grant AFOSR-77-3469, February 1981.
2. G. K. Huddleston, H. L. Bassett, J. M. Newton, "Parametric Investigation of Radome Analysis Methods: Salient Results", Final Technical Report, Volume I of IV, Grant AFOSR-77-3469, February 1981.
3. R. E. Collin and F. J. Zucker, Antenna Theory, Part 1, Section 4-2, McGraw-Hill, New York, 1969.
4. S. Silver, Microwave Antenna Theory and Design, Ch. 2, McGraw-Hill, New York, 1949.
5. Ibid, Ch. 3.
6. J. H. Richmond, "Calculation of Transmission and Surface Wave Data for Plane Multilayers and Inhomogeneous Plane Layers", Air Force Contract AF 33(615)-1081, The Antenna Laboratory, Ohio State University, Columbus, Ohio, October 1963.

## Chapter 2

### PROGRAM SIIRACP

2-1. Purpose: SIIRACP is a Fortran computer program used to analyze the effects of a tangent ogive radome on the performance of a monopulse aperture antenna. It consists of a main program and 28 sub-routines, 22 of which are identical to those used in Program RTFRACP [1]. It uses complex arithmetic and requires 66600 octal words of core memory for execution on the CDC Cyber 70 system (60-bit words) at Georgia Institute of Technology. Execution time to compute bore-sight error on the Cyber 70 is approximately 255 seconds per look direction when the small antenna aperture is represented by  $7 \times 7 = 49$  sample data points and the radome is represented by 826 sample points; i.e., approximately 1.26 millisecond per aperture sample point per radome sample point.

The computer-aided radome analysis uses a receiving formulation based on the Lorentz reciprocity theorem as described earlier [1,2]. The voltage produced at the terminals of a linear antenna by an incident plane wave is given by

$$V_R(\hat{k}) = \iint_S (\underline{E}_T \times \underline{H}_R - \underline{E}_R \times \underline{H}_T) \cdot \hat{n} \, da \quad (1)$$

where  $\underline{E}_T, \underline{H}_T$  are the fields produced on the surface  $S$  enclosing the antenna when the antenna is transmitting;  $\underline{E}_R, \underline{H}_R$  are the incident fields produced on  $S$  by the incident plane wave or perturbations thereof;  $\hat{k}$  is a unit vector which points from the antenna toward the direction from which the plane

wave arrives; and  $\hat{n}$  is a unit vector normal to the surface S and pointing into the source-free region.\* The fields  $\underline{E}_T$ ,  $\underline{H}_T$  are taken to be those produced by the planar aperture on surface S when the antenna is transmitting in the absence of the radome. The geometrical optics approximation

$$\underline{H}_T + \frac{\hat{n} \times \underline{E}_T}{\eta} \quad (2)$$

is used to generate the magnetic field in the aperture from the aperture illumination specified by  $\underline{E}_T$ .

The surface S is taken to be the inner surface of the radome. At each sample point P' on this surface, the plane wave fields  $\underline{E}_R$ ,  $\underline{H}_R$  incident from the outside are weighted with the flat panel normal voltage transmission coefficients as determined by the radome wall configuration, the angle of incidence, and the plane of incidence. The fields  $\underline{E}_T$ ,  $\underline{H}_T$  at P' are found by aperture integration. The individual contributions are summed up as indicated in Equation (1) and was illustrated in Figure 1-2.

The parameters of the tangent ogive radome are indicated in Figure 2-1. The outside base diameter  $D_{os}$  and fineness ratio  $F_{os}$  determine the outside length according to

$$F_{os} = L_{os} / D_{os} \quad (3)$$

A similar relation holds for the inside dimensions; viz.,

$$F_{is} = L_{is} / D_{is} \quad (4)$$

\*By choosing  $\hat{n}$  this way, the minus sign in Figure (1-1) is removed.

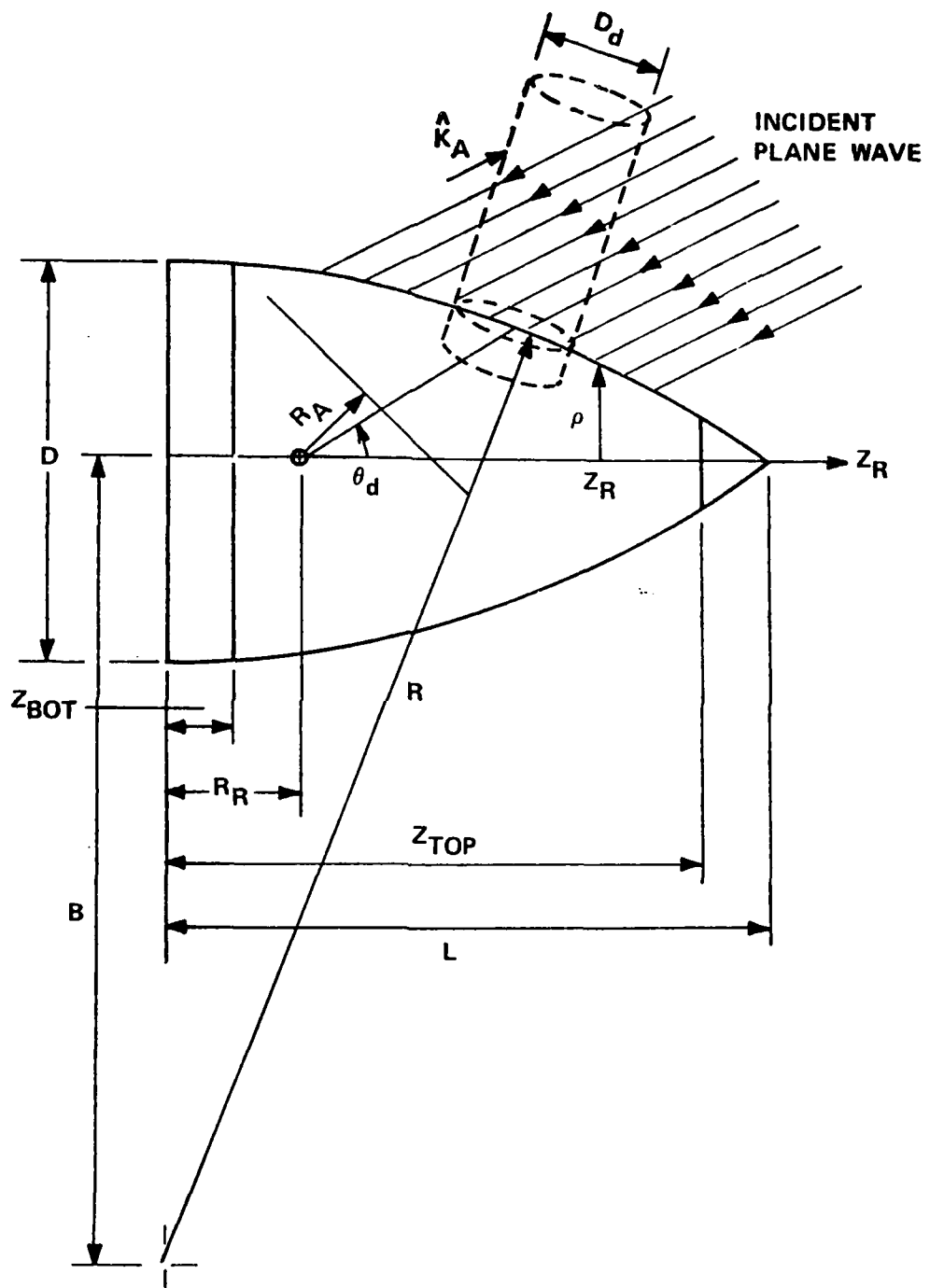


Figure 2-1. Tangent Ogive Radome Geometry.



The radius of curvature of the outside wall  $R_{OS}$  is given by

$$R_{OS} = F_{OS} D_{OS} / \sin (\pi - 2 \tan^{-1}(2F_{OS})) \quad (5)$$

and the dimension B is given by

$$B = R_{OS} - D_{OS}/2 \quad (6)$$

The placements of a bulkhead (bottom disk) and metal tip (top disk) can be specified by  $Z_{BOT}$  and  $Z_{TOP}$ , respectively. The thickness, dielectric constant, and loss tangent of the wall may also be specified for up to N=5 layers. The radome is assumed to be a body of revolution with uniform wall dimensions independent of location. The dashed cylindrical shape of a diameter  $D_d$  in Figure 2-1 was used earlier to simulate a laser-induced defect and is not pertinent here.

The subroutine which generates the antenna aperture fields represents three types of antennas: circular or square aperture with tapered ( $\cos x$ ) illumination and any one of four polarizations (vertical, horizontal, RHC, LHC); flat plate antenna with tapered illumination and vertical polarization. For either antenna, the fields are computed for one of three selected channels: sum, azimuth difference, elevation difference. Inputs include the number of samples  $N_X$ ,  $N_Y$  and the aperture diameter  $D_{AP}/\lambda$  in wavelengths.

The antenna/radome orientation is specified according to the parameters defined in Figure 2-2. The angle  $\phi_p$  selects the plane of scan of the radome tip with respect to the antenna coordinate system:  $\phi_p = 0^\circ$  selects the azimuth plane;  $\phi_p = 90^\circ$  selects the elevation plane. The angle  $\theta_L$  scans the tip in the selected plane.

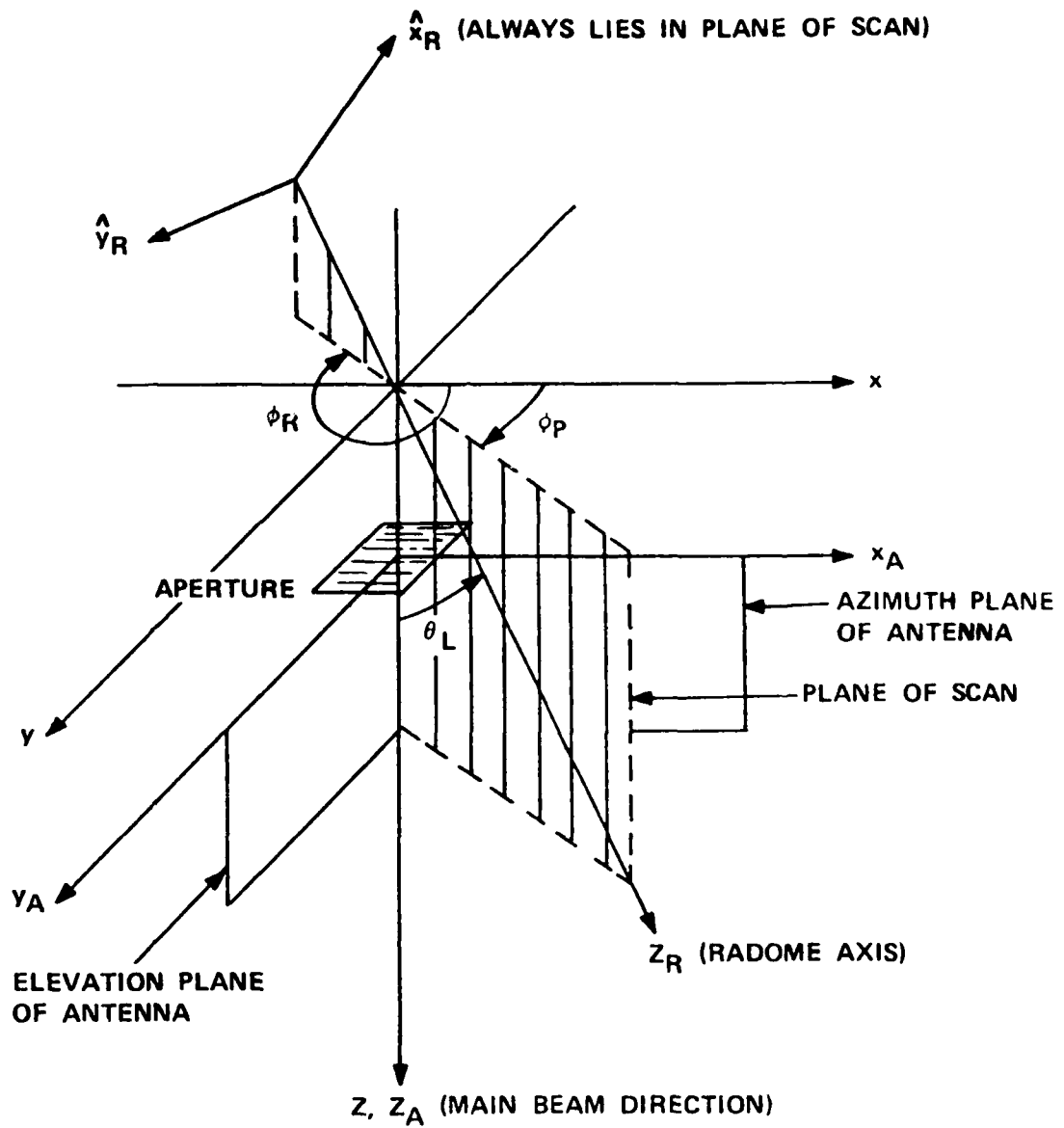


Figure 2-2. Coordinate Systems Used in Radome Analysis.

The program computes boresight errors in the azimuth and elevation planes of the antenna. The radome orientation is specified by  $\phi_P$  and  $\phi_L$ . The first target return (plane wave) is made to arrive from the direction

$$k_1 = x_A \sin \theta_{os} + y_A \sin \theta_{os} + z_A \sqrt{1 - 2 \sin^2 \theta} \quad (7)$$

where  $\theta_{os}$  is the initial specified offset angle; e.g., 2°. The voltage received by each channel is computed and stored. The second return is made to arrive from

$$k_2 = x_A (-\sin \theta_{os}) + y_A (-\sin \theta_{os}) + z_A \sqrt{1 - 2 \sin^2 \theta_{os}} \quad (8)$$

and the voltages are again computed. The data from these two points are used to construct a linear tracking model in the two planes, and a direction of arrival  $k$  is predicted which will yield null indications in both planes. The process is repeated until a desired error tolerance is satisfied or a maximum number of iterations is exceeded. Upon completion, the output  $k$  indicates the direction from which the plane arrives which yields an electrical boresight indication. If  $\alpha$  and  $\beta$  represent the boresight error angles in the azimuth and elevation planes, respectively, then they are related to the direction  $k = x_A k_x + y_A k_y + z_A k_z$  by

$$\sin \alpha = \frac{k_x}{\sqrt{1 - k_y^2}} \quad (9)$$

$$\sin \beta = \frac{k_y}{\sqrt{1 - k_x^2}} \quad (10)$$

where

$$k_z = \sqrt{1 - k_x^2 - k_y^2} \quad (11)$$

Options are also provided whereby principal plane patterns as shown in Figure 2-3 and additional outputs around boresight can be computed and printed. These options are useful when preparing software for a new type of antenna and to ensure correct operation whenever curious results are obtained.

2-2. Usage:	<u>Line No.</u>
DATA APIN/0./	47
DATA ZBOTIN/0.00/	49
DATA RADIUS/1E0/	52
DATA THETAA, PHIA, AGAM3A/0.0,90.0,0.0/	53
DATA NX, NY, NYE, NXY/4,4,1,512/	56
DATA MY/1/,NREC/61	57
READ (5,6) TITLE	63
READ (5,*) GRAF3D, GRAFSA, GRAFTR, GRAFRV, SUPPRS, IPENCD, SQUARE	65
READ (5,*) NFINE, NPHI, NTHE, DIAOS, RAIN, RRIN, ZTOPIN, FREQ, OSANG	67
READ (5,*) LMAX, DMRAD, IOPT, RAPMAX, VAIRM, IPOL, ICASE, N, IPWR, KMAX, NXE	76
READ (5,*) DSTHIN, DSPHIN, NTHMIN, NPHIMIN	79
READ (5,*) DIN(I), ER(I), TD(I) (I=1,N)	115
READ (5,*) FINR(I) (I=1,NFINE)	124
READ (5,*) PHI(I) (I=1, NPHI)	127
READ (5,*) THETA(I) (I=1,NTHE)	129

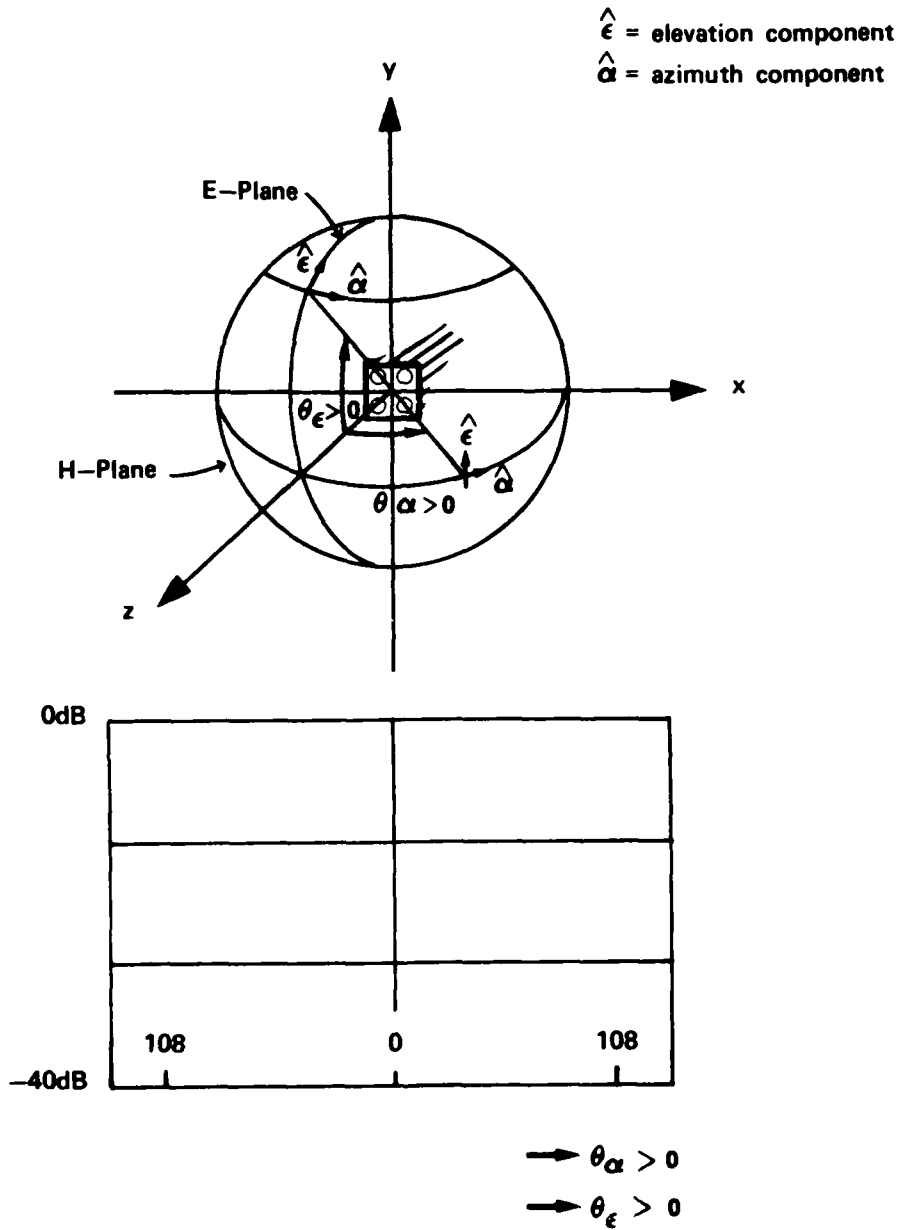


Figure 2.3 Coordinate System for Far Field Patterns

### 2-3. Arguments

a. Inputs. Units of arguments on input are distances in inches, angles in degrees, and frequency in gigahertz, unless otherwise noted. Units of arguments passed to subroutines are centimeters, radians, and gigahertz. An asterisk is used to denote those DATA arguments that do not normally need to be changed by the user.

- APIN\* - Height of a cylindrical base section of the tangent ogive radome. It is no longer included in the ray tracing algorithms and should not be changed from its zero value.
- ZBOTIN - Distance from base of tangent ogive radome to missile bulkhead (Figure 2-1).
- RADIUS\* - The radius R used in the far field factor  $e^{-jkR}/R$  by Subroutine FAR. Do not change.
- THETAA\* - Angle  $\theta_a$  between z-axis and the position vector  $\underline{r}_a$  to the antenna origin. This angle was used in earlier work to locate the antenna origin in the reference system using spherical coordinates  $(r_a, \theta_a, \phi_a)$ . Do not change.
- PHIA\* - Angle  $\phi_a$  between the projection of  $z_A$  axis onto the xy-plane and the x-axis. Do not change.
- AGAM3A\* - Angle between  $z_A$ -axis and z-axis in Figure 2-2. Do not change.
- NX,NY - Integer powers of two equal to the number of sample points in the antenna aperture; e.g., 16, 32, 64, etc. Changing NX and NY necessitates compatible changes in Lines 16-18.

- NYE  
 (NXE)
- Integer powers of two which specify the expanded number of sample points desired when computing the transmitting patterns of the antenna by inverse Fourier transforming the aperture fields. Subroutine JOYFFT provides this capability of increased resolution in one or both dimensions. Changes in NXE, NYE necessitate compatible changes in Lines 16, 20, 22 and 23. Note that  $NXE * NYE < NX * NY$  and either  $NXE < NX$  or  $NYE < NY$ .
- NXY
- Integer power of two used by Subroutine JOYFFT for dimension of complex working array XYFFT. Note that  $MX * NX < NXY$  and  $MY * NY < NSY$ . See below for MX and MY.
- NREC
- Integer variable equal to the number of points at which to compute the receiving pattern in either principal plane. The received voltage is computed at points  $\theta_i$  equally spaced in  $\sin\theta$ , where  $\theta$  is the angle measured from the  $z_A$ -axis as indicated in Figure 2-3, where  $\sin \theta_i = -KMAX + (I-1) * 2 * KMAX / NREC$ , and where  $KMAX = \sin \theta_{max} < 1.0$ .
- NS
- Not used. It was originally used by Subroutine RECBS. Do not remove.
- MX,MY
- Integer powers of two equal to the magnification factors desired in the  $k_x$  (H-plane) and  $k_y$  (E-plane) directions, respectively, of the transmitting antenna patterns. Note that the restrictions  $MX * NY < NXY$  and  $MY * NY < NXY$  must be observed. The data cited

above indicates increased resolutions in the NX direction of  $MX=16$  and no magnification ( $MY=1$ ) in the NY direction. Consequently, note that  $NXE=MX*NX=256$ .

- TITLE** - A Hollerith string of up to 72 characters which describes briefly the analysis being done. A format of 18A4 is specified and should work for machines with word length greater than or equal to 32 bits. The dimension of TITLE (Line 31) should be at least 18.
- GRAF3D** - A logical variable used to control the plotting of the incident fields on the antenna aperture. This feature has been removed from the program, and GRAF3D should always be FALSE.
- GRAFSA** - A logical variable which (if TRUE) controls the plotting of the transmitting power patterns of the antenna as follows: E-plane sum, E-plane difference equation ( $\Delta_{EL}$ ), H-plane sum, and H-plane difference azimuth ( $\Delta_{AZ}$ ). The radome is absent.
- GRAFTR** - A logical variable which controls the plotting of the amplitude and phase of the antenna aperture fields in the following order:  
 $E_{X\Sigma}, E_{Y\Sigma}, E_{X\Delta EL}, E_{Y\Delta EL}, E_{X\Delta AZ}, E_{Y\Delta AZ}$ .
- GRAFRV** - A logical variable which controls the plotting of the receiving patterns of the antenna with radome in the same order as specified under GRAFSA above.



- SUPPRS - A logical variable which controls the printing of numerous results. When TRUE, the printing of these numerous results are suppressed. This feature is convenient to aid in debugging new portions of software prior to making production runs.
- IPENCD - An integer variable which selects pen and paper for the Calcomp. This variable may be system dependent. For the Cyber 70, IPENCD=00 yields ballpoint pen and 11" wide plain paper; IPENCD=40 yields a heavier ink pen and the same paper.
- SQUARE - Logical input variable which selects a square aperture (TRUE) in Subroutine TRECNF.
- NFINE - Integer variable equal to the number of fineness ratios to be considered for the tangent ogive radome; e.g., NFINE=1.
- NPHI - Integer variable equal to the number of scan planes; e.g., NPHI=2.
- NTHE - Integer variable equal to the number of angles in each scan plane at which to compute boresight errors, etc. Note: The program is set up to iterate on fineness ratio, scan plane, and scan angle as outer loop, middle loop, and inner loop, respectively. Therefore, for each of NFINE fineness ratios, the analysis will be done for NTHE scan angles in NPHI different scan planes.
- DIAOS - Real variable equal to the outside base diameter (in.) of the radome. See Figure 2-1.

- RAIN - Real variable equal to the distance (in.) from the gimbal point to the antenna aperture.
- RRIN - Real variable equal to the distance (in.) from the gimbal point to the base of the radome.
- ZTOPIN - Real variable equal to the distance (in.) from the base of the radome to the face of a metal tip on the radome.
- FREQ - Real variable equal to the frequency of operation in gigahertz.
- OSANG - Real variable equal to the offset angle in degrees at which the first target return is to arrive on the antenna; e.g., OSANG=3.0.
- LMAX - Integer variable equal to the maximum number of iterations allowed by Subroutine RECBS in computing boresight error; e.g., LMAX=5.
- DMRAD - Real variable equal to the tolerance in milliradians allowed on computing boresight error; e.g., DMRAD=0.1.
- IOPT - Integer variable which selects the polarization of the incident plane wave as follows:
1. Linear, elevation component
  2. Linear, azimuth component
  3. Right hand circular
  4. Left hand circular
- RAPMAX - Real variable equal to the maximum radius (in.) of the antenna aperture.
- VAIRM - Real variable equal to the maximum amplitude of sum channel received voltage without radome. Any

real value can be entered for this variable since a subsequent program modification (Lines 345-362) causes VAIRM to be computed automatically.

- IPOL - Integer variable which selects the polarization of the antenna when ICASE=1 according to the same code as used above for IOPT.
- ICASE - Integer variable which selects the type of antenna aperture for the analysis: ICASE=1 or 2 selects a circular or square aperture with tapered illumination; ICASE=3 selects a flat plate antenna with programmed illumination. See Subroutine TRECNE in Chapter 4.
- N - Integer variable equal to the number of layers (up to 5) in the radome wall. For cases where more than 5 layers are required, the dimensional arrays on Line 37 must be changed to NN=N+1.
- IPWR - Integer variable which selects the component for which to compute the transmitting power patterns as follows:
1. Elevation Components
  2. Azimuth Component
  3. Total power
- KMAX - Real variable equal to the sine of the maximum angle at which receiving patterns are to be computed.
- NXE - Integer variable used by JOYFFT as explained above.
- DSTHIN, DSPHIN - Real variables equal to the distance between adjacent sample points on the radome surface in the

longitudinal ( $\theta$ ) and circumferential ( $\phi$ ) directions, respectively. See Chapter 3.

- NTHMIN, NPHIMIN - Integer variables equal to the minimum acceptable number of radome sample points in the two directions.
- DIN, ER, TD - Subscripted real variables equal to the thickness (in.), dielectric constant ( $\epsilon_r$ ), and loss tangent ( $\tan \delta$ ) of each layer of the radome wall. I=1 corresponds to the first layer and is the layer on exit side of the wall. Layer N is the first layer encountered by the incident plane wave. See Subroutine WALL.
- FINR - Subscripted real variable equal to NFINE fineness ratios.
- PHI - Subscripted real variable equal to NPFI angles (degrees) which specify the scan planes.
- THETA - Subscripted real variable equal to NTHE angles (degrees) which specify the scan angles in the scan plane.

b. Outputs. The parameters of analysis which are computed and outputted by the program depend on whether SUPPRS is true. In what follows, it is assumed that SUPPRS=FALSE so that all possible outputs are obtained. Since many of the original input parameters are printed directly, only those parameters not already explained above will be included below. Additional clarification may be found in Section 2-6.

- TABLE - Logical variable which, if TRUE, causes a look-up table to be used in computing transmission coefficients. When SUPPRS=FALSE, an abbreviated table

of transmission coefficients of the radome wall is printed by Subroutine WALL with variables as explained immediately below.

- ANGLE - Real variable equal to the angle of incidence (degrees) of the plane wave on a plane sheet of infinite extent having the layered configuration specified for the radome wall. The entries in the table are computed at 250 equal increments in  $\sin \theta_i$ , but only every fifth result is printed.
- TPERI, TPARI - Complex variables equal to the normal voltage transmission coefficients of the sheet for the two cases of  $E_i$  perpendicular to the plane of incidence ( $T_{\perp}$ ) and  $E_i$  parallel to the plane of incidence ( $T_{\parallel}$ ). In the printed table, the power transmission coefficients  $|T_{\perp}|^2$  and  $|T_{\parallel}|^2$  are printed; adjacent to each, the phases of  $T_{\perp}$  and  $T_{\parallel}$  are also printed.
- RPERI, RPARI - Complex variables equal to the reflection coefficients  $R_{\perp}$ ,  $R_{\parallel}$  of the plane dielectric sheet. Actually,  $|R_{\perp}|^2$  and  $|R_{\parallel}|^2$  are printed, accompanied by the phases of  $R_{\perp}$  and  $R_{\parallel}$ .
- KXMAX - Real variable equal to the folding wavenumber associated with sampling the aperture fields according to  $KXMAX = 1./2(\Delta x/\lambda)$ , where  $x$  is the distance between samples.
- DXWL - Real variable equal to  $\Delta x/\lambda$ .
- KXM, KYM - Real variables equal to the folding wavenumbers of the principal plane patterns after magnification

for increased resolution.  $KXM = KYMAX * NXE / (MX * NX)$  and applies to the H-plane.  
 $KYM = KYMAX * NYE / (MY * NY)$  and applies to the E-plane.  
 Usually, the expanded dimension NXE and magnification factor MX are selected so that  $KXM = KXMAX$ .  
 Also, NYE and MY are usually selected so that  $KYM \ll KYMAX$ .

- MIN,MAX - Real variables equal to the minimum and maximum values of the amplitude of the complex arrays containing the aperture fields are processed by Subroutine NORMH in preparation for 3D plotting by Subroutine PLT3DH.
- ROS - Real variable equal to the radius of curvature of the outside shape of the tangent ogive radome.
- BOS - Real variable equal to the distance B in inches defined in Figure 2-1.
- FINOS - Real variable equal to the fineness ratio of the radome as based on the outside dimensions.
- FINIS - Real variable equal to the fineness ratio of the radome as based on the inside dimensions.

The following variables are printed when the receiving patterns are computed and printed:

- ICUT - Integer variable which defines the E-plane (ICUT=1) or H-plane (ICUT=2) pattern. See Figure 2-3.
- ICOMP - Integer variable which defines the field component of the plane wave incident on the receiving antenna: ICOMP=1 for elevation component; ICOMP=2 for azimuth component.

- KMAX - Real variable equal to the sine of the maximum angle off broadside for which the received voltage is computed.
- NREC - Integer variable (power of 2) equal to the number of points at which the receiving pattern is computed. The pattern is computed at NREC points spaced equally in  $k_{xy} = \sin\theta$  according to  $\Delta k_{xy} = 2 \text{ KMAX}/\text{NREC}$ .
- DK - Real variable equal to  $2*\text{KMAX}/\text{NREC}$ .
- ANGMAX - Real variable equal to  $\sin^{-1}(\text{KMAX})$ .

The receiving pattern is computed at NREC points and magnified using Subroutine MAGFFT to 256 points equally spaced in  $\sin \theta$  over the range  $(-\text{KMAX}, \text{KMAX}-\text{DK})$ . Three parameters are printed: angle in degrees, amplitude in decibels, and phase in degrees. Only every fourth point in the 256 points is printed. The receiving patterns are printed in the following order:

E-Plane:  $\Sigma_{EL}, \Delta_{EL}$

H-Plane:  $\Sigma_{AZ}, \Delta_{AZ}$

Subroutine RECBS computes the boresight error of the antenna as produced by the radome. When SUPPRS=FALSE, the following parameters are printed:

- K1, K2 - Real subscripted variables containing the direction cosines  $(k_{xi}, k_{yi}, k_{zi})$  of the last and next to last true directions to the target. One of these variables is equal to K, the subscripted variable containing the direction cosines of the last target return.

AZTM,ELTM - Real variables equal to the boresight error in the H-plane and E-plane associated with the last target return  $(k_x, k_y, k_z)$ . Expressed in milliradians, these errors are computed according to

$$AZTM = \sin^{-1}(k_x / \sqrt{1 - k_y^2}) * 1000.$$

$$ELTM = \sin^{-1}(k_y / \sqrt{1 - k_x^2}) * 1000.$$

Let  $\hat{k} = \hat{x}_A k_x + \hat{y}_A k_y + \hat{z}_A k_z$ . Then AZTM is the angle between the  $z_A$ -axis and the projection of  $\hat{k}$  onto the  $x_A z_A$  (azimuth) plane. ELTM is the angle between the  $z_A$ -axis and the projection of  $\hat{k}$  onto the  $y_A z_A$  (elevation) plane.

MESAZ,MESEL - Real variables equal to the monopulse error slopes in the azimuth and elevation channels expressed in units of volts per degree, where the maximum signal received by the sum channel is considered to be one volt.

UAZ,UEL - Real subscripted variables equal to the received tracking functions  $I_{\text{mag}} \{\Delta/\Sigma\}$  corresponding to the target returns K1 and K2 above; e.g.,  $UAZ(1) = I_{\text{mag}} \{\Delta_{AZ}/\Sigma_{AZ}\}$  for K1.

SMAX - Real variable equal to the maximum amplitude of the received sum channel voltage.



LCTR - Integer variable equal to the number of iterations (target returns) used by Subroutine RECBS to compute boresight error.

Subroutine RECBS also computes and prints six additional monopulse outputs around the apparent boresight direction  $\hat{k}_0$ . The directions  $\hat{k}$  chosen lie in the plane  $k_x = k_y$  and are spaced one milliradian apart over the range  $\pm 3$  mrad and centered on the direction  $\hat{k}_0$ . The variables printed are as follows:

ANG - Real variable equal to the angle in milliradians between  $\hat{k}_0$  and  $\hat{k}$ .

VRAZ, VREL - Real variables equal to  $I_{\text{mag}} \{ \Delta / i \}$  for the target return from direction  $\hat{k}$  for the azimuth and elevation channels, respectively.

DAZ, DEL - Amplitude and phase (degrees) of the complex voltages received on the  $\Delta_{\text{AZ}}$  and  $\Delta_{\text{EL}}$  channels, respectively, for target return  $\hat{k}$ .

SLPAZ, SLPEL - Average values of the monopulse error slopes (volts/degree) in the azimuth and elevation channels, respectively, obtained by a linear approximation of the tracking functions based on their values at  $\text{ANG} = \pm 3$  mrad. For example,

$$\text{SLPAZ} = [\text{VRAZ}(3 \text{ mrad}) - \text{VRAZ}(-3 \text{ mrad})] / (.006 * 57.3)$$

The main program always prints the boresight error in azimuth (BSEAZ) and elevation (BSEEL), and the values printed are identical to AZTM and

ELTM defined above. Main also computes the gain of the antenna in decibels with the radome in place according to

$$\text{GAIN} = 20. * \text{ALOG10}(\text{SMAX}/\text{VAIRM})$$

For other than an "air radome", GAIN is negative and indicates a loss in antenna maximum gain due to radome reflections and ohmic ( $\tan \delta$ ) losses. The amplitude of received sum voltage, VAIRM, is always printed as the last item prior to termination of the program.

#### 2-4. Comments and Method

a. Method. The method of analysis has been presented in Section 2.1. Additional details of analysis are presented in the descriptions of each subroutine, especially Subroutine RECM.

b. Supporting Subroutines. Twenty eight supporting subroutines are required by SIIRACP, 22 of which are identical to those used by RTFRACP. The purpose of each one is briefly described below. Those subroutines peculiar to SIIRACP and explained in Chapters 3-8 are denoted by asterisks below.

- \* (1) TRECNF--Computes complex vector aperture electric fields of antenna for all three monopulse channels at  $NX \times NY$  sample points.
- (2) ORIENT--Computes matrices ROTATE and TRANSLATE used for coordinate transformations by Subroutines POINT and VECTOR.
- (3) POINT--Transforms a point  $P(x_A, y_A, z_A)$  in antenna system to the same point  $P(x_R, y_R, z_R)$  in radome coordinate system, and vice versa.
- (4) VECTOR--Transforms a vector from radome to antenna coordinate system, and vice versa.

- (5) INCPW--Computes the rectangular electric field components of a plane wave incident from the direction  $\hat{k}_\Lambda$  in antenna coordinates. The power density of the plane wave is unity.
- \* (6) RECM--Computes the voltage received by each channel of the antenna for a plane wave  $EINC(E_x, E_y, E_z)$  incident on the radome from the direction  $KA(k_x, k_y, k_z)$ .
- (7) OGIVEN--Computes the unit inward normal to the tangent ogive radome surface at a specified point.
- (8) RXMIT--Computes the transmitted electric fields of the plane wave traveling in direction  $-\hat{k}$  and incident on a flat dielectric wall with unit inner normal  $\hat{n}$ . The unit vectors  $\hat{k}$ ,  $\hat{n}$  are used to resolve the incident plane wave into vector components perpendicular and parallel to the plane of incidence, and to determine the angle of incidence.
- \* (9) WALL--Computes the normal voltage transmission coefficients of flat panel model of the radome wall as function of the sine of the incidence angle.
- (10) AXB--Computes real vector cross product  $\underline{C} = \underline{A} \times \underline{B}$ .
- (11) CAXB--Computes the complex vector cross product  $\underline{C} = \underline{A} \times \underline{B}$ , where  $\underline{A}$  is complex and  $\underline{B}$  is real.
- (12) RECBS--Computes boresight errors of antenna enclosed by the radome for the specified orientation, fineness ratio, etc.
- (13) RECPTN--Computes receiving patterns of all three channels.
- \* (14) APINT--Computes the fields of specified planar aperture fields using equivalent currents.
- \* (15) DIPOLES--Computes the fields of electric and magnetic dipoles located on a planar surface as required by Subroutine APINT.

- \* (16) CAXCB--Computes the complex vector product  $\underline{C} = \underline{A} \times \underline{B}$ ,  
where  $\underline{A}$  and  $\underline{B}$  are complex.
- (17) FAR--Computes the amplitude of the power pattern from the  
complex plane wave spectra  $A_x(k_x, k_y)$ ,  $A_y(k_x, k_y)$  of an  
antenna.
- (18) AMPHS--Converts a complex number from rectangular to polar  
form. This subroutine utilizes the intrinsic function  
ATAN2. The amplitude produced is linear (not decibels),  
and the phase is in degrees on the range (-180, 180).
- (19) DBPV--Converts a real, two-dimensional array from linear  
to logarithmic values in decibels on the range 0 to -40 dB.
- (20) NORMH--Normalizes a two-dimensional real array to values  
between 0 and 1.
- (21) CNPLTH--Plots single dimensional far field patterns on axes  
patterned after standard pattern recorder paper. CNPLTH  
calls Subroutine PSI in addition to the usual Calcomp sub-  
routines.
- (22) PSI--Used by Subroutine CNPLTH to compute the azimuthal  
angle  $\psi$ .
- (23) PLT3DH--Yields three-dimensional plots of the data in the  
two-dimensional real array FIELD. PLT3DH calls Subroutines  
PLTT, NORMH as well as the usual Calcomp sub-routines.
- (24) PLTT--Used by Subroutine PLT3DH to eliminate moving the  
pen for hidden lines.
- (25) FFTA--Computes the Fast Fourier Transform of a one-  
dimensional complex array having  $2^{**IEXP}$  elements. Proper  
operation is machine dependent.

- (26) MAGFFT--Provides increased resolution of a sampled function using FFT and Discrete Fourier Transform techniques.
- (27) JOYFFT--Provides increased resolution of selected portions of a two-dimensional Fourier transform. JOYFFT calls Subroutines FFTA and PWRTWO.
- (28) PWRTWO--Used by Subroutine JOYFFT to ensure that a given integer is a power of 2.

#### 2-5. Program Flow

For the following, refer to the program listing in Section 2-8 and the line numbers shown on the right-hand margin of that listing.

<u>Line Nos.</u>	<u>Explanation</u>
15	All variables beginning with the letter K in the main program are real.
16-31	Declare variables and array dimensions. Note equivalence statements in Lines 23-25. The dimension of IBUF in Line 25 may be computer system dependent. Note in Line 31 that only twenty fineness ratios, scan planes, and scan angles can be accommodated.
32-35	Label common is used as a convenient means to transmit variables to subroutines not directly called by MAIN. The labels are generated from the names of the subroutines which receive the variables, and each label is terminated with the letter C to denote common; e.g., RECMC denotes variables common to MAIN and Subroutine RECM.

- 40-42            Declare namelists for printing data. These name-  
lists are no longer used except for occasional de-  
bugging purposes.
- 43-57            Set data in DATA statements as described above in  
Section 2-3.
- 61-62            Set SMAX and VMAX to unity to prevent division by zero.
- 63-64            Read and write TITLE according to 18A4 format.
- 65-67            Read input data using free-field format.
- 68                Compute sine of the offset angle  $\theta_{OS}$ .
- 69                Set TABLE=FALSE so that normalizing factor VAIRM  
can be computed via a call to Subroutines RECM and  
RXMIT. In the latter, TABLE=FALSE causes  $T_1$ ,  $T_{11}$  to  
be set unity as in the case of no radome.
- 71-75            Write input data.
- 76-80            Read input data and set VAIRM needlessly.
- 81-111           Comments explaining input variables.
- 112              Set NN=N+1= Number of wall layers plus one.
- 113              Initialize DINCH= total thickness of radome wall  
in inches.
- 114              Read wall data and compute total thickness.
- 117              Compute DIAIN= inside base diameter of the radome  
in inches.
- 118-119          Compute indices of the center element of near-field  
arrays corresponding to  $x_A, y_A$ .
- 120-121          Write array dimensional data.
- 122-129          Read fineness ratios, scan planes, and scan angles.

130-133      Compute wavelength in inches and centimeters.  
                  Compute  $\beta = 2\pi/\lambda_{\text{cm}}$ .

134            Compute DAPWL= diameter of antenna aperture in  
                  wavelengths.

135-148       Convert variables in inches to centimeters for input  
                  to subroutines. Some variables are multiply defined  
                  to avoid conflicts in labeled common; e.g., ZBOT and  
                  Z1. Note that DIACM is the inside diameter of the  
                  radome in centimeters.

149-153       Convert angles from degrees to radians using  $\text{RAD} = \pi/180$ .

154-160       Compute near fields of three channel monopulse antenna  
                  using Subroutine TRECNF.

161-168       Set KYMAX=KXMAX, compute magnified folding wavenumbers  
                  KXM, KYM, and print results.

169-187       Initialize Calcomp plotter, if required. The commented  
                  initialization (Lines 175-185) applies to the IBM 3033  
                  system at JHU/APL.

Note:          Lines 188-268 are used to plot the near fields of the  
                  antenna and/or the transmitting principal plane power  
                  patterns.

189-199       Initialize the maximum values FMXEL, FMXDAZ of the E-  
                  and H-plane patterns so that when used initially as  
                  inputs to Subroutine FAR, the resulting pattern will  
                  be normalized with respect to its own maximum and FMXEL  
                  and FMXDAZ will be set equal to these respective maxima.  
                  On subsequent call to FAR, the resulting patterns will  
                  be normalized with respect to FMXEL and FMXDAZ. Hence,

the relative gain of the difference and sum patterns will be correctly displayed in the graphs.

191 Iterate for each of three monopulse antenna channels.

192-201 Equate complex arrays EXT, EYT to the selected near field and compute the amplitude NF of EXT.

202 Assume transmitting near fields are to be plotted (GRAFTR=T).

204 Call Subroutine PLT3DH to plot the amplitude of EXT. The inputs XSIZE=6., YSIZE=2.5, HEIGHT=2.5 yield a 3D plot that will fit on a 8½" x 11" report page. The inputs NF, NX, NY specify the real array to be plotted and its dimensions. The input NMZ=.TRUE. directs the subroutine to normalize NF so that its values be between 0 and 1. The input LDB=.FALSE indicates that the array NF contains linear values rather than logarithmic values (decibels).

205-212 Compute and plot phase of EXT on a scale of -180 degrees to +180 degrees. Note that Line 210 ensures that the real array NF contains these phase values scaled to the required 0 to 1 range.

213-226 Repeat amplitude and phase 3D plots for EYT.

227 Assume GRAFSA=T so that principal plane patterns are plotted.

230 If IP=3, go to Line 254 and plot H-plane patterns; otherwise, plot E-plane patterns.

233 Call Subroutine JOYFFT to calculate the inverse Fourier transform of the  $x_A$ -component of near field EXT to



produce the plane wave spectrum XEEL from which the radiation field can be computed. In the process of computing the transform, provide increased resolution from NX x NY points to NYE x NXE points through point (NXC, NYC) in the array EXT. In the  $k_x$  direction, the plane wave spectrum is magnified by MY; it is magnified by MX in the  $k_y$  direction. The array FFTXY is a working array.

- 234 Repeat for EYT to produce the plane wave spectrum YEEL for the  $y_A$ -component of field.
- 235 Call Subroutine FAR to calculate the E-plane elevation (IPWR=3) power pattern FFSEL of the near field at equal samples in  $\sin\theta$  over the range  $(-KXM, KXM - \Delta K)$ . If  $FMXEL < 0$  (and it is for IP=1), normalize FFSEL with respect to its own maximum.
- 237 Call Subroutine DBPV and convert the power pattern to decibels on a scale of 0 to -40 dB.
- 238-241 Scale the values in FFSEL to the range of 0 to 1 for plotting.
- 242 Call Subroutine CNPLTH and plot the power pattern. If  $KXM < 1$ , the pattern is plotted over the angular range corresponding to  $\sin^{-1}(KXM)$ ; if  $KXM > 1$ , the angular range is  $(-90^\circ, 90^\circ)$ . Subroutine CNPLTH actually plots conical cuts corresponding to  $k_x = \text{constant}$  or  $k_y = \text{constant}$  as specified by inputs KXC, KYC. In the call here,  $KXY = KYC = 0$  so that a principal pattern is produced.

243-247 Write a figure title for the plot and establish a new origin for the next plot.

248 If IP=2, the E-plane patterns are finished.

249-253 Since JOYFFT changes the input arrays EXT,EYT it is necessary to recompute them so that increased resolution can be obtained in the plane wave spectra in the H-plane.

254-269 Repeat computation and plotting for H-plane power patterns.

271 Iterate the radome analysis for NFINE fineness ratios.

272 Set FINE = outside fineness ratio.

273-277 Calculate and write  $R_{OS}$ , B,  $F_{OS}$ ,  $F_{IS}$  as defined in Figure 2-1 for the radome geometry.

278 Compute RDML = distance from the base of the radome to the theoretical tip on the inside of the radome.

279-283 If ZTOPIN<RDML, the radome has a metal tip, and a message is written to that effect.

284-309 Compute parameters needed by Subroutine OGIVE to describe the radome shape. R and B are in centimeters and apply to the inside dimensions. AP, the height of the cylinder in centimeters, is not used. RTSQ= square of the radius of the top disk. RBSQ= square of the radius of the bottom disk (bulkhead). The other variables, BSQ, RINV, RSQ1, RP, and RP2, are precalculated here to speed later computations in OGIVE.

310            Compute conversion factor DPMR for converting milli-  
radians to degrees.

311-314        Initialize the "last" values of boresight error in  
azimuth (AZL) and elevation (ELL) and the "last"  
value THL of scan angle. These variables are used  
later to compute boresight error slope in degrees  
per degree from the present and last values of bore-  
sight error.

315-316        Write title for analysis results.

317-319        Write parameters of radome wall.

320-322        Write heading for table of boresight error and gain  
data.

323-334        Write this same data to logical unit 7 for subsequent  
storage as a disk file, if desired.

335            Iterate the radome analysis for NPFI scan planes.

336-338        Compute  $\phi_r$  in radians as required by Subroutine ORIENT.

339            Iterate the analysis for NTHE scan angles in each  
scan plane.

340-342        Compute  $\theta_r$  in radians as required by Subroutine ORIENT.

343            Call Subroutine ORIENT and compute the rotation matrix  
ROTATE and translation matrix TRANSL required for coor-  
dinate transformations using Subroutines POINT and  
VECTOR.

344            On the first iteration, TABLE is false so that the  
maximum amplitude of the received voltage on the sum  
channel is computed without the radome.

345-347 Set the direction cosines of the incident plane wave so that it arrives from the  $\hat{z}_A$  direction.

348 Call Subroutine INCPW and compute the rectangular components PWI of the incident plane wave having polarization specified by IOPT.

349-354 Set TSUP=T and TABLE=F so that an air radome will be used and so that printing by Subroutine RXMIT and RECM will be suppressed.

355-356 Call Subroutine RECM and compute the complex voltages VR received on the sum, difference elevation, and difference azimuth channels, respectively, corresponding to VR(I), I=1,3.

360 Compute VAIRM=|VR(1)|.

362 Set TABLE=T so that on subsequent iterations VAIRM will not be recomputed, and so that the table of transmission coefficients will be utilized when RXMIT is called.

363 If SUPPRS=F, compute and print the E-plane and H-plane receiving power patterns of the antenna with the radome in place.

366 Iterate in J for E-plane (ICUT=1) and H-plane (ICUT=2) patterns.

368 Set the desired far field component.

369 Set the temporary logical variable TSUP=T so that printing will be suppressed.

370-371 Call Subroutine RECPTN and compute the complex received voltages on each of three channels at NREC points over the range  $(-KMAX, KMAX - DK)$ .

372-375 Increase the resolution and print results for all three channels. Do not print results that are known to be identically zero.

376-377 Transfer the received voltage into a one-dimensional array VREC.

378 If  $NREC > NXE$ , there is no need to increase the resolution.

379 Call Subroutine MAGFFT to increase the resolution of VREC from NREC points to NXE points. The result is contained in complex array XYFFT on output.

380-384 Compute linear power pattern.

385 Select  $NXX =$  larger of  $NXE$  and  $NREC$ .

386 Write heading for printed results from Subroutine NORMH.

388 Call Subroutine NORMH to normalize the  $NXX$  values in real array MVREC to be between zero and one. The input argument  $LDB = .FALSE.$  since the values are not in decibels.

389 Call Subroutine DBPV to convert the power pattern in MVREC to decibels.

390-391 Write correct heading for E-plane or H-plane.

392 Compute the increment in  $\sin\theta$  at which power pattern has been computed and resolved.

393-404 Scale the power pattern to have values between 0 and 1. If  $SUPPRS = F$ , compute the angle  $\theta = ANG$  and the phase

of the pattern, and print the results for every fourth angle.

405 If GRAFRV=T, plot the receiving power patterns.

406-416 Call Subroutine CNPLTH and plot the receiving patterns in turn. Write an appropriate figure title following each pattern plot. Re-originate the plotter pen for subsequent plots. The result of Lines 330-383 is four principal plane patterns: E-plane sum, E-plane  $\Delta_{EL}$ , H-plane sum, H-plane  $\Delta_{AZ}$ .

417-419 Call Subroutine RECBS and compute the boresight errors AZT, ELT in the azimuth and elevation planes of the antenna as caused by the radome. On output, the real array KA contains the direction cosines of the last target return and, hence, gives the true direction to the target at the time that the tracking functions in the azimuth and elevation planes indicated the electrical boresight direction.

420 If this is the first iteration in scan angle, do not attempt to compute boresight error slope.

421-422 Compute boresight error slope (degrees/degree) in azimuth and elevation channels.

423-425 Set the "last" values of boresight errors and scan angle to the current values in preparation for next iteration.

426-428 Compute loss in maximum gain of the antenna sum channel due to the radome.

429-430            Write results to logical units 6 and 7.  
434-435            Write maximum amplitude of received sum voltage  
                    VAIRM without radome.  
436                Terminate plotting software.  
  
                    STOP  
  
                    END

2-6. Test Case

A test case has been delivered to JHU/APL under separate cover.

Typical input data are shown in Table 2-1.

2-7. References

1. G. K. Huddleston and E. B. Joy, "Development of Fabrication and Processing Techniques for Laser Hardened Missile Radomes: Radome Electrical Design Analysis", Martin Marietta Purchase Agreement 573712, April 1977.
2. G. K. Huddleston, H. L. Bassett, and J. M. Newton, "Parametric Investigation of Radome Analysis Methods", IEEE AP-S Symposium Digest, pp. 199-202, May 1978; also, Proc. Fourteenth Symposium on Electromagnetic Windows, pp. 21-28, June 1978.
3. E. B. Joy and G. K. Huddleston, "Radome Effects on the Performance of Ground Mapping Radar," U.S. Army Missile Command, DAAH-01-72-C-0598, March 1973.

2-8. Program Listing: See following pages.

TEST SIIRACP FEB AC  
 F.F.F.F,00,T  
 1.1,1.1,1241,.01,.01,1.70,35.,.3.  
 5.,.5,1.,.159,1.6,1,1,1,1.,.5,4  
 .1241.,.1241,8,8  
 .001,1.00,0.000  
 1.505  
 0.  
 0.

1 2 3 4 5 6 7 8 9

Table 2-1. Input Data for SIIRACP.



C	THIS RADOME ANALYSIS COMPUTER PROGRAM, SIIRACP, WAS PREPARED FOR	1
C	JOHNS HOPKINS APL BY G.K. HUDDLESTON, JANUARY 1980, UNDER THE	2
C	COGNIZANCE OF ROBERT C. MALLALIEU.	3
C	SUBR TRECNF COMPUTES NEAR FIELDS SUITABLE FOR THIS SURFACE	4
C	INTEGRATION (INNER RADOME SURFACE) ANALYSIS APPROACH.	5
C	COMPUTED RESULTS ARE ALSO WRITTEN TO TAPE7 FOR LATER USE.	6
C		7
C	-----	8
C		9
C	IMPLEMENTATION AT APL/JHU 2/11/80 FOR IBM 3033	10
C		11
C	-----	12
C	*** LIBRARIES LSIIRAC AND MISCFFT ARE REQUIRED FOR EXECUTION ***	13
C	PROGRAM SIIRACP(INPUT,OUTPUT,TAPE5=INPUT,TAPE6=OUTPUT,TAPE7)	14
	IMPLICIT REAL(K)	15
	REAL NF(4,4),MVREC(256),KA(3)	16
	COMPLEX SUMX(4,4),SUMY(4,4),DELX(4,4),DELY(4,4)	17
	COMPLEX DAZX(4,4),DAZY(4,4),EXT(4,4),EYT(4,4)	18
	COMPLEX VR(16),VREC3(6,3),VREC(32)	19
	REAL FFS(256,1),FFSEL(1,256)	20
	COMPLEX XE(256,1),YE(256,1),XYFFT(512),PWI(3)	21
	COMPLEX XEEL(1,256),YEEL(1,256)	22
	EQUIVALENCE(XE(1,1),XEEL(1,1))	23
	EQUIVALENCE(YE(1,1),YEEL(1,1))	24
	EQUIVALENCE(FFS(1,1),MVREC(1),FFSEL(1,1))	25
C		26
	LOGICAL GRAF3D,GRAFSA,GRAFTR,GRAFRV, TABLE, SUPPRS, TSUP, SQUARE	27
	INTEGER IBUF(512)	28
C		29
	REAL ROTATE(3,3),TRANSL(3),TITLE(18)	30
	REAL FINR(20),PHI(20),THETA(20)	31
	COMMON/RECIC/DSTH,DSPHI,NTHMIN,NPHIMIN, AREA, NPOINTS, ROS, RIS,	32
	\$ZBOTCM, ZTOPCM, BCM, RR	33
	COMMON/TDISKC/ZTOP, RTSQ	34
	COMMON/TRACC/Z2, Z1	35
	COMMON/BDISKC/ZBOT, RBSQ	36
	COMMON/TRANSC/DIN(6), ER(6), TD(6), TZ, WALTOL, N, NN, D(6), ZB, TK	37
	COMMON/OGIVC/ RP, BSQ, AP, RINV, B, RSQ1, RP2	38

C	NAMELIST/GEOM/RR, RA, APIN, ZBOTIN, NX, NY, NXE, NYE, NXY, MX, MY, NXC, NYC	39
	NAMELIST/KDATA/KXMAX, KYMAX, KXM, KYM	40
	NAMELIST/NEW/LMAX, DMRAD, IOPT, RAPMAX, VAIRM	41
C	BOUNDARY VALUES NEEDED BY SUBR TRACE (INCHES, CONVERT TO CM BELOW)	42
C	Z1=ZR COORDINATE OF BOTTOM DISK	43
C	Z2=ZR COORDINATE OF TOP DISK (Z1, Z2 IN CM)	44
C	APIN IS HEIGHT OF CYLINDER IN INCHES, CONVERT TO CM BELOW	45
	DATA APIN/0./	46
C	ZBOTIN IS ZR COORD OF BOTTOM DISK (BULKHEAD) IN RADOME COORD IN INCHE	47
	DATA ZBOTIN/0.00/	48
C	KXMAX, KYMAX ARE OUTPUTS OF NEAR FIELD SUBR	49
C	INITIALIZE CONSTANTS	50
	DATA RADIUS/1E0/	51
	DATA THETAA, PHIA, AGAM3A/0.0, 90.0, 0.0/	52
	DATA PI/3.1415926535898/	53
C*****		54
	DATA NX, NY, NYE, NXY/4, 4, 1, 512/	55
	DATA MY/1/, NREC/6/	56
C*****		57
C		58
C	READ IN DESCRIPTION OF RADOME WALL	59
	SMAX=1.0	60
	VMAX=1.0	61
	READ(5,6)TITLE	62
	WRITE(6,6) TITLE	63
	READ(5,*) GRAF3D, GRAFSA, GRAFTR, GRAFRV, SUPPRS, IPENCD, SQUARE	64
260	FORMAT(4L6)	65
	READ(5,*) NFINE, NPHI, NTHE, DIAOS, RAIN, RRIN, ZTOPIN, FREQ, OSANG	66
	SINOS=SIN(OSANG*PI/180.)	67
	TABLE=.FALSE.	68
C	TABLE IS SET FALSE SO THAT NORMALIZING FACTOR CAN BE COMPUTED.	69
	WRITE(6,265) GRAF3D, GRAFSA, GRAFTR, GRAFRV, TABLE	70
265	FORMAT(" GRAF3D=", L2, " GRAFSA=", L2, " GRAFTR=", L2, " GRAFRV=", L2,	71
	\$ " TABLE=", L2)	72
	WRITE(6,270) NFINE, NPHI, NTHE, OSANG	73
270	FORMAT(/" NFINE=", I5, " NPHI=", I3, " NTHETA=", I3, " OSANG= ", F5.2/)	74
	READ(5,*) LMAX, DMRAD, IOPT, RAPMAX, VAIRM, IPOL, ICASE, N, IPWR, KMAX, NXE	75
		76

MX=NXE/NX	77
IF (MX.LT.1) MX=1	78
READ(5,*) DSTHIN,DSPHIN,NTHMIN,NPHIMIN	79
IF (VAIRM.LE.0.) VAIRM=1.0	80
C DIAOS=OUTSIDE DIAMETER OF BASE OF TANGENT OGIVE RADOME	81
C VAIR=MAXIMUM REC'D VOLTAGE W/O RADOME AT KX=0.,KY=0.	82
C NFINE=NO. OF FINENESS RATIOS	83
C NPHI=NUMBER OF SCAN PLANES	84
C NTHE=NUMBER OF ANGLES IN EACH SCAN PLANE	85
C DIAIN=INSIDE BASE DIAMETER OF RADOME IN INCHES	86
C ZTOPIN=ZR COORD (IN) OF TOP DISK (METAL TIP)	87
C FREQ=FREQUENCY IN GHZ	88
C GRAF3D=.TRUE. GIVES 3D PLOTS OF INCIDENT FIELDS ON APERTURE (DELETED)	89
C GRAFRV=.TRUE. GIVES SA PLOTS OF RECEIVING PATTERNS (AZ & EL)	90
C GRAFSA=.TRUE. GIVES SA PLOTS OF TRANSMITTING PATTERN WITHOUT RADOME	91
C SUPPRS=.TRUE. SUPPRESSES THE PRINTING OF NUMEROUS RESULTS	92
C RAPMAX=MAX RADIUS OF ANTENNA APERTURE IN INCHES.	93
C IOPT SELECTS POLARIZATION OF INCIDENT PLANE WAVE:	94
C     =1 ELEV (VERTICAL)	95
C     =2 AZIMUTH (HORIZONTAL)	96
C     =3 RHC	97
C     =4 LHC	98
C IPOL SELECTS POLARIZATION OF ANTENNA WHEN ICASE=1:	99
C     = SAME CODE AS FOR IOPT	100
C ICASE=1 OR 2 FOR CIRC APERTURE, UNIFORM ILLUMINATION	101
C     =3 FOR FLAT PLATE WITH SPECIFIED ILLUM, VERT POL (CASE III)	102
C N=NUMBER OF LAYERS IN RADOME WALL	103
C OSANG=ANGLE IN DEG IN 45 PLANE OFF BORESIGHT OF FIRST TARGET RETURN	104
C     USED BY SUBR RECBS IN GETTING INITIAL DATA.	105
C IPWR=1 FOR POWER IN ELEV COMP OF FAR FIELD PATTERN	106
C     =2 FOR AZIMUTH COMP, =3 FOR TOTAL POWER.	107
C DSTHIN=SAMPLE DISTANCE (IN.) ON RADOME SURFACE IN THETA DIRECTION	108
C DSPHIN= -DITTO-   PHI DIRECTION	109
C NTHMIN=MINIMUM NUMBER OF SAMPLES IN THETA DIRECTION	110
C NPHIMIN= -DITTO-   PHI DIRECTION	111
NN=N+1	112
DINCH=0.	113
DO 5 I=1,N	114

```

READ(5,*) DIN(I),ER(I),TD(I)
5 DINCH=DIN(I)+DINCH
DIAIN=DIAGS-DINCH*2.
NXC=NX/2+1
NYC=NY/2+1
WRITE(6,4) NX,NY,NXE,NYE,NXY,MX,MY
4 FORMAT(" NX,NY,NXE,NYE,NXY,MX,MY:",7I4)
C READ FINENESS RATIOS FOR THIS RUN--BASED ON OUTSIDE DIMENSIONS
DO 13 I=1,NFINE
13 READ(5,*) FINR(I)
C READ ORIENTATIONS FOR THIS RUN (DEGREES)
DO 14 I=1,NPHI
14 READ(5,*) PHI(I)
DO 15 I=1,NTHE
15 READ(5,*) THETA(I)
C COMPUTE WAVELENGTH:
WLIN=29.97925/(FREQ*2.54)
WLCM=WLIN*2.54
BETA=2.*PI/WLCM
DAPWL=2.*RAPMAX/WLIN
C CONVERT TO CENTIMETER AND RADIANS
ZBOT=ZBOTIN*2.54
Z1=ZBOT
RSQMAX=(2.54*RAPMAX)**2
DIACM=DIAIN*2.54
ZTOP=ZTOPIN*2.54
ZB=ZTOP
Z2=ZTOP
ZTOPCM=ZTOP
ZBOTCM=ZBOT
RA=RAIN*2.54
RR=RRIN*2.54
DSTH=DSTHIN*2.54
DSPHI=DSPHIN*2.54
RAD=PI/180.0
6 FORMAT(18A4)
THETAA=THETAA*RAD
PHIA=PHIA*RAD

```

A JAM (A JAM) A *RA.	153
ME (E FIELD) E ANTENNA WHEN XMAX IN Y:	154
ALL THE NE (OMA, NX, NY, Z, P, Q, R, APWL, DXWL, KXMAX, ZBASE, SQUARE)	155
ALL THE NE (OMY, NX, NY, Z, P, Q, R, APWL, DXWL, KXMAX, ZBASE, SQUARE)	156
ALL THE NE (EEX, NX, NY, Z, P, Q, R, APWL, DXWL, KXMAX, ZBASE, SQUARE)	157
ALL THE NE (EY, NX, NY, Z, P, Q, R, APWL, DXWL, KXMAX, ZBASE, SQUARE)	158
ALL THE NE (EXX, NX, NY, Z, P, Q, R, APWL, DXWL, KXMAX, ZBASE, SQUARE)	159
ALL THE NE (EY, NX, NY, Z, P, Q, R, APWL, DXWL, KXMAX, ZBASE, SQUARE)	160
*XMAX *YMAX	161
*XMAX *YMAX *ZBASE *XMAX	162
*XMAX *YMAX *ZBASE *YMAX	163
*XMAX *YMAX	164
WRITE (X, Y, Z, XMAX, YMAX, KX, KY, ZBASE, ZPHIN, NTRMIN, NPHMIN)	165
*FORMAT "XMAX=YMAX=ZBASE=XMAX YMAX=ZBASE=YMAX=XMAX YMAX=ZBASE=YMAX=XMAX" WAVELENGTHS"	166
PHASE="EEX" "EY" "EXX" "EY" "ZPHIN" "EEX" "EY" "ZPHIN"	167
PHASE="NTRMIN" "NPHMIN" "ZPHIN" "NTRMIN" "NPHMIN" "ZPHIN"	168
	169
STOP (E FIELD) E TWAVE	170
DE (GRAPH) E (GRAPH) A (GRAPH) B (GRAPH) C (GRAPH) D (GRAPH)	171
E (GRAPH) A (GRAPH) B (GRAPH) C (GRAPH) D (GRAPH)	172
CONTINUE	173
	174
----- ALL ME INITIALIZATION -----	175
	176
READ ME ANALYSIS (ME) (PROGRAM)	177
* (ME) (PROGRAM) (ME) (PROGRAM)	178
* (ME) (PROGRAM) (ME) (PROGRAM)	179
WRITE (ME) (PROGRAM)	180
	181
READ ME ANALYSIS (ME) (PROGRAM)	182
ALL ME INITIALIZATION	183
	184
-----	185
	186
DE (GRAPH) E (GRAPH) A (GRAPH) B (GRAPH) C (GRAPH) D (GRAPH)	187
E (GRAPH) A (GRAPH) B (GRAPH) C (GRAPH) D (GRAPH)	188
*ME (PROGRAM)	189
*ME (PROGRAM)	190

DO 30 IP=1,3	191
DO 35 I=1,NX	192
DC 35 J=1,NY	193
IF (IP.EQ.1) EXT(I,J)=SUMX(I,J)	194
IF (IP.EQ.1) EYT(I,J)=SUMY(I,J)	195
IF (IP.EQ.2) EXT(I,J)=DELX(I,J)	196
IF (IP.EQ.2) EYT(I,J)=DELY(I,J)	197
IF (IP.EQ.3) EXT(I,J)=DAZX(I,J)	198
IF (IP.EQ.3) EYT(I,J)=DAZY(I,J)	199
NF(I,J)=CABS(EXT(I,J))	200
35 CONTINUE	201
IF (.NOT.GRAFTR) GO TO 215	202
C PLOT 3D NEAR FIELDS X-COMPONENTS	203
CALL PLT3DH(6.,2.5,2.5,NF,NX,NY,.TRUE.,.FALSE.)	204
C PLOT PHASE ALSO	205
DO 40 I=1,NX	206
DO 40 J=1,NY	207
NF(I,J)=0.	208
CALL AMPHS(EXT(I,J),RLF,AIF)	209
NF(I,J)=(AIF+180.)/360.	210
40 CONTINUE	211
CALL PLT3DH(6.,2.5,2.5,NF,NX,NY,.FALSE.,.FALSE.)	212
C PLOT 3D NEAR FIELDS Y-COMPONENTS	213
DO 45 I=1,NX	214
DO 45 J=1,NY	215
NF(I,J)=CABS(EYT(I,J))	216
45 CONTINUE	217
CALL PLT3DH(6.,2.5,2.5,NF,NX,NY,.TRUE.,.FALSE.)	218
C PLOT PHASE ALSO	219
DO 50 I=1,NX	220
DO 50 J=1,NY	221
NF(I,J)=0.	222
CALL AMPHS(EYT(I,J),RLF,AIF)	223
NF(I,J)=(AIF+180.)/360.	224
50 CONTINUE	225
CALL PLT3DH(6.,2.5,2.5,NF,NX,NY,.FALSE.,.FALSE.)	226
IF (GRAFSA) GO TO 215	227
GO TO 30	228

215	CONTINUE		229
	IF (IP.EQ.3) GO TO 220		230
C	CALC EL CUT OF SUM		231
C	NOTE THAT JOYFFT CHANGES EXT,EYT.		232
	CALL JOYFFT(EXT,NX,NY,MY,MY,MY,NXC,NYC,XEEL,NYE,NXE,XYFFT,NXY,3)		233
	CALL JOYFFT(EYT,NX,NY,MY,MY,MY,NXC,NYC,YEEL,NYE,NXE,XYFFT,NXY,3)		234
	CALL FAR(FFSEL,XEEL,YEEL,NYE,NXE,FREQ,KYM,KXM,RADIUS,IPWR,FMXEL)		235
C	SA PLOTS OF ELEVATION RESULTS		236
	CALL DBPV(FFSEL,NYE,NXE,1)		237
	DO 216 I=1,NYE		238
	DO 216 J=1,NXE		239
	FFSEL(I,J)=1.0+FFSEL(1,J)/40.		240
216	CONTINUE		241
	CALL CNPLTH(FFSEL,NXE,KXM,0.,0.)		242
	CALL SYMBOL(.5,6.5,.140000,39HFIGURE TRANSMITTING ELEVATION PO		243
	\$WER,0.,39)		244
	RPWR=FLOAT(IPWR)		245
	CALL NUMBER(999.,999...14,RPWR,0.,0)		246
	CALL PLOT(8.5,0.,-3)		247
	IF (IP.EQ.2) GO TO 30		248
C	RECOMPUTE SUMX,SUMY FOR JOYFFT:		249
	CALL TRECNF(EXT,NX,NY,1,IPOL,1,DAPWL,DXWL,KXMAX,ICASE,SQUARE)		250
	WRITE(6,219) IPWR		251
219	FORMAT(" IPOWER OF PATTERN=",I2)		252
	CALL TRECNF(EYT,NX,NY,1,IPOL,?,DAPWL,DXWL,KXMAX,ICASE,SQUARE)		253
220	CALL JOYFFT(EXT,NX,NY,MY,MY,MY,NXC,NYC,YE,NXE,NYE,XYFFT,NXY,3)		254
	CALL JOYFFT(EYT,NX,NY,MY,MY,MY,NXC,NYC,YE,NXE,NYE,XYFFT,NXY,3)		255
	CALL FAR(FFS,XE,YE,NXE,NYE,FREQ,KXM,KYM,RADIUS,IPWR,FMXDAZ)		256
C	SA PLOTS OF AZIMUTH RESULTS		257
	CALL DBPV(FFS,NXE,NYE,1)		258
	DO 10 I=1,NXE,1		259
	DO 10 J=1,NYE		260
	FFS(I,J)=1.0+FFS(I,J)/40.0		261
10	CONTINUE		262
	CALL CNPLTH(FFS,NXE,KXM,0.,0.)		263
226	CALL SYMBOL(.5,6.5,.140000,37HFIGURE TRANSMITTING AZIMUTH POWER		264
	\$.0.,37)		265
	CALL NUMBER(999.,999...14,RPWR,0.,0)		266

CALL PLOT(8.5,0.,-3)	267
30 CONTINUE	268
205 CONTINUE	269
C	270
DO 100 NG=1,NFINE	271
FINE=FINR(NG)	272
C CALCULATE INSIDE FINENESS RATIO	273
RIN=FINE*DIAOS/(SIN(PI-2.*ATAN(2.*FINE)))	274
ROS=RIN*2.54	275
BIN=RIN-DIAOS/2.	276
FINE=SQRT((RIN-DINCH)**2-BIN**2)/DIAIN	277
RDML=FINE*DIAIN+APIN	278
IF (ZTOPIN.LT.RDML) WRITE(6,25) ZTOPIN	279
20 FORMAT(" TANGENT OGIVE PARAMETERS: "," ROS(IN)="	280
\$ ,F9.5," BOS(IN)=" ,F9.5,/26X," FINOS=" ,F5.3,	281
\$ " FINIS=" ,F8.5," RINV=" ,E12.5)	282
25 FORMAT(/" THIS RADOME HAS A TOP DISK AT ZTOPIN= " ,E12.5/)	283
C COMPUTE PARAMETERS NEEDED BY SUBR OGIVE	284
R=FINE*DIACM/(SIN(PI-2.*ATAN(2.*FINE)))	285
RIS=R	286
TLIS=DIAIN*FINE	287
IF (ZTOPIN.GT.TLIS) ZTOPIN=TLIS	288
ZTOP=ZTOPIN*2.54	289
ZB=ZTOP	290
Z2=ZTOP	291
ZTOPCM=ZTOP	292
IF (ZTOPCM.GT.RIS) ZTOPCM=RIS	293
B=R-DIACM/2.	294
BCM=B	295
AP=APIN*2.54	296
RTSQ=R**2-(ZTOP-AP)**2	297
IF (RTSQ.LT.0.) RTSQ=0.	298
RTSQ=(SQRT(RTSQ)-B)**2	299
RBSQ=R**2-(ZBOT-AP)**2	300
IF (RBSQ.LT.0.) RBSQ=0.	301
RBSQ=(SQRT(RBSQ)-B)**2	302
BSQ=B**2	303
RINV=1./R	304



	RSQ1=R**2	305
	RP=RSQ1-BSQ	306
	RP2=RSQ1+BSQ	307
	WRITE(6,20) RIN,BIN,FINR(NG),FINE,RINV	308
C		309
	DPMR=180./(PI*1000.)	310
	AZL=0.	311
	ELL=0.	312
	THL=0.	313
	TLOS=DIAOS*FINR(NG)	314
	WRITE(6,2) TITLE,FINR(NG),DIAOS,TLOS,FREQ,RAIN,RRIN,DAPWL,IPOL,	315
	\$ICASE,IOPT	316
	DO 8 I=1,N	317
	8 WRITE(6,7) I,DIN(I),ER(I),TD(I)	318
	7 FORMAT(2X,I3,F13.5,F10.3,F9.4)	319
	WRITE(6,9)	320
	9 FORMAT(//" PHI THETA BSEEL BSEAZ SLPEL SLPAZ GAIN"/	321
	\$ " (DEG) (DEG) (MRAD) (MRAD) (DEG/DEG) (DEG/DEG) (DB)"/)	322
	WRITE(7,2) TITLE,FINR(NG),DIAOS,ZTOPIN,FREQ,RAIN,RRIN,DAPWL,IPOL,	323
	\$ICASE,IOPT	324
	DO 18 I=1,N	325
	18 WRITE(7,7) I,DIN(I),ER(I),TD(I)	326
	WRITE(7,9)	327
	2 FORMAT(1H1,5X," RESULTS OF RADOME ANALYSIS USING INSIDE SURFACE IN	328
	1TEGRATION"/18A4/" FINENESS RATIO=",F8.5,2X,	329
	2"DIAMETER=",F8.5," IN. LENGTH=",F8.5," IN."/" FREQUENCY=",	330
	3F8.5," GHZ "/	331
	4" RA=",F8.5," IN. RR=",F8.5," IN. ANTENNA D=",F8.4,	332
	5" WAVELENGTHS"/" IPOL=",I2," ICASE=",I2," IOPT=",I2//	333
	6" LAYER THICKNESS(IN.) ER TAND"/)	334
	DO 100 IPHI=1,NPHI	335
	PHIP=PHI(IPHI)	336
	PHIR=PHIP	337
	PHIR=PHIR*RA.	338
	DO 100 ITHE=1,N.	339
	THETAL=THETA(ITHE)	340
	THETAR=180.-THETAL	341
	THETAR=THETAR*RAD	342

CALL ORIENT(RA, THETAA, PHIA, RR, THETAR, PHIR, AGAM3A, ROTATE, TRANSL)	343
IF (TABLE) GO TO 23	344
C COMPUTE NORMALIZING FACTOR:	345
KA(1)=0.	346
KA(2)=0.	347
KA(3)=1.	348
CALL INCPW(KA, PWI, IOPT)	349
TSUP=SUPPRS	350
TABLE=.FALSE.	351
ZTEMP=ZTOPCM	352
ZTOPCM=DIACM*FINE	353
IF (ZTOPCM.GT.RIS) ZTOPCM=RIS	354
CALL RECM(PWI, KA, NX, NY, KXMAX, KYMAX, FREQ, ROTATE, TRANSL,	355
\$SUMX, SUMY, DELX, DELY, DAZX, DAZY, VR, TABLE, TSUP, RSQMAX)	356
C SET ZTOPCM BACK TO THE INPUTTED VALUE.	357
IF (ZTOPCM.LT.ZTEMP) ZTEMP=ZTOPCM	358
ZTOPCM=ZTEMP	359
VAIRM=CABS(VR(1))	360
WRITE(6, 105) VAIRM	361
TABLE=.TRUE.	362
23 IF (.NOT.SUPPRS) GO TO 24	363
GO TO 350	364
24 CONTINUE	365
DO 320 J=1,2	366
ICUT=J	367
ICOMP=IOPT	368
TSUP=.TRUE.	369
CALL RECPTN(SUMX, SUMY, DELX, DELY, DAZX, DAZY, NX, NY, ICUT, ICOMP, KMAX,	370
\$NREC, VREC3, KXMAX, KYMAX, FREQ, ROTATE, TRANSL, TABLE, TSUP, RSQMAX)	371
DO 325 MM=1,3	372
ICHAN=MM	373
IF ((ICUT.EQ.1).AND.(ICHAN.EQ.3)) GO TO 325	374
IF ((ICUT.EQ.2).AND.(ICHAN.EQ.2)) GO TO 325	375
DO 26 I=1,NREC	376
26 VREC(I)=VREC3(I, ICHAN)	377
IF (NREC.GE.NXE) GO TO 31	378
CALL MAGFFT(VREC, NREC, XYFFT, NXE)	379
DO 305 I=1, NXE	380

305	MVREC(I)=CABS(XYFFT(I))**2		381
	GO TO 33		382
31	DO 32 I=1,NREC		383
32	MVREC(I)=CABS(VREC(I))**2		384
33	NXX=MAX0(NXE,NREC)		385
	WRITE(6,306)		386
306	FORMAT(/" MIN AND MAX VALUES OF REC"G PATTERN: "/)		387
	CALL NORMH(MVREC,NXX,1,.FALSE.)		388
	CALL DBPV(MVREC,NXX,1,1)		389
	IF (J.EQ.1) WRITE(6,308)		390
	IF (J.EQ.2) WRITE(6,309)		391
	DK=2.*KMAX/NXX		392
	IMOD=4		393
	IF (NREC.GE.NXE) IMOD=1		394
	DO 307 I=1,NXX,1		395
	IF (SUPPRS) GO TO307		396
	ANG=ASIN(-KMAX+(I-1)*DK)*180./PI		397
	CALL AMPHS(XYFFT(I),AMP,PHS)		398
	IF (NREC.GE.NXE) CALL AMPHS(VREC(I),AMP,PHS)		399
	IF (MOD(I,IMOD).EQ.0) WRITE(6,310) ANG,MVREC(I),PHS		400
307	MVREC(I)=1.0+MVREC(I)/40.		401
308	FORMAT(/" REC"G PATTERN, EL CUT, EL COMP (DB): "/)		402
309	FORMAT(/" REC"G PATTERN, AZ CUT,EL COMP (DB): "/)		403
310	FORMAT(F9.1,5X,F8.3,3X,F6.1)		404
	IF (.NOT.GRAFRV) GO TO 325		405
	CALL CNPLTH(MVREC,NXX,KMAX,0.,0.)		406
	IF (J.EQ.1) CALL SYMBOL(.5,6.5,.140,43HFIGURE	RECVG POWER PA	407
	\$TTERN-ELEV PLANE,0.,43)		408
	IF (J.EQ.2) CALL SYMBOL(.5,6.5,.140,41HFIGURE	RECVG POWER PA	409
	\$TTERN-AZ PLANE,0.,41)		410
	CALL PLOT(8.5,0.,-3)		411
325	CONTINUE		412
320	CONTINUE		413
350	CONTINUE		414
C	COMPUTE BORESIGHT ERROR		415
275	CONTINUE		416
	CALL RECBS(SUMX,SUMY,DELX,DELY,DAZX,DAZY,NX,NY,		417
	\$ LMAX,NS,IOPT,VR,DMRAD,ROTATE,TRANSL,FREQ,KXMAX,KYMAX,		418

\$	TABLE, SINOS, KA, AZT, ELT, RSQMAX, VMAX, SMAX, SUPPRS)	419
	IF (ITHE.EQ.1) GO TO 300	420
	SLPAZ=(AZT-AZL)*DPMR/(THETAL-THL)	421
	SLPEL=(ELT-ELL)*DPMR/(THETAL-THL)	422
300	AZL=AZT	423
	ELL=ELT	424
	THL=THETAL	425
	GAINM=SMAX/VAIRM	426
	IF (GAINM.LT.1E-2) GAINM=1E-2	427
	GAINM=20.*ALOG10(GAINM)	428
	WRITE(6,11) PHIP, THETAL, ELT, AZT, SLPEL, SLPAZ, GAINM	429
	WRITE(7,11) PHIP, THETAL, ELT, AZT, SLPEL, SLPAZ, GAINM	430
	11 FORMAT(1X, F5.1, F6.1, F8.2, F8.2, F9.4, F10.4, F7.1)	431
C	GRAF3D OPTION HAS BEEN REMOVED.	432
100	CONTINUE	433
	WRITE(6,105) VAIRM	434
105	FORMAT(// " RECEIVED SUM VOLTAGE WITHOUT RADOME=" , E12.5 //)	435
	IF (GRAF3D.OR.GRAFSA.OR.GRAFTR.OR.GRAFRV) CALL PLOT(0.,0.,999)	436
	STOP	437
	END	438

```
C      BLOCK DATA
C      COMMON/TRANSC/DIN(6),ER(6),TD(6),TZ,WALTOL,N,NN,D(6),ZB,TK
C      DATA WALTOL,TK,TZ/0.,0.,0./
C      END
```

```
1
2
3
4
5
6
7
```

## Chapter 3

### SUBROUTINE RECM

3-1. Purpose: To compute the complex voltages produced at the terminals of the three channels of a radome enclosed monopulse antenna by a plane wave of specified polarization and direction of arrival.

3-2. Usage: CALL RECM (EINC, KA, NX, NY, KXMAX, FREQ, ROTATE, TRANSL, SUMX, SUMY, DELX, DELY, DAZX, DAZY, VREC, TABLE, SUPPRS, RSQMAX)  
COMMON/RECIC/DSTH, DSPHI, NTHMIN, NPHIMIN, AREA, NPOINTS, ROS, RIS, ZBOTCM, ZTOPCM, BCM, RR

#### 3-3. Arguments

- EINC - A complex array of three elements containing  $E_x$ ,  $E_y$ ,  $E_z$  of the incident plane wave. See Subroutine INCPW.
- KA - A real array of three elements containing the direction cosines  $k_{xA}$ ,  $k_{yA}$ ,  $k_{zA}$  of the unit vector  $k_A$  which points from the antenna origin in the direction from whence the plane wave emanates.
- NX,NY - The even integer number of sample points in  $x_A$  and  $y_A$  directions used to represent the antenna aperture fields.
- KXMAX,KYMAX - Real variables which represent the normalized folding wavenumbers corresponding to the sample distances  $\Delta x_A$ ,  $\Delta y_A$  according to  $\Delta x_A = \lambda / (2 * KXMAX)$ ,  $\Delta y_A = \lambda / (2 * KYMAX)$ , where  $\lambda$  is the free space wavelength.

- FREQ - Frequency in gigahertz of the monochromatic plane wave.
- ROTATE,TRANSL- Real matrices of direction cosines and translation distances used to carry out coordinate transformations of points and vectors from antenna to radome coordinate systems, and vice versa. See Subroutine ORIENT.
- SUMX,SUMY - Two dimensional (NX X NY) complex arrays of the x and y vector components of the antenna aperture fields for the sum channel of a three-channel monopulse antenna. The element at  $I=NX/2+1$ ,  $J=NY/2+1$ , corresponds to that at  $x_A=0$ ,  $y_A=0$  in the aperture. The general correspondence is given by

$$x_A = x_{\max} + (I-1) \Delta x_A = (I-MIDNX) \Delta x_A$$

$$y_A = y_{\max} + (J-1) \Delta y_A = (J-MIDNY) \Delta y_A$$

where  $x_{\max} = \Delta x_A * NX/2$  and  $y_{\max} = \Delta y_A * NY/2$ .

Also see Subroutine TRECNF.

- DELX,DELY - Antenna aperture fields for the difference elevation channel.
- DAZX,DAZY - Antenna aperture fields for the difference azimuth channel.
- VREC - Complex array of three elements which on output contains the complex terminal voltage of the antenna

for the sum, elevation difference, and azimuth difference channels, respectively.

- TABLE - Logical variable required by Subroutine RXMIT: if TRUE, a look-up table is used to calculate the transmission coefficients of the radome wall; if FALSE, these coefficients are calculated exactly for each angle of incidence specified.
- SUPPRS - Logical variable used to control the printing of results from Subroutine RXMIT: if FALSE, a table of power transmission and reflection coefficients for equal increments in the sine of the incidence angle is printed. The phases of the complex voltage transmission and reflection coefficients of the radome wall are also printed.
- RSQMAX - Real variable denoting the maximum radius of the antenna aperture such that any point  $(x_A^2 + y_A^2) > RSQMAX$  is omitted from the summation procedure used to compute the received voltages VREC.
- DSTH, DSPHI - Real input variables which specify the sample distance in the  $\theta$  and  $\phi$  directions on the radome surface; e.g.,  $\lambda/3$ .
- NTHMIN, NPHIMIN - Integer input variables which specify the minimum acceptable number of samples  $N_\theta, N_\phi$  in the two directions; e.g.,  $N_{\phi MIN} = 4$ .
- AREA - Real output variable equal to the surface area of the radome included in the surface integration.



- NPOINTS - Integer output variable equal to the number of sample points on the radome surface.
- ROS,RIS - Real input variables equal to the generating radii of the inside and outside surfaces of the tangent ogive radome shape (Figure 3-1).
- ZBOTCM, ZTOPCM - Real input variables which specify the  $Z_R$  coordinates of the bulkhead and opaque tip (if any), respectively (Figure 3-1).
- BCM,RR - Real input variables defined in Figure 3-1.

#### 3-4. Comments and Method

a. Subroutines Required: APINT, VECTOR, POINT, RXMIT, CAXB, OGIVEN, CAXCB.

b. Method: The voltage  $V_R$  induced at the terminals of a linear antenna by a "received" electromagnetic plane wave  $\underline{E}_R, \underline{H}_R$  is given by the Lorentz reciprocity theorem as [1]

$$V_R(\hat{k}_A) = C \oint_S (\underline{E}_T \times \underline{H}_R - \underline{E}_R \times \underline{H}_T) \cdot \hat{n} da \quad (1)$$

where  $\hat{k}_A$  is the unit vector which points in the direction from whence the plane wave emanates and where  $\underline{E}_T, \underline{H}_T$  are the electromagnetic fields of the antenna as produced on the closed surface  $S$  which surrounds the antenna when it is transmitting. The unit vector  $\hat{n}$  is the normal to  $S$  pointing into the region not containing any sources, and  $C$  is a complex constant.

When the inside surface of the radome is chosen as (closed) surface of integration, the source-free volume is that inside the radome, excluding the space occupied by the antenna; hence,  $\hat{n}$  is equal to the unit inward

normal  $\hat{n}_{is}$  to the inside radome surface. The surface can be divided into elemental areas  $\Delta A_{lm}$ , and the received voltage can be approximated by

$$V_R(\hat{k}_A) = C \sum_l \sum_m (\underline{E}_T \times \underline{H}_R - \underline{E}_R \times \underline{H}_T) \cdot \hat{n}_{is} \Delta A_{lm} \quad (2)$$

where the fields are evaluated at the same points  $P'_{lm}$  on the radome surface. The elemental areas  $\Delta A_{lm}$  differ, in general, from point to point, and must be included under the summation.

It is assumed that the fields  $\underline{E}_T, \underline{H}_T$  on  $S$  with the radome in place are the same as those that would exist in the absence of the radome. They are computed at points  $P'$  from their specified aperture values  $\underline{E}_{ap}, \underline{H}_{ap}$  via the Huygens-Fresnel principle as explained in Chapters 5 and 6. The received fields  $\underline{E}_R, \underline{H}_R$  at  $P'$  are computed by applying the flat panel normal transmission coefficients  $T_{n\perp}, T_{n\parallel}$  to the incident plane wave  $\underline{E}_i, \underline{H}_i = \underline{E}_i \times \hat{k}_A / \eta$  at the point  $P$  on the outside surface of the radome that is co-linear with the inside point  $P'$  with respect to the unit normal  $\hat{n}_{is}$ . (See Figure 1-2).

The tangent ogive radome surface is divided into elemental (trapezoidal) areas by sections made in the longitudinal ( $\theta$ ) and circumferential ( $\phi$ ) directions. In both cases, desired sampling intervals  $\Delta S_\theta, \Delta S_\phi$  (e.g.,  $\lambda/3$ ) are specified as input data. For the  $\theta$  direction of Figure 3-1, the number of samples  $N_\theta$  is given by

$$N_\theta = \text{MAX} \left\{ \frac{R(\theta_{TOP} - \theta_{BOT})}{\Delta S_\theta}, N_{\theta MIN} \right\} \quad (3)$$

where  $R$  is the generating radius of the ogive surface

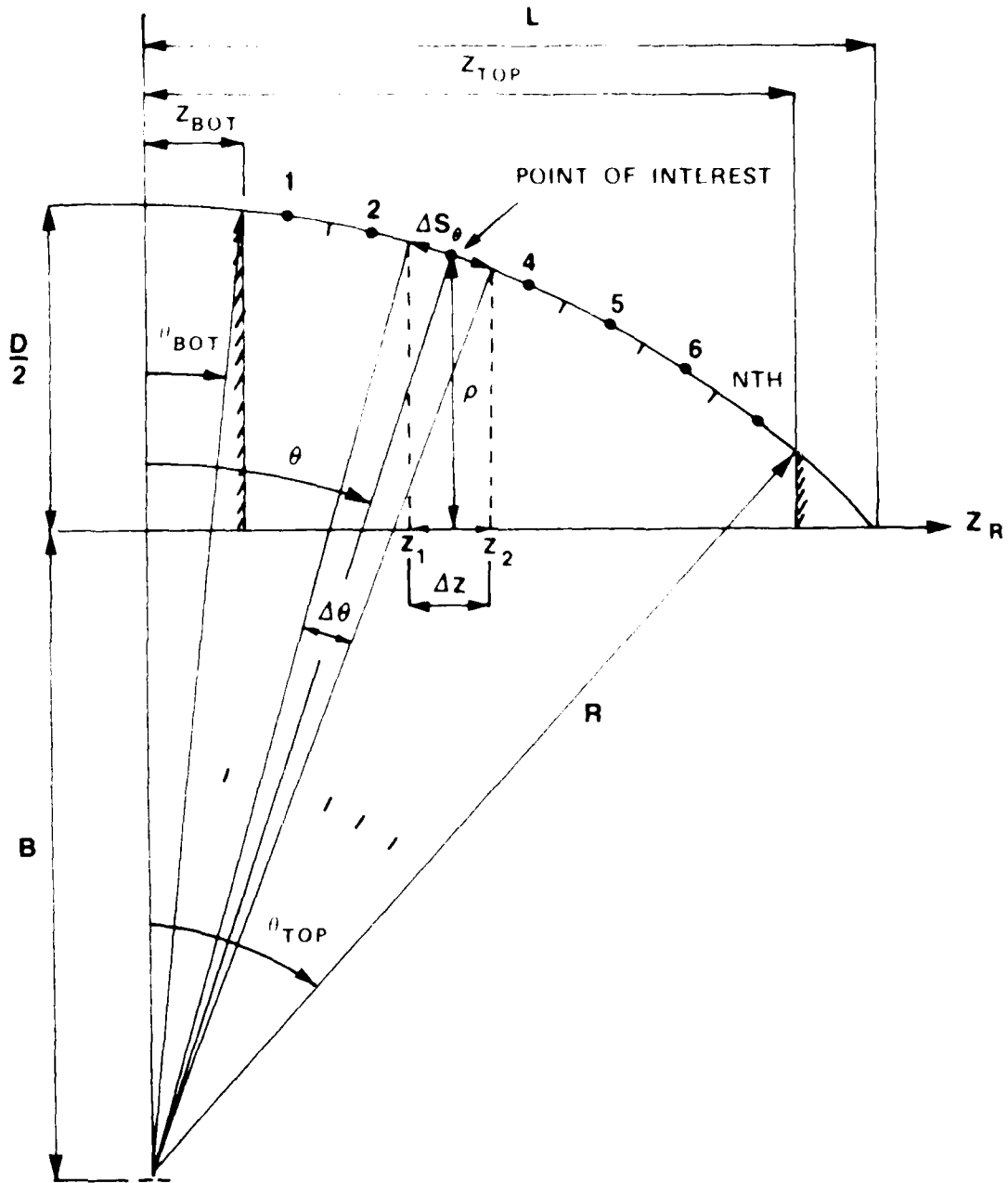


FIGURE 3-1. RADOME GEOMETRY FOR DEFINING ELEMENTAL SURFACE AREA IN  $\theta$  DIRECTION.

$$R = L / \sin(\pi - 2 \tan^{-1}(2L/D)) \quad (4)$$

and where the other variables are defined in Figure 3-1. (A minimum acceptable number of samples  $N_{\theta \text{MIN}}$  is also specified). The angular limits are given by

$$\theta_{\text{BOT}} = \sin^{-1} (Z_{\text{BOT}}/R) \quad (5)$$

$$\theta_{\text{TOP}} = \sin^{-1} (Z_{\text{TOP}}/R) \quad (6)$$

Since  $N_{\theta}$  is an integer, the sample interval  $\Delta S_{\theta}$  must be recomputed as

$$\Delta S_{\theta}' = R(\theta_{\text{TOP}} - \theta_{\text{BOT}})/N_{\theta} = R\Delta\theta \quad (7)$$

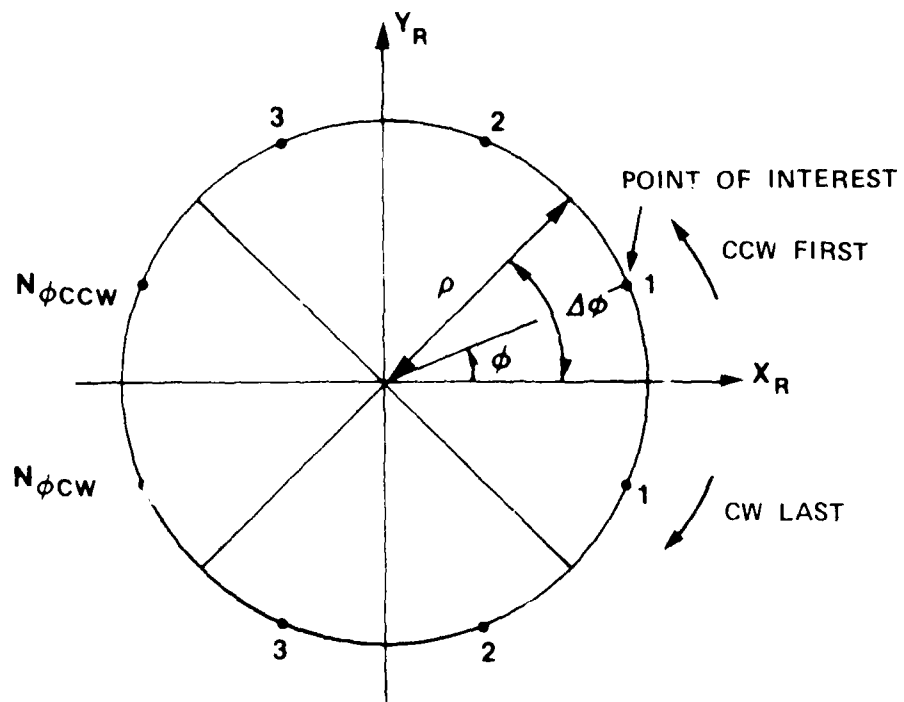
For iteration in  $I$ , a sample point at the center of an elemental area on the radome surface is specified by

$$\theta = \theta_{\text{BOT}} + \Delta\theta/2 + (I-1)*\Delta\theta, \quad (8)$$

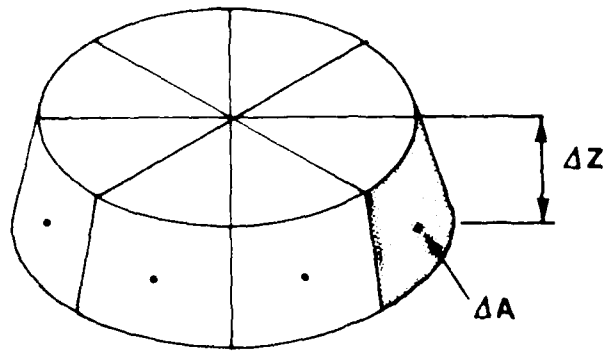
and the corresponding  $Z_R$  coordinate is given by

$$Z_R = R \sin \theta \quad (9)$$

The elemental areas are formed in the circumferential ( $\phi$ ) direction as indicated in Figure 3-2. Using  $\Delta S_{\phi}$  as input data, the number of samples  $N_{\phi}$  in the  $\phi$  direction is given by



(a) DEFINITIONS IN  $\phi$ -DIRECTION



(b) TYPICAL ELEMENTAL VOLUME

FIGURE 3-2 DEFINITION OF ELEMENTAL SURFACE AREA IN  $\phi$  DIRECTION.

$$N_{\phi} = \text{MAX} \left\{ \frac{2\pi\rho}{\Delta S_{\phi}}, N_{\phi\text{MIN}} \right\} \quad (10)$$

where  $\rho$  is defined in Figure 3-1 and is given by

$$\rho = \sqrt{R^2 - Z_R^2} - B \quad (11)$$

Since  $N_{\phi}$  is an integer, the sampling distance in  $\phi$  must be recomputed as

$$\Delta S'_{\phi} = 2\pi\rho/N_{\phi} \quad (12)$$

The sample point at the center of an elemental area is specified in  $\phi$  by  
(for iteration J)

$$\phi = \phi_0 + (J-1)\Delta\phi \quad (13)$$

where  $\Delta\phi = 2\pi/N_{\phi}$  and where  $\phi_0$  is a specified initial point in  $\phi$ . The area  $\Delta A$  of a surface element specified by  $(\theta, \phi)$  is given by

$$\Delta A = R(\Delta Z - B\Delta\theta) \quad (14)$$

where

$$\Delta Z = Z_2 - Z_1 = R \left[ \sin\left(\theta + \frac{\Delta\theta}{2}\right) - \sin\left(\theta - \frac{\Delta\theta}{2}\right) \right] \quad (15)$$

It is deemed advantageous to set  $\phi_0$  above in Equation (13) to some midpoint of the illuminated surface of the radome. This is done by transforming the unit vector  $\hat{k}_A$  to radome coordinates; i.e.,

$$\hat{k}_A = x_A \hat{k}_{xA} + y_A \hat{k}_{yA} + z_A \hat{k}_{zA} = x_R \hat{k}_{xR} + y_R \hat{k}_{yR} + z_R \hat{k}_{zR} \quad (16)$$

The angle  $\phi_0$  follows as

$$\phi_0 = \cos^{-1} \left( \frac{k_{xR}}{\sqrt{k_{xR}^2 + k_{yR}^2}} \right) \quad (17)$$

The computations in  $\phi$  proceed first in the counterclockwise (CCW) direction and then in the clockwise (CW) direction as indicated in Figure 3-2(a). For the CCW direction, the coordinates of the sample point are given by ( $J=1, N_\phi/2+1$ )

$$x_R = \rho \cos (\phi_0 + (J-1)\Delta\phi) \quad (18)$$

$$y_R = \rho \sin (\phi_0 + (J-1)\Delta\phi) \quad (19)$$

For the CW direction, there results

$$x_R = \rho \cos (\phi_0 - J\Delta\phi) \quad (20)$$

$$y_R = \rho \sin (\phi_0 - J\Delta\phi) \quad (21)$$

where  $J$  is incremented from unity to  $N_\phi/2$ . (The  $z_R$  coordinate is given by Equation (9).)

For each elemental area specified, two tests may be performed to determine if the contribution of the fields on that surface element should be included in the received voltage. The first test consists of ensuring that the sample point  $(x_R, y_R, z_R)$  lies forward of the aperture plane of the antenna; i.e., that  $z_A \geq 0$ . The second test (which may be disabled as deemed appropriate) determines if the surface element is directly illuminated by the incident plane wave. The test is performed by computing the angle of incidence  $\theta$  according to

$$\cos \theta = n_{is} \cdot \hat{k}_A \quad (22)$$

If  $\cos \theta < 0$ , the point is illuminated and should certainly be included in the summation indicated in Equation (2); if  $\cos \theta \geq 0$ , the point lies in the shadow region, and, under certain circumstances, may be omitted from the computation to save time. The effect of this omission is not completely understood in all cases.

3-5. Program Flow (Refer to Program Listing below)

<u>Line Number(s)</u>	<u>Comments</u>
1-39	Declare variables, initialize constants.
40-52	Initialize Subroutines DIPOLES and APINT; compute and write fields $\underline{E}_T, \underline{H}_T$ at point $(0, 0, 2D^2/\lambda)$ for reference.
53-55	Initialize Subroutine RXMIT.
56-67	Compute $\theta_{TOP}, \theta_{BOT}, N_{\theta}, AS'_{\theta}, \Delta\theta$ .
68-76	Compute $\phi_0$ and initialize summation of $V_{REC}$ .
77-85	Iterate in $\theta$ on radome surface.



86-90 Compute  $Z_{ROS}$ ,  $Z_{RIS}$ ,  $r_{OS}$ ,  $r_{IS}$  and ensure that surface element does not lie forward of metal tip or aft of bulkhead.

91-97 Compute  $N_{\uparrow}$  and  $\Delta S'_{\phi}$ .

98-104 Compute  $N_{\uparrow CCW}$ ,  $N_{\uparrow CW}$ , and  $\Delta\phi$ .

105-106 Compute  $\Delta Z$  and  $\Delta A$ .

107-119 Iterate in 4: CCW first, CW second.

120-125 Compute inside coordinates  $x_{RIS}$ ,  $y_{RIS}$ .

126-135 Compute unit inward normal  $\hat{n}_{IS}$  and apply illumination test (disabled).

136-141 Convert coordinates of sample point on surface to antenna coordinates to ensure  $z_A \geq 0$ .

142-152 Compute phase of incident plane wave at outside point  $(x_{ROS}, y_{ROS}, z_{ROS})$  with respect to the antenna origin. Adjust phase of the specified incident plane wave and store temporarily as  $\underline{H}_{RP}$ .

153-156 Compute antenna coordinates of inside point in wavelengths.

157-163 Compute transmitted plane wave  $\underline{E}'_R$ ,  $\underline{H}'_R$  at inside point.

164-171 Use aperture integration to compute the transmitted fields  $\underline{E}_{Ti}$ ,  $\underline{H}_{Ti}$  of the antenna at the inside point for each channel of the monopulse antenna.

172-176 Disabled statements pertaining to surface integration using the outside radome surface.

177-179 Form the vector cross products  $\underline{S}_1 = \underline{E}_T \times \underline{H}'_R$ ,  $\underline{S}_2 = \underline{E}'_R \times \underline{H}_T$ .

180-182      Add contribution to received voltage  $V_{Ri}$ .  
183-184      Increment AREA.  
185-186      Increment NCUS = number of points omitted.  
187-189      Increment NPOINTS.  
190-197      If SUPPRS=.FALSE., compute and write total sur-  
                 face area, received voltages, number of points  
                 used, and number of points omitted.

3-6. Test Case: None

3-7. References

1. G. K. Huddleston, H. L. Bassett, and J. M. Newton, "Parametric Investigation of Radome Analysis Methods", 1978 IEEE AP-S Symposium Digest, pp. 199-201, May 1978.

3-8. Program Listing (See following pages)

```

SUBROUTINE RECM(EINC,KA,NX,NY,KXMAX,KYMAX,FREQ,ROTATE,TRANSL,      1
$ SUMX,SUMY,DELX,DELY,DAZX,DAZY,VREC,TABLE,SUPPRS,RSQMAX)      2
C SUBR RECM COMPUTES THE RECEIVED VOLTAGE OF AN ANTENNA INSIDE A TANGENT
C OGIVE RADOME AS PRODUCED BY A PLANE WAVE INCIDENT FROM THE DIRECTION      4
C SPECIFIED BY KA. THE INSIDE SURFACE OF THE RADOME IS USED AS THE SURFACE
C OF INTEGRATION IN THE RECIPROCITY INTEGRAL, AND THE NORMAL TRANSMISSION
C COEFFICIENT IS USED TO TRANSFER THE INCIDENT PLANE WAVE FROM THE POINT
C P ON THE OUTSIDE SURFACE TO THE POINT P' ON THE INSIDE SURFACE, WHERE      8
C P AND P' ARE COLINEAR WITH THE NORMAL TO EITHER SURFACE.      9
C THE CALL TO THIS SUBR IS IDENTICAL TO THE CALL TO SUBR RECM      10
C USED IN THE RAY TRACING FORMULATION HOWEVER, ADDITIONAL VARIABLES      11
C ARE NEEDED BY THIS SUBR AND ARE PASSED FROM MAIN PROGRAM VIA LABEL      12
C COMMON/RECIC/ AS SHOWN BELOW.      13
  COMPLEX ET(3),HT(3),ERP(3),HRP(3)      14
  COMPLEX S1(3),S2(3),U,C,EINC(3),VREC(3)      15
  COMPLEX SUMX(NX,NY),SUMY(NX,NY),DELX(NX,NY),DELY(NX,NY),
$ DAZX(NX,NY),DAZY(NX,NY)      17
  REAL KXMAX,KYMAX,ROTATE(3,3),TRANSL(3),LAMBDA,NISA(3)      18
  REAL PIR(3),NIS(3),KR(3),KA(3),PT(3),PISR(3),PO(3),PTWL(3)      19
  LOGICAL TABLE,ATOR,RTOA,SUPPRS,INIT      20
  COMMON/RECIC/DSTH,DSPHI,NTHMIN,NPHIMIN,AREA,NPOINTS,ROS,RIS,      21
$ZBOTCM,ZTOPCM,BCM,RR      22
  NAMELIST/ATDR/DSTH,BETA,DKX,DKY,DKXY,THTOP,THBOT,STH,NTH      23
  DATA ATOR/.TRUE./,RTOA/.FALSE./      24
  DATA PI/3.14159265/      25
  DATA ZERO/1E-6/      26
  DATA TUPI/6.28318530/      27
  DATA ETA/376.9911185/,NDO/0/      28
  DATA NISA/0.,0.,-1./,PT/0.,0.,0./      29
  AREA=0.      30
  B=BCM      31
  NPOINTS=0      32
  NCUS=0      33
  DKX=2.*KXMAX/NX      34
  DKY=2.*KYMAX/NY      35
  NXMID=NX/2+1      36
  NYMID=NY/2+1      37
  DXWL=.5/KXMAX      38

```

	DYWL=.5/KYMAX	39
	IF (NDO.CT.0) GO TO 4	40
C	INITIALIZE CONSTANTS IN SUBR DIPOLES:	41
	LAMBDA=29.97925/FREQ	42
	BETA=2.*PI/LAMBDA	43
	INIT=.TRUE.	44
	PTWL(1)=0.	45
	PTWL(2)=0.	46
	PTWL(3)=2.*4.*RSQMAX/LAMBDA	47
	CALL APINT(PTWL,SUMX,SUMY,NX,NY,NXMID,NYMID,DXWL,DYWL,ET,HT,INIT)	48
	WRITE(6,3) PTWL(3),ET,HT	49
3	FORMAT(" SUBR DIPOLES INITIALIZED BY SUBR RECI"/	50
	\$" AT Z=2*D**2/WL= ",E12.5," ET= ",6E12.5/	51
	\$30X," HT= ",6E12.5/)	52
	RTD=180./PI	53
	CALL RXMIT(HRP,ERP,KA,NISA,PT,TABLE,SUPPRS,BETA)	54
4	CONTINUE	55
	DKXY=DKX*DKY	56
	THTOP=ASIN(ZTOPCM/RIS)	57
	THBOT=ASIN(ZBOTCM/RIS)	58
	STH=RIS*(THTOP-THBOT)	59
	NTHP=STH/DSTH	60
	IF(NTHP.GE.NTHMIN) GO TO 10	61
	NTH=NTHMIN	62
	GO TO 15	63
10	NTH=NTHP	64
15	DSTHP=STH/NTH	65
	DTH=(THTOP-THBOT)/NTH	66
	IF (.NOT.SUPPRS) WRITE(6,ATDR)	67
C	DETERMINE ANGLE PHIO OF CENTER OF ILLUMINATED AREA ON RADOME:	68
	CALL VECTOR(KA,KR,ATOR,ROTATE)	69
	RAD=KR(1)**2+KR(2)**2	70
	IF (RAD.GT.ZERO) GO TO 16	71
	PHIO=0.	72
	GO TO 31	73
16	PHIO=ACOS(KR(1)/SQRT(RAD))	74
31	DO 32 I=1,3	75
32	VREC(I)=(0.,0.)	76

C	SELECT CIRCLE ON SURFACE OF RADOME AT CONSTANT THETA	77
C	AND ITERATE IN I	78
	TH=THBOT-DTH/2.	79
	IF ((NDO.EQ.0).AND.(.NOT.SUPPRS)) WRITE(6,33)	80
33	FORMAT(3X,"THDEG",4X,"PHIDEG",12X,"PT",23X,"NIR"/)	81
	DO 20 I=1,NTH	82
	TH=TH+DTH	83
	THD=TH*RTD	84
	SINTH=SIN(TH)	85
	PIR(3)=ROS*SINTH	86
	RHOOS=SQRT(ROS**2-PIR(3)**2)-B	87
	PISR(3)=RIS*SINTH	88
	IF ((PISR(3).GT.ZTOPCM).OR.(PISR(3).LT.ZBOTCM)) GO TO 20	89
	RHOIS=SQRT(RIS**2-PISR(3)**2)-B	90
	NPHIP=TUPI*RHOIS/DSPHI	91
	IF(NPHIP.GE.NPHIMIN) GO TO 40	92
	NPHI=NPHIMIN	93
	GO TO 50	94
40	NPHI=NPHIP	95
C	DIVIDE THE INNER SURFACE INTO NPHI EQUAL PARTS	96
50	DSPHIP=TUPI*RHOIS/NPHI	97
	NPHI2=NPHI/2	98
	NPHICW=NPHI2	99
	NPHICCW=NPHI2	100
	IF(2.*NPHICCW.LT.NPHI) GO TO 55	101
	GO TO 60	102
55	NPHICCW=NPHICW+1	103
60	DPHI=TUPI/NPHI	104
	DZ=RIS*(SIN(TH+DTH/2.)-SIN(TH-DTH/2.))	105
	DA=RIS*(DZ-B*DTH)*DPHI	106
110	DO 61 J1=1,2	107
	JMAX=NPHICCW	108
	IF(J1.EQ.2) JMAX=NPHICW	109
C	SELECT A POINT ON INNER SURFACE OF RADOME AT CONSTANT PHI	110
C	AND ITERATE IN J, FIRST CCW, THEN CLOCKWISE.	111
	PHI=PHIO-DPHI	112
	IF (J1.EQ.2) PHI=PHIO	113
120	DO 62 J=1,JMAX	114

IF (J1.EQ.2) GO TO 41	115
PHI=PHI+DPHI	116
GO TO 42	117
41 PHI=PHI-DPHI	118
42 CONTINUE	119
PHID=PHI*RTD	120
CPHI=COS(PHI)	121
SPHI=SIN(PHI)	122
PISR(1)=RHOIS*CPHI	123
PISR(2)=RHOIS*SPHI	124
C THE POINT OF INTEREST ON INSIDE SURFACE HAS RADOME COORD PISR(XR,YR,ZR).	
C CALL OGIVEN TO FIND INNER UNIT NORMAL NIS TO RADOME SURFACE	126
CALL OGIVEN(PISR,NIS)	127
IF ((NDO.EQ.0).AND.(.NOT.SUPPRS)) WRITE(6,56) THD,PHID,PISR,NIS	128
56 FORMAT(2(2X,F7.2),6E10.3)	129
C TEST NOW IF THIS POINT IS ILLUMINATED BY PLANE WAVE	130
C CUS=NIS(1)*KR(1)+NIS(2)*KR(2)+NIS(3)*KR(3)	131
C IF CUS IS GREATER THAN ZERO, AREA IS NOT ILLUMINATED	132
C IF(CUS.GT.0.) GO TO 59	133
C IF(CUS.LT.0.) GO TO 65	134
C GO TO 59	135
C CONVERT INSIDE POINT PISR(XR,YR,ZR) TO ANTENNA COORD PT(XA,YA,ZA):	136
65 CALL POINT(PISR,PT,RTOA,ROTATE,TRANSL)	137
C TEST TO INSURE THAT POINT XR,YR,ZR IS ILLUMINATED	138
C BY THE ANTENNA INSIDE THE RADOME	139
C IF ZA>0.,POINT IS ILLUMINATED	140
IF (PT(3).LT.0.) GO TO 59	141
C COMPUTE PHASE OF INCIDENT PLANE WAVE AT OUTSIDE POINT:	142
PIR(1)=RHOOS*CPHI	143
PIR(2)=RHOOS*SPHI	144
CALL POINT(PIR,PO,RTOA,ROTATE,TRANSL)	145
PHS=AMOD(BETA*(KA(1)*PO(1)+KA(2)*PO(2)+KA(3)*PO(3)),TUPI)	146
U=CMPLX(0.,PHS)	147
C=CEXP(U)	148
C ADJUST PHASE OF INCIDENT ELECTRIC FIELD AT OUTSIDE POINT AND STORE AS HRP:	
HRP(1)=EINC(1)*C	150
HRP(2)=EINC(2)*C	151
HRP(3)=EINC(3)*C	152

C	COMPUTE ANTENNA FIELDS AT INSIDE POINT PISR:	153
	PTWL(1)=PT(1)/LAMBDA	154
	PTWL(2)=PT(2)/LAMBDA	155
	PTWL(3)=PT(3)/LAMBDA	156
C	TRANSMIT INCIDENT PLANE WAVE THRU WALL USING NORMAL XMN COEFS:	157
	CALL VECTOR(NIS,NISA,RTOA,ROTATE)	158
	IF ((NDO.EQ.0).AND.(.NOT.SUPPRS)) WRITE(6,57) THD,PHID,PT,NISA	159
57	FORMAT(2(2X,F7.2),6E10.3/)	160
	CALL RXMIT(HRP,ERP,KA,NISA,PT,TABLE,SUPPRS,BETA)	161
C	COMPUTE CORRESPONDING MAGNETIC FIELD*ETA:	162
	CALL CAXB(ERP,KA,HRP)	163
	DO 58 ICH=1,3	164
	IF (ICH.EQ.1)	165
	\$CALL APINT(PTWL,SUMX,SUMY,NX,NY,NXMID,NYMID,DXWL,DYWL,ET,HT,INIT)	166
	IF (ICH.EQ.2)	167
	\$CALL APINT(PTWL,DELX,DELY,NX,NY,NXMID,NYMID,DXWL,DYWL,ET,HT,INIT)	168
	IF (ICH.EQ.3)	169
	\$CALL APINT(PTWL,DAZY,DAZY,NX,NY,NXMID,NYMID,DXWL,DYWL,ET,HT,INIT)	170
C	SUBR APINT COMPUTES HT*ETA.	171
C	*****	172
C	THE NEXT TWO STATEMENTS ARE FOR OUTSIDE SURFACE CASE.	173
C	CALL POYNTIN(E,H,S)	174
C	CALL RXMIT(ETR,HTR,STR,NIS,PISP,TABLE,BETA,ETRP,HTRP)	175
C	*****	176
C	FORM CONTRIBUTION TO RECEIVED VOLTAGE	177
	CALL CAXCB(ET,HRP,S1)	178
	CALL CAXCB(ERP,HT,S2)	179
	VREC(ICH)=VREC(ICH)-((S1(1)-S2(1))*NIS(1)+(S1(2)-S2(2))*NIS(2)+	180
	\$ (S1(3)-S2(3))*NIS(3))*DA	181
58	CONTINUE	182
	AREA=AREA+DA	183
	GO TO 62	184
59	NCUS=NCUS+1	185
62	CONTINUE	186
	NPOINTS=NPOINTS+JMAX	187
61	CONTINUE	188
20	CONTINUE	189
	NDO=1	190

```
IF (SUPPRS) RETURN 191
PERCNT=100.*(1.-FLOAT(NCUS)/FLOAT(NPOINTS)) 192
WRITE(6,25) AREA,VREC,NPOINTS,PERCNT,NCUS 193
25 FORMAT(//" SUBR RECI: AREA=",E12.5/" VREC=",6E12.5/" NPOINTS=", 194
&I5," PERCENT=",F5.1," NCUS=",I6//) 195
RETURN 196
END 197
```



## Chapter 4

### SUBROUTINE TRECNF

- 4-1. Purpose: To compute near-field aperture distributions for four types of three-channel monopulse antennas: (1) circular aperture with tapered amplitude and uniform phase distributions; (2) flat plate antenna with a programmed amplitude distribution and uniform phase; (3) square aperture with  $\cos x$  amplitude and uniform phase; (4) single element. Four polarizations can be selected for the circular and square apertures. The flat plate antenna is vertically ( $\hat{y}_A$ ) polarized only.
- 4-2. Usage: CALL TRECNF (E, NX, NY, ICHAN, IPOL, IXY, DAPWL, DXWL, KXMAX, ICASE, SQUARE)
- 4-3. Arguments
- |       |  |
|-------|--|
| E     | - Complex array of NX by NY elements which, on output, contains the values of the specified (IXY) rectangular component ( $x_A$ or $y_A$ ) of the electric field distribution over the specified (ICASE) antenna aperture having the specified (IPOL) polarization for the specified (ICHAN) channel of a three-channel monopulse antenna. |
| NX,NY | - Even integer number of points in a rectangular array at which the aperture distribution is computed in the $x_A$ and $y_A$ directions, respectively. The point $I=NX/2 + 1$ , $J=NY/2 + 1$ corresponds to $x_A=0$ , $y_A=0$ . For the single element case, $NX=NY=2$ .   |

- ICHAN - Integer control variable with values 1, 2, or 3 which selects the sum, elevation difference, or azimuth difference channel, respectively.
- IPOL - Integer control variable which selects the antenna polarization as follows:
- 1 - Vertical ( $y_A$ ) polarization
  - 2 - Horizontal ( $x_A$ ) "
  - 3 - Right-hand circular "
  - 4 - Left-hand circular "
- IXY - Integer control variable having values 1 or 2 to select the  $x_A$  or  $y_A$  component of aperture electric field.
- DAPWL - Diameter, in wavelengths, of the antenna aperture.
- DXWL - Spacing, in wavelengths, between samples in aperture in  $x_A$  and  $y_A$  directions (output).
- KXMAX - Maximum value of normalized wavenumber corresponding to  $KXMAX = 1./(2.*DXWL)$  (output).
- ICASE - Integer control variable having values 1 or 2 to specify a circular aperture antenna with uniform amplitude and phase. If ICASE=3, a flat plate antenna having a programmed amplitude distribution (see Table 4-2) with vertical polarization is selected.
- SQUARE - Logical input variable; if TRUE, square aperture is used.

#### 4-4. Comments and Method

a. The integers NX,NY must each be equal to each other and even; e.g., NX=NY=16. In addition, when ICASE=3 (flat plate antenna), NX and NY must equal 16. If NX=NY=2, the fields of a single element at  $x_A=y_A=0$  are specified. If NX=NY=32, only the central 15 x 15 elements are non-zero.

b. The actual shape of the circular aperture, as approximated by a rectangular array of sample points, is shown in Figure 4-1 for the case of NX=NY=16. Row 1 and Column 1 of the array contain null elements. The elements inside and on the boundary of the aperture may contain non-zero values as shown in Table 4-1 for the various cases when ICHAN=1 (sum channel). Note that specification of  $D_{AP}$  in Figure 4-1 determines the sample spacings according to

$$\Delta x_A = \Delta y_A = \frac{D_{AP} \cos \alpha}{(N_x - 2)} = \frac{D_{AP} \cos \alpha}{(N_y - 2)} \quad (1)$$

where  $\alpha = \tan^{-1}(2/7)$ .

The aperture distributions for three monopulse channels are formed by phasing the elements in the four quadrants of the aperture appropriately. The sum channel distribution is formed by assigning equal phases to all elements. The azimuth difference channel is formed by multiplying all elements in Quadrants II and III of the sum distribution by minus one and by zeroing all elements along  $x_A=0$ . For the elevation difference channel, Quadrants III and IV are negated, and all elements along the line  $y_A=0$  are made zero for symmetry reasons.

The phasing chosen models a tracking antenna and provides outputs in two orthogonal channels from which the direction of arrival of a target return can be mathematically determined. Let  $k$  be a unit vector which

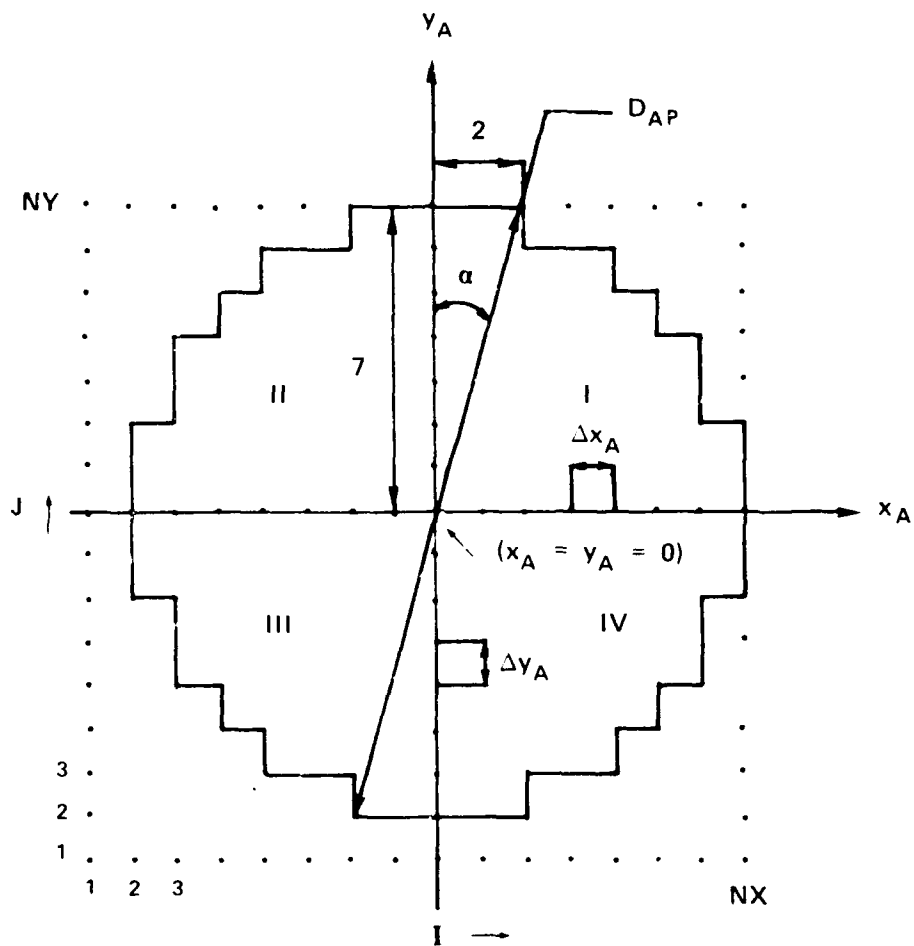


FIGURE 1-1. APPROXIMATION OF CIRCULAR APERTURE BY RECTANGULAR GRID OF SAMPLE POINTS.

points from the antenna origin toward the direction from whence the plane wave (target return) emanates; i.e.,

$$\hat{k} = \hat{x}_A k_x + \hat{y}_A k_y + \hat{z}_A k_z \quad (2)$$

Define the tracking functions for this plane wave as

$$f_i(k_x, k_y) = \frac{\Delta_i(k_x, k_y)}{\Sigma(k_x, k_y)} \quad (3)$$

where  $\Delta_i$  represents the output of the elevation ( $\epsilon$ ) or azimuth ( $\alpha$ ) difference channel and  $\Sigma$  represents the sum channel output. Then for small  $k_x > 0$ , the phase of  $f_\alpha$  is  $+\pi/2$ ; for small  $k_x < 0$ , the phase of  $f_\alpha$  is  $-\pi/2$ . Similarly, for small  $k_y > 0$ ,  $\arg(f_\epsilon) = \pi/2$ ; for small  $k_y < 0$ ,  $\arg(f_\epsilon) = -\pi/2$ . Hence, the change in phase by  $\pi$  in either channel represents the boresight direction of the antenna, and tracking is done using the imaginary parts of the tracking functions rather than their real parts.

c. The shape and sampling grid used to model the flat plate antenna are shown in Figure 4-2. In Subroutine TRECNF, the integers NX and NY must both equal 16, and only linear polarization ( $\hat{y}_A$ ) is applicable to the flat plate antenna (ICASE=3). The phasing of the four quadrants is done as described above to model the three monopulse channels so that tracking can be simulated. Note that specification of  $D_{Ap}$  determines the sample spacing according to

$$\Delta x_A = \Delta y_A = \frac{D_{Ap} \cos \alpha}{N \left( \frac{x}{2} - 2 \right)} \quad (4)$$

where  $\alpha = \tan^{-1} (4/6)$ .

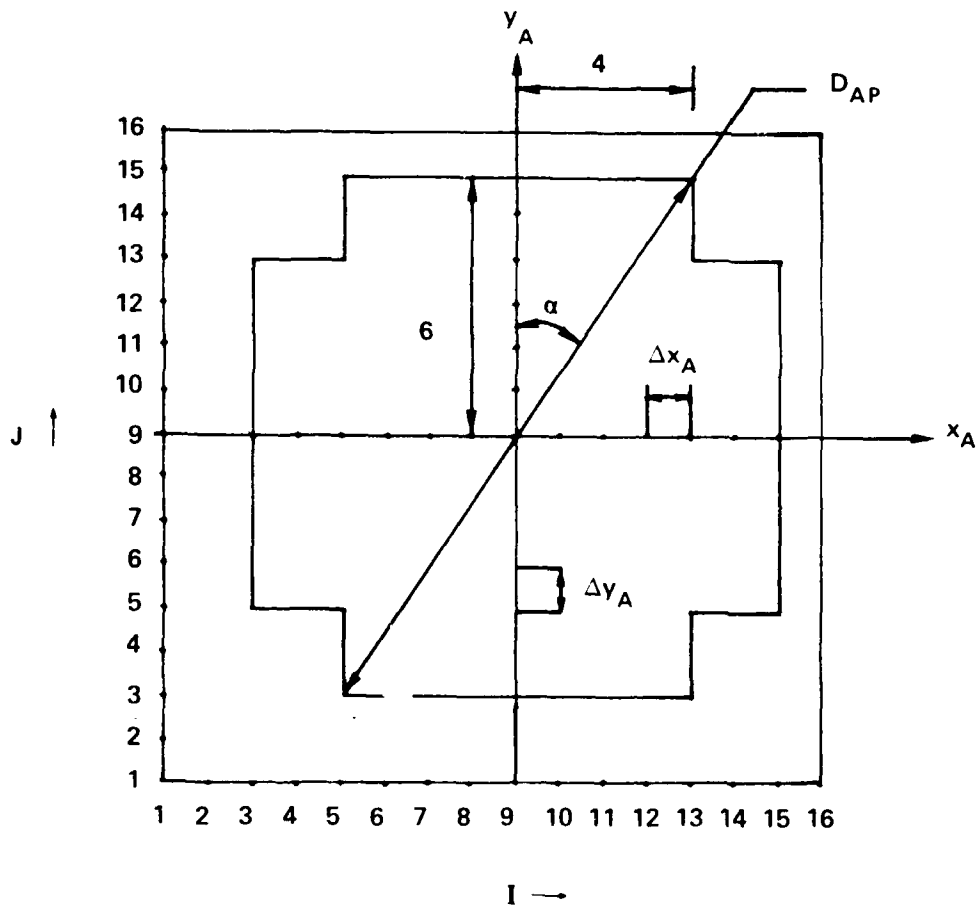


FIGURE 4-2. GEOMETRY OF FLAT PLATE ANTENNA.

Table 4-1. Values of Non-Zero Elements in Circular Aperture  
(ICHAN=1, ICASE=1 or 2)

<u>IPOL</u>	<u>IXY</u>	<u>Value</u>	<u>Polarization Type</u>
1	1	(0 + j0)	Vertical
1	2	(1 + j0)	"
2	1	(1 + j0)	Horizontal
2	2	(0 + j0)	"
3	1	(0 + j1)	RHC
3	2	(1 + j0)	"
4	1	(0 - j1)	LHC
4	2	(1 + j0)	"

The phase of each sample point in Figure 4-2 for the sum channel is made equal, but the amplitudes are tapered in the  $x_A$  and  $y_A$  directions as shown in Table 4-2. The amplitude distribution is separable and symmetrical so that

$$E_{y_A}(x_A, y_A) = g(x_A)h(y_A) = E_{y_A}(-x_A, y_A) = E_{y_A}(x_A, -y_A) \quad (5)$$

It is noted that samples 10, 12, 14, and 16 are actually specified in the program, and samples 9, 11, 13, and 15 are obtained from them by averaging.

d. The square aperture is formed by setting to zero Row 1 and Column 1 of the array of Figure 4-1 for symmetry reasons. The values of field at the other points in the aperture are computed to yield a  $\cos x$  amplitude taper in the  $x_A$  direction and a uniform amplitude in  $y_A$ ; i.e.,

$$E(x, y) = \cos \frac{\pi x}{2 x_{\max}} \quad (5)$$

where  $x_{\max}$  corresponds to the sample at  $I=NX$ .

### 3-5. Program Flow

<u>Line Nos.</u>	<u>Comments</u>
19	Assign complex values to CFAC to use in generating vertical, horizontal, RHC, and LHC polarization according to IPOL.
20-22	Compute the angle $\alpha$ and the upper bound $R_{\max}$ of the radius of the circular aperture.
23-24	Ensure that IPOL has correct values of 1, 2, 3, or 4.



Table 4-2. Symmetrical Amplitude Distribution for Flat Plate Antenna

<u>Sample No.</u>	<u><math>\frac{x}{A}</math></u>	<u>Amplitude</u>	<u><math>\frac{y}{A}</math></u>	<u>Amplitude</u>
9	0	1.0280	0	1.0280
10	$\Delta x$	1.0280	$\Delta y$	1.0280
11	$2\Delta x$	.9120	$2\Delta y$	.9170
12	$3\Delta x$	.7959	$3\Delta y$	.8060
13	$4\Delta x$	.6077	$4\Delta y$	.6155
14	$5\Delta x$	.4194	$5\Delta y$	.4250
15	$6\Delta x$	.2097	$6\Delta y$	.2125
16	$7\Delta x$	0.0	$7\Delta y$	0.0

25 If  $NX \neq NY$  and  $SQUARE=FALSE$ , write error message and stop the program.

26-29 Compute indices of midpoint  $\pm 7$ .

30-31 Ensure that  $IXY=1$  or  $2$ .

32 If  $NX$  and  $NY$  are not even, stop the program.

33 Test value of  $ICASE$ : if  $ICASE=3$  generate fields of flat plate antenna (Lines 64-105); otherwise, generate fields of circular or square aperture (Lines 34-60).

34-56 Assign complex field value to each sample point  $(x_A, y_A, 0)$  in the circular aperture according to the values shown in Table 4-1. If  $\sqrt{x_A^2 + y_A^2} > R_{\max}$ , make the field value zero. Multiply the non-zero elements by  $CFAC(IPOL)$  to generate the correct polarization. For the square aperture, zero Column 1 and Row 1, and insert  $\cos x$  taper (Line 37).

57-60 Compute sample spacing  $\Delta x_A/\lambda$  and go to statement 60.

61-63 Error message and STOP.

64-65 Flat plate antenna-- if  $NX \neq 16$ , write error message and STOP (Lines 131-133).

66-67 Compute sample spacing  $\Delta x_A/\lambda$ .

68 Ensure  $NX=NY$

69-72 Zero all elements in the aperture. If  $IXY=1$  ( $x_A$ -component), to to statement 60.

73-80 Assign tapered amplitude values to eight "even" elements in Quadrant III.

81-89 Compute amplitude values for the "odd" elements in Quadrant III.

90-93 Compute amplitude values for elements 3-9 along  $y_A=0$  line and along  $x_A=0$  line.

94-97 Generate symmetrical amplitude values in Quadrant IV.

98-105 Generate symmetrical amplitude values in Quadrants I and II.

106 Compute  $k_{x_{max}}$  and  $d_x/\lambda$ .

107-111 Test to determine if the sum channel data generated should be phased to produce the aperture distribution for a specified difference channel (ICHAN).

112-120 Form aperture distribution for difference elevation channel by zeroing all elements along  $y_A=0$  and negating all elements for  $y_A < 0$ . RETURN.

121-129 Form aperture distribution for difference azimuth channel by zeroing all elements along  $x_A=0$  and negating all elements  $x_A < 0$ . RETURN.

130-134 Error messag for ICASE=3 and NX≠16.

END

4-6. Test Case: None.

4-7. References

1. D. R. Rhodes, Introduction to Monopulse, McGraw Hill, New York, 1959.

4-8. Program Listing: See following pages.

SUBROUTINE TRECNF(E,NX,NY,ICHAN,IPOL,IXY,DAPWL,DXWL,KXMAX,ICASE, &SQUARE)	1
C *** MODIFIED JAN 80 FOR SQUARE APERTURE AND FOR SINGLE ELEMENT***	2
C SUBR TRECNF COMPUTES ELECTRIC FIELDCOMPONENTS OVER A CIRCULAR APERTURE	3
C OF RADIUS RMAX=(NX/2-1)/COS(ATAN(2/7)) AND RETURNS SAME IN E(NX,NY).	4
C NX MUST EQUAL NY AND MUST BE EVEN.	5
C ICHAN=1 FOR SUM CHANNEL    IPOL=1 FOR VERT-Y POL.    IXY=1 FOR X-COMP.	6
C      =2 FOR ELEV DIFF          =2 FOR HORIZ-X POL      =2 FOR Y-COMP.	7
C      =3 FOR AZ DIFF          =3 FOR RHC POL	8
C      =                          =4 FOR LHC POL	9
C DAPWL=DIAMETER OF APERTURE IN WAVELENGTHS (INPUT)	10
C DXWL=SAMPLE SPACING IN APERTURE (OUTPUT)	11
C KXMAX=MAXIMUM WAVENUMBER (OUTPUT)	12
C ICASE=1 OR 2 FOR UNIFORM, CIRCULAR APERTURE (ADA M.'S CASE I AND II)	13
C      =3 FOR FLAT-PLATE ANTENNA, VERTICAL POL (CASE III).	14
COMPLEX E(NX,NY),CFAC(4)	15
REAL KXMAX	16
LOGICAL SQUARE	17
DATA CFAC/(1.,0.),(1.,0.),(0.,+1.),(0.,-1.)	18
ANG=ATAN(2./7.)	19
IF (ICASE.EQ.3) ANG=ATAN(4./6.)	20
RMAX=(NX/2-1)/COS(ANG)+.001	21
IF (IPOL.GT.4) IPOL=4	22
IF (IPOL.LT.1) IPOL=1	23
IF ((.NOT.SQUARE).AND.(NX.NE.NY)) GO TO 15	24
NXMM7=NX/2+1-7	25
NXMP7=NX/2+1+7	26
NYMM7=NY/2+1-7	27
NYMP7=NY/2+1+7	28
C FOR NX,NY=32, ONLY THE CENTRAL 15 X 15 ELEMENTS ARE NONZERO.	29
IF ((IXY.LT.1).OR.(IXY.GT.2)) IXY=2	30
IF (MOD(NX,2).NE.0) GO TO 15	31
IF (ICASE.EQ.3) GO TO 25	32
TUXMX=FLOAT(NX)	33
DO 10 I=1,NX	34
X=FLOAT(-(NX/2)+I-1)	35
COSX=COS(3.14159265*X/TUXMX)	36
DO 10 J=1,NY	37
	38

IF ((I.EQ.1).OR.(J.EQ.1)) GO TO 9	39
IF (NX.EQ.16) GO TO 1	40
IF ((I.LT.NXMM7).OR.(I.GT.NXMP7).OR.(J.LT.NYMM7).OR.(J.GT.NYMP7))	41
\$GO TO 9	42
1 IF(SQUARE) GO TO 8	43
Y=FLOAT(-(NY/2)+J-1)	44
R=SQRT(X**2+Y**2)	45
IF (R.GT.RMAX) GO TO 9	46
8 IF ((IPOL.EQ.1).AND.(IXY.EQ.1)) GO TO 9	47
IF ((IPOL.EQ.2).AND.(IXY.EQ.2)) GO TO 9	48
C IF RHC, EY=(1,0), EX=(0,1) I.E., EX LEADS EY BY 90 DEG.	49
C IF LHC, EY=(1,0), EX=(0,-1) I.E., EX LAGS EY BY 90 DEG.	50
E(I,J)=CPLX(COSX,0.)	51
IF ((IPOL.LT.3).OR.(IXY.EQ.2)) GO TO 10	52
E(I,J)=E(I,J)*CFAC(IPOL)	53
GO TO 10	54
9 E(I,J)=(0.,0.)	55
10 CONTINUE	56
IF (NX.EQ.2) GO TO 56	57
DXWL=(DAPWL/2.)*COS(ANG)/(NX/2-1)	58
IF(SQUARE) DXWL=(DAPWL/SQRT(2.))/(NX-2)	59
GO TO 60	60
15 WRITE(6,20)	61
20 FORMAT(//" NX.NE.NY OR NX NOT EVENIN SUBR TRECNF"//)	62
STOP	63
C THE FOLLOWING IS FOR ADA M.'S CASE III (ICASE=2):	64
25 IF (NX.NE.16) GO TO 90	65
DXWL=(DAPWL/2.)*COS(ANG)/(NX/2-2)	66
IF(SQUARE) DXWL=(DAPWL/SQRT(2.))/(NX-2)	67
NY=NX	68
DO 26 I=1,NX	69
DO 26 J=1,NY	70
26 E(I,J)=(0.,0.)	71
IF (IXY.EQ.1) GO TO 60	72
E(6,4)=(.2824,0.)	73
E(8,4)=(.4250,0.)	74
E(4,6)=(.2888,0.)	75
E(6,6)=(.5218,0.)	76

E(8,6)=(.8060,0.)	77
E(4,8)=(.4194,0.)	78
E(6,8)=(.7959,0.)	79
E(8,8)=(1.028,0.)	80
DO 30 J=4,8,2	81
DO 30 I=3,8,1	82
IF ((MOD(J,2).EQ.0).AND.(MOD(I,2).EQ.0)) GOTO 30	83
E(I,J)=(E(I-1,J)+E(I+1,J))/2.	84
30 CONTINUE	85
DO 35 I=3,8,1	86
DO 35 J=3,8,2	87
E(I,J)=(E(I,J-1)+E(I,J+1))/2.	88
35 CONTINUE	89
DO 40 I=3,9	90
40 E(I,J)=E(I,8)	91
DO 45 J=3,9	92
45 E(9,J)=E(8,J)	93
DO 50 J=3,9	94
DO 50 I=1,6	95
E(9+I,J)=E(9-I,J)	96
50 CONTINUE	97
DO 55 I=3,15	98
DO 55 J=1,6	99
E(I,9+J)=E(I,9-J)	100
55 CONTINUE	101
GO TO 60	102
56 DXWL=DAPWL/SQRT(2.)	103
KXMAX=.5/DXWL	104
RETURN	105
60 KXMAX=1./(2.*DXWL)	106
IF (ICHAN.EQ.1) RETURN	107
IF ((IXY.EQ.1).AND.(ICASE.EQ.3)) RETURN	108
IF ((IXY.EQ.1).AND.(IPOL.EQ.1)) RETURN	109
IF ((IXY.EQ.2).AND.(IPOL.EQ.2)) RETURN	110
IF (ICHAN.EQ.3) GO TO 75	111
C LOAD ELEVATION DIFFERENCE CHANNEL:	112
J=NY/2+1	113
DO 65 I=1,NX	114

65	E(I,J)=(0.,0.)	115
	JMAX=NY/2	116
	DO 70 J=1,JMAX	117
	DO 70 I=1,NX	118
70	E(I,J)=-E(I,J)	119
	RETURN	120
C	LOAD AZIMUTH DIFFERENCE CHANNEL:	121
75	I=NX/2+1	122
	DO 80 J=1,NY	123
80	E(I,J)=(0.,0.)	124
	IMAX=NX/2	125
	DO 85 I=1,IMAX	126
	DO 85 J=1,NY	127
85	E(I,J)=-E(I,J)	128
	RETURN	129
C	DAPWL=5.047 FOR ADA M.'S CASE III	130
90	WRITE(6,95)	131
95	FORMAT(//"****ERROR EXIT! NX NOT EQUAL TO 16 IN SUBR TRECNF****"//)	132
	STOP	133
	END	134

## Chapter 5

### SUBROUTINE APINT

- 5-1. Purpose: To compute the electromagnetic fields  $\underline{E}$ ,  $\underline{H}$  of a rectangular aperture in the  $z=0$  plane at a point  $P(x,y,z>0)$ , where the amplitude and phase of the aperture electric fields  $E_{xap}$ ,  $E_{yap}$  are specified at  $N_x$  by  $N_y$  discrete points spaced  $d_x/\lambda$  and  $d_y/\lambda$  apart. The aperture magnetic fields  $H_{xap}$ ,  $H_{yap}$  are derived from  $\underline{E}_{ap}$  via the geometrical optics approximation.
- 5-2. Usage: CALL APINT (PFWL, EX, EY, NX, NY, MIDX, MIDY,  
DXWL, DYWL, E, H, INIT)
- 5-3. Arguments
- |               |  |
|---------------|--|
| PFWL          | - Real input array of three elements which specifies the Cartesian coordinates in wavelengths of the point $P(x/\lambda, y/\lambda, z/\lambda)$ at where the fields are to be computed; i.e., $PFWL(1) = x/\lambda$ , etc. |
| EX,EY         | - Complex input arrays of $NX$ by $NY$ elements each which specify the aperture electric field.  |
| NX,NY         | - Integer input variables equal to the number of sample points in the aperture in the $x$ and $y$ directions, respectively. $NX$ and $NY$ must be even.  |
| MIDX,<br>MIDY | - Integer input variables equal to the indices in the arrays $EX$ , $EY$ corresponding to $x=y=0$ ; i.e., $MIDX = NX/2+1$ , $MIDY = NY/2+1$ .  |
| DXWL,<br>DYWL | - Real input variables equal to the sample spacings in wavelengths in the $x$ and $y$ directions, respectively.  |



- E,H - Complex output arrays of three elements each equal to the rectangular vector components of the electric and magnetic fields at P; i.e.,  $E(1)=E_x$ , etc.
- INIT - Logical input variable which controls initialization of subroutine DIFOLES.

#### 6-4. Comments and Method

The fields at P(x,y,z) due to the sampled aperture fields are computed by summing the individual fields of equivalent electric and magnetic dipoles located at each sample point as explained in Section 6-4.

#### 6-5. Program Flow

- 1-1. Declare variables, initialize constants.
- 13-14. Compute initial source point, minus  $d_x/\lambda$ . Set z-coordinate of source points to zero.
- 15-16. Initialize summations of the fields E,H.
- 17-17. Compute first source point  $P_x(x,y,0)$ .
- 18-18. Compute electric  $J_x^e, J_y^e$  and magnetic  $J_x^m, J_y^m$  currents according to  $J_x^e = z \times H_{-ay}$  and  $J_y^m = \frac{E}{-ay} \times z$ .
19. Call subroutine DIFOLES to compute the fields of the electric and magnetic dipoles  $J_x^e, J_y^e$  located at the specified source point.
- 20-21. Add contribution of each dipole to the field at P(x,y,z).
22. Repeat for all source points.

6-6. Test and/or Use Chapter 6.

6-7. Bibliography: See Chapter 6.

6-8. Program Bibliography: See Bibliography.



SUBROUTINE APINT(PFWL,EX,EY,NX,NY,MIDX,MIDY,DXWL,DYWL,E,H,INIT)	1
C SUBR APINT COMPUTES FRESNEL FIELDS OF RECTANGULAR APERTURE WITH	2
C APERTURE FIELDS GIVEN BY EX,EY( H FIELDS ARE DERIVED USING G.O. APPROX.)	
C FIELDS E,H ARE COMPUTED AT THE POINT PFWL.	4
COMPLEX E(3),H(3),EX(NX,NY),EY(NX,NY),JE(2),JM(2),ES(3),HS(3)	5
C JE,JM ARE ELECTRIC AND MAGNETIC SURFACE CURRENT DENSITIES FOUND FROM	6
C EAPXZHAT AND ZHAT X HAP.	7
LOGICAL INIT	8
REAL PSWL(3),PFWL(3)	9
DATA ETA/376.9911185/	10
C NX,NY MUST BE EVEN SO THAT OMITTING ROW 1 AND COL 1 YIELDS SYM APERTURE	
C INIT=.TRUE. TO INITIALIZE CONSTANTS IN SUBR DIPOLES	12
PSWL(1)=(1-MIDX)*DXWL	13
PSWL(3)=0.	14
DO 1 L=1,3	15
E(L)=(0.,0.)	16
H(L)=(0.,0.)	17
1 CONTINUE	18
DO 10 I=2,NX	19
PSWL(1)=PSWL(1)+DXWL	20
PSWL(2)=(1-MIDY)*DYWL	21
DO 10 J=2,NY	22
PSWL(2)=PSWL(2)+DYWL	23
JE(1)=-EX(I,J)/ETA	24
JM(1)=EY(I,J)	25
JE(2)=-EY(I,J)/ETA	26
JM(2)=-EX(I,J)	27
CALL DIPOLES(JE,JM,PSWL,PFWL,DXWL,DYWL,ES,HS,INIT)	26
DO 5 L=1,3	29
E(L)=E(L)+ES(L)	30
H(L)=H(L)+HS(L)	31
5 CONTINUE	32
10 CONTINUE	33
RETURN	34
END	35

## Chapter 6

### SUBROUTINE DIPOLES

6-1. Purpose: To compute the electromagnetic fields  $\underline{E} = \hat{x} E_x + \hat{y} E_y + \hat{z} E_z$  and  $\underline{H} = \hat{x} H_x + \hat{y} H_y + \hat{z} H_z$  at point  $P_f(x/\lambda, y/\lambda, z/\lambda)$  as produced by electric  $\underline{J}^e = \hat{z} \times \underline{H}$  and magnetic  $\underline{J}^m = \underline{E} \times \hat{z}$  surface currents flowing on the planar rectangular surface of dimensions  $\Delta x/\lambda$ ,  $\Delta y/\lambda$  located at source point  $P_s(x'/\lambda, y'/\lambda, z'/\lambda)$  and oriented in the  $z=z'$  plane. All dimensions are in wavelengths.

6-2. Usage: CALL DIPOLES (JE, JM, PSWL, PFWL, DXWL, DYWL, E, H, INIT)

#### 6-3. Arguments

- JE,            - Complex input arrays of two elements each containing the x and y components of the electric and magnetic surface current densities at the center of the planar element as found from  $\underline{E} \times \hat{z}$  and  $\hat{z} \times \underline{H}$ , respectively, where  $\hat{z}$  is the unit normal to the element and  $\underline{E}$ ,  $\underline{H}$  are the fields at the center of the element.
- JM
- PSWL,        - Real input arrays of three elements each which contain the coordinates  $P_s(x'/\lambda, y'/\lambda, z'/\lambda)$ ,  $P_f(x/\lambda, y/\lambda, z/\lambda)$  of the center of the source element and the point at which the field is to be computed, respectively.
- PFWL
- DXWL,        - Real input variables equal to the dimensions  $\Delta x/\lambda$ ,  $\Delta y/\lambda$  of the rectangular source element.
- DYWL

- E, H - Complex output arrays of three elements each containing the fields  $\underline{E}$ ,  $\eta \underline{H}$  at the point  $P_f$ . Note that  $\eta \underline{H}$  is computed rather than  $\underline{H}$  above (to save time).
- INIT - Logical input variable which controls initialization of various constants for repetitive calls to the subroutine: if TRUE, the constants are computed; if FALSE, the constants are not computed, and their last computed values are used.

#### 6-4. Comments and Method

a. Comment. The source and field points cannot be any closer together than  $r = .01\lambda$ . This restriction is necessary to prevent division by zero due to the  $r^{-1}$  variation of the dipole fields as explained below. Actually, field points should be removed to the order of  $r = \sqrt{(\Delta x/\lambda)^2 + (\Delta y/\lambda)^2}$  for validity of the discretized approximation to the physical model.

b. Method. The subroutine computation is motivated by the problem of computing the fields of a rectangular antenna aperture located in the  $z=z'$  plane as illustrated in Figure 1. Let the electric and magnetic fields  $\underline{E}_{ap}$ ,  $\underline{H}_{ap}$  be specified at discrete points  $(x_m, y_n, 0)$ . Then, at each point, the equivalent surface current densities  $\underline{J}^e$  and  $\underline{J}^m$  are given by [1]

$$\underline{J}^e = \hat{z} \times \underline{H}_{ap} = \hat{x} (-H_{yap}) + \hat{y} H_{xap} = \hat{x} J_x^e + \hat{y} J_y^e \quad (1)$$

$$\underline{J}^m = \underline{E}_{ap} \times \hat{z} = \hat{x} E_{yap} + \hat{y} (-E_{xap}) = \hat{x} J_x^m + \hat{y} J_y^m \quad (2)$$

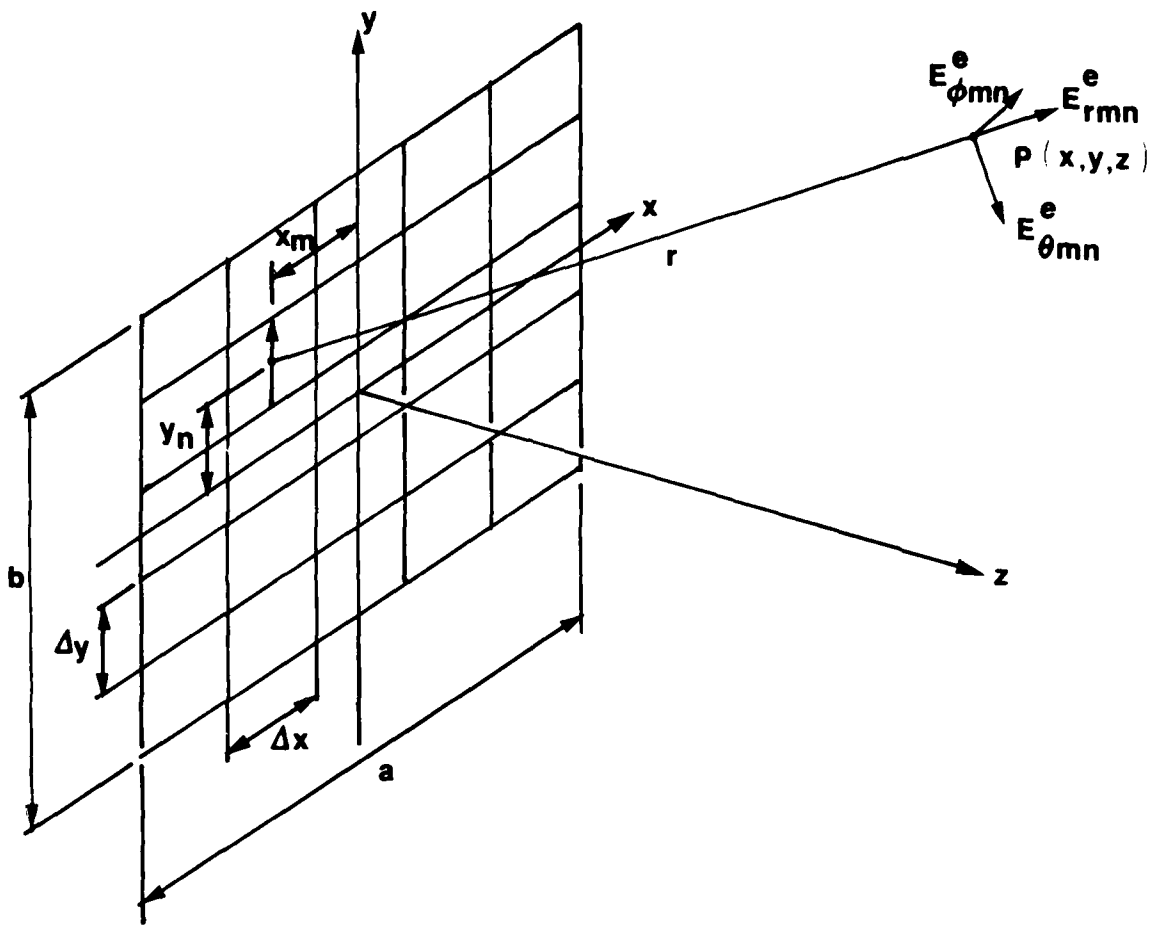


Figure 6-1. Geometry of Rectangular Aperture Antenna Approximated by Elementary Dipoles.

The surface current densities so defined can be discretized for each element  $\Delta x \Delta y$  as follows. Consider the current density  $\underline{J}_y^e$ . The total current entering the lower boundary and leaving the upper boundary of the element is  $\underline{J}_y^e \Delta x$  and can be regarded as an elementary dipole concentrated at the center of the element. The dipole moment is

$$p_o = ql = \frac{\underline{J}_y^e \Delta x}{j\omega} \Delta y \quad (3)$$

where  $q$  is the charge and  $l$  is the separation [2], and where the following relation for the sinusoidal steady state has been used:

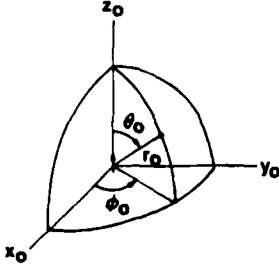
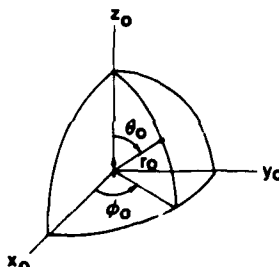
$$q = \int I dt = \frac{I}{j\omega} \quad (4)$$

Similar relations hold for the other component of  $\underline{J}^e$  and, by duality, for  $\underline{J}^m$  as will be summarized below.

The next step in the development is to obtain expressions for the dipole fields of  $\underline{J}^e$  and  $\underline{J}^m$ . To facilitate this step, first consider the fields radiated by electric and magnetic dipoles oriented along the  $z_o$  axis as shown in Table 1 [2]. Note that these expressions require  $r_o$  in wavelengths, and that  $\Delta x$  and  $\Delta y$  refer to the element size in the original aperture.

Matters are simplified if the spherical coordinate components of Table 1 are transformed to their corresponding rectangular components according to [3]

Table 6-1. Elementary Dipole Fields of Z-Directed Currents.

Electric	← Duality →	Magnetic
	$\underline{E}^e$ $\underline{H}^e$ $\epsilon$ $\mu$ $\eta$	
$E_{r_o}^e = J_{z_o}^e e_o \left[ \frac{1}{r_o^3} + \frac{j2\pi}{r_o^2} \right] \cos \theta_o e^{-j2\pi r_o}$		$H_{r_o}^m = J_{z_o}^m h_o \left[ \frac{1}{r_o^3} + \frac{j2\pi}{r_o^2} \right] \cos \theta_o e^{-j2\pi r_o}$
$E_{\theta_o}^e = J_{z_o}^e \frac{e_o}{2} \left[ \frac{1}{r_o^3} + \frac{j2\pi}{r_o^2} - \frac{(2\pi)^2}{r_o} \right] \sin \theta_o e^{-j2\pi r_o}$		$H_{\theta_o}^m = J_{z_o}^m \frac{h_o}{2} \left[ \frac{1}{r_o^3} + \frac{j2\pi}{r_o^2} - \frac{(2\pi)^2}{r_o} \right] \sin \theta_o e^{-j2\pi r_o}$
$H_{\phi_o}^e = J_{z_o}^e e_o \frac{j\pi}{r_o} \left[ \frac{1}{r_o^2} + \frac{j2\pi}{r_o} \right] \sin \theta_o e^{-j2\pi r_o}$		$E_{\phi_o}^m = -J_{z_o}^m h_o j\pi \left[ \frac{1}{r_o^2} + \frac{j2\pi}{r_o} \right] \sin \theta_o e^{-j2\pi r_o}$
$\epsilon_o = \frac{\left(\frac{\partial \Delta}{\partial x}\right) \left(\frac{\partial \Delta}{\partial y}\right) \eta}{j(2\pi)^2}$		$h_o = \frac{\left(\frac{\partial \Delta}{\partial x}\right) \left(\frac{\partial \Delta}{\partial y}\right)}{j(2\pi)^2 \eta}$
$r_o$ in wavelengths		$r_o$ in wavelengths



$$A_{x_0} = (A_{r_0}^- \cos \theta_0) \sin \theta_0 \cos \phi_0 + (A_{\theta_0}^- \sin \theta_0) \cos \theta_0 \cos \phi_0 \quad (5a)$$

$$A_{y_0} = (A_{r_0}^- \cos \theta_0) \sin \theta_0 \sin \phi_0 + (A_{\theta_0}^- \sin \theta_0) \cos \theta_0 \sin \phi_0 \quad (5b)$$

$$A_{z_0} = (A_{r_0}^- \cos \theta_0) \cos \theta_0 - (A_{\theta_0}^- \sin \theta_0) \sin \theta_0 \quad (5c)$$

$$C_{x_0} = - (C_{\phi_0}^- \sin \theta_0) \sin \phi_0 \quad (5d)$$

$$C_{y_0} = (C_{\phi_0}^- \sin \theta_0) \cos \phi_0 \quad (5e)$$

$$C_{z_0} = 0 \quad (5f)$$

In the above, the trigonometric function in parentheses comes from the field expressions in Table 1; hence, the "minus" superscript indicates the field expression from Table 1 without the orientation factor  $\cos \theta_0$  or  $\sin \theta_0$ , weighting  $e_0$  or  $h_0$ , and without the current  $J_{z_0}^n$  or  $J_{z_0}^e$ .

Define direction cosines  $k_{x_0}$ ,  $k_{y_0}$ ,  $k_{z_0}$  related to  $\theta_0$ ,  $\phi_0$  according to

$$k_{x_0} = \sin \theta_0 \cos \phi_0 \quad (6a)$$

$$k_{y_0} = \sin \theta_0 \sin \phi_0 \quad (6b)$$

$$k_{z_0} = \cos \theta_0 \quad (6c)$$

Then Equations (5) can be rewritten succinctly as

$$A_{x_0} = (A_{r_0}^- + A_{\theta_0}^-) k_{x_0} k_{z_0} \quad (7a)$$

$$A_{y_0} = (A_{r_0}^- + A_{\theta_0}^-) k_{y_0} k_{z_0} \quad (7b)$$

$$A_{z_0} = (A_{r_0}^- + A_{\theta_0}^-) k_{z_0}^2 - A_{\theta_0}^- \quad (7c)$$

$$C_{x_0} = - C_{\phi_0}^- k_{y_0} \quad (7d)$$

$$C_{y_0} = C_{\phi_0}^- k_{x_0} \quad (7e)$$

$$C_{z_0} = 0 \quad (7f)$$

Similar expressions for cases of x-directed and y-directed dipoles may be derived from those given above merely redefining the axes in Table 1. When this is done, the generalized expressions shown in Table 2 result for all three cases.

When both electric and magnetic currents are present (x-directed and y-directed components) the expressions for  $\underline{E}$  and  $\underline{H}$  are obtained by adding the contributions due to each current as given in Table 2. Note that  $A_r^-$ ,  $A_\theta^-$ , and  $A_\phi^-$  are identical for both types and directions of currents so that the expressions for the field components may be written, for example, as follows:

$$E_x = e_0 \left\{ J_x^e [(A_r^- + A_\theta^-) k_x^2 - A_\theta^-] + J_y^e k_x k_y (A_r^- + A_\theta^-) \right\} - h_0 j \pi n J_y^m k_z C_\phi^- \quad (8a)$$

Table 6-2. Rectangular Field Components of Elementary Dipoles

Field Component	Dipole Orientation		
	x-directed	y-directed	z-directed
$A_x^-$	$A_{r\theta}^- k_x^2 - A_\theta^-$	$A_{r\theta}^- k_x k_y$	$A_{r\theta}^- k_x k_z$
$A_y^-$	$A_{r\theta}^- k_x k_y$	$A_{r\theta}^- k_y^2 - A_\theta^-$	$A_{r\theta}^- k_y k_z$
$A_z^-$	$A_{r\theta}^- k_x k_z$	$A_{r\theta}^- k_y k_z$	$A_{r\theta}^- k_z^2 - A_\theta^-$
$C_x^-$	0	$C_\phi^- k_z$	$-C_\phi^- k_y$
$C_y^-$	$-C_\phi^- k_z$	0	$C_\phi^- k_x$
$C_z^-$	$C_\phi^- k_y$	$-C_\phi^- k_x$	0

where:

$$A_{r\theta}^- = (A_r^- + A_\theta^-)$$

$$A_r^- = \left( \frac{1}{r_o^3} + \frac{j2\pi}{r_o^2} \right) e^{-j2\pi r_o}$$

$$A_\theta^- = \frac{1}{2} \left( \frac{1}{r_o^3} + \frac{j2\pi}{r_o^2} - \frac{(2\pi)^2}{r_o} \right) e^{-j2\pi r_o}$$

$$C_\phi^- = \left( \frac{1}{r_o^2} + \frac{j2\pi}{r_o} \right) e^{-j2\pi r_o}$$

$$\eta H_x = \eta h_o \left\{ J_x^m [(A_r^- + A_\theta^-) k_x^2 - A_\theta^-] + J_y^m k_x k_y (A_r^- + A_\theta^-) \right\} + e_o j\pi J_y^c k_z C_\phi^- \quad (8b)$$

Similar expressions may be obtained for the other rectangular components of  $\underline{E}$  and  $\underline{H}$  as given in Table 6-3 and by Lines 56-57 and 62-65 of the program listing.

#### 6-6. Program Flow

<u>Lines</u>	<u>Comment</u>
15	If INIT=.TRUE., compute constants in Lines 18-29.
18-29	Compute $(2\pi)^2$ , $j$ , $e_o$ , $h_o$ , $j2\pi$ , $j\pi$ , $h_{oe} = -h_o\eta$ , $e_{oh} = e_o/\eta$ . Lines 26-27 have been added to cause $\eta\underline{H}$ to be computed instead of $\underline{H}$ to save time in Subroutine RECM (See Chapter 3).
30-33	Compute $r$ in wavelengths; i.e., the distance from the source point to the field point.
34	If $r < .01\lambda$ , write error message and stop (Lines 67-69).
35-37	Compute direction cosines $k_x$ , $k_y$ , $k_z$ .
38-40	Compute exponential phase factor $e^{-j2\pi r}$ .
41-45	Compute $A_{ro}^-$ , $A_{\theta o}^-$ , $C_{\phi o}^-$ , $(A_{ro}^- + A_{\theta o}^-)$ , and $C_\theta = (A_{ro}^- + A_{\theta o}^-) k_x^2 - A_{\theta o}^-$
46-49	These commented lines contain only $1/r$ terms and can be used to replace lines 41-45.
50-51	Precalculate $(A_{ro}^- + A_{\theta o}^-) k_x k_y$ and $C_{\phi o}^- k_z$ to facilitate computation of $E_x$ and $H_x$ .

Table 6-3. Fields of Elementary x-Directed and y-Directed Dipoles

$$\underline{E} = \underline{E}^e + \underline{E}^m$$

$$\underline{H} = \underline{H}^e + \underline{H}^m$$

$$E_x = e_o [J_x^e(A_{r\theta}^- k_x^2 - A_\theta^-) + J_y^e(k_x k_y A_{r\theta}^-)] - h_o j^{\pi n} J_y^m k_z c_\phi^-$$

$$E_y = e_o [J_x^e(k_x k_y A_{r\theta}^-) + J_y^e(A_{r\theta}^- k_y^2 - A_\theta^-)] + h_o j^{\pi n} J_x^m k_z c_\phi^-$$

$$E_z = e_o [J_x^e(k_x k_z A_{r\theta}^-) + J_y^e(k_y k_z A_{r\theta}^-)] + h_o j^{\pi n} c_\phi^- (-J_x^m k_y + J_y^m k_x)$$

$$H_x = e_o \frac{j^n}{n} J_y^e k_z c_\phi^- + h_o [J_x^m(A_{r\theta}^- k_x^2 - A_\theta^-) + J_y^m k_x k_y A_{r\theta}^-]$$

$$H_y = -e_o \frac{j^n}{n} J_x^e k_z c_\phi^- + h_o [J_x^m(k_x k_y A_{r\theta}^-) + J_y^m(A_{r\theta}^- k_y^2 - A_\theta^-)]$$

$$H_z = e_o \frac{j^n}{n} c_\phi^- (k_y J_x^e - k_x J_y^e) + h_o [J_x^m(k_x k_z A_{r\theta}^-) + J_y^m(k_y k_z A_{r\theta}^-)]$$

Where:

$$e_o = \frac{(\frac{\Delta A}{2}) n}{j(2^n)^2} \qquad h_o = \frac{(\frac{\Delta A}{2})}{j(2^n)^2 n}$$

52-53      Compute  $E_x$  and  $H_x$  due to the x-directed and y-directed electric and magnetic currents:  $J_x^e = JE(1)$ ,  $J_y^e = JE(2)$ ,  $J_x^m = JM(1)$ ,  $J_y^m = JM(2)$ .

54          Precalculate  $(A_{\rho 0}^- + A_{\theta 0}^-) k_y^2 - A_{\theta 0}^-$ .

55          See lines 46-49 above.

56-57      Compute  $E_y$  and  $H_y$ .

58-61      Precalculate common variables for  $E_z$ ,  $H_z$ .

62-65      Compute  $E_z$  and  $H_z$ .

            RETURN

67-69      Error message and halt.

            END

#### 6-6. Test Case

Selected test cases shown in Figure 2-15 of Reference 1 were executed. The square, 4" x 4", uniform aperture ( $\lambda = 1.18"$ ) was sampled at  $M=15$ ,  $N=15$  points in the x and y directions, respectively. Cases were done for  $\underline{E}_{ap} = \hat{y}(1)$ ,  $\underline{H}_{ap} = 0$ , and for  $\underline{E}_{ap} = \hat{y}(1)$ ,  $\underline{H}_{ap} = -\hat{x}(1/\eta)$ . In the latter case, the amplitudes obtained were twice as large (as expected). Although exact comparison to the graphical results in Figure 2-15 was not possible, agreement was obtained so far as could be determined. Some benchmarks as computed by Subroutine DIPOLES are shown in Tables 4 through 6.

#### 6-7. References

1. C. H. Walter, Traveling Wave Antennas, McGraw-Hill, New York, 1965, Ch. 2.
2. S. Silver, Microwave Antenna Theory and Design, McGraw-Hill, New York, 1949, Ch. 3.
3. D. T. Paris and F. K. Hurd, Basic Electromagnetic Theory, McGraw-Hill, New York, 1969, Ch. 1.

6-8. Program Listing. See following pages.

SUBROUTINE DIPOLES(JE, JM, PSWL, PFWL, DXWL, DYWL, E, H, INIT)	1
C *** MODIFIED 1-23-80 TO INCLUDE ONLY 1/R TERMS **** NULLIFIED 1-24-80**	
C SUBR DIPOLES COMPUTES THE RECTANGULAR COMPONENTS OF THE FIELDS E, H OF	3
C ELECTRIC AND MAGNETIC DIPOLES LOCATED AT PSWL(X', Y', Z')	4
C AND ORIENTED IN THE X' AND Y' DIRECTIONS. THE FIELDS ARE COMPUTED AT	5
C THE POINT PFWL(X, Y, Z). ALL DIMENSIONS ARE IN WAVELENGTHS. MKS SYSTEM	
C IS USED. FREE SPACE (ETA=377 OHMS) IS ASSUMED.	7
COMPLEX JE(2), JM(2), E(3), H(3), JAY, HO, EO, CPHS, JPI, JAY2PI	8
COMPLEX ARO, ATO, CPO, ARTO, CT, ARTOK, CPOK, EOH, HOE	9
REAL PSWL(3), PFWL(3), KX, KY, KZ	10
LOGICAL INIT	11
C DXWL, DYWL=X' AND Y' DIMENSIONS OF THE RECTANGULAR ELEMENT OVER WHICH	12
C CURRENT DENSITIES JE AND JM FLOW TO MAKE THE DIPOLES.	13
DATA TUPI/6.283185301/, ETA/376.9911185/	14
IF (INIT) GO TO 1	15
GO TO 2	16
C COMPUTE EO, HO (SEE DERIVATION DATED 7-23-79):	17
1 TUPI2=TUPI**2	18
JAY=(0., 1.)	19
EO=DXWL*DYWL*ETA/(JAY*TUPI2)	20
HO=DXWL*DYWL/(JAY*TUPI2*ETA)	21
JAY2PI=JAY*TUPI	22
JPI=JAY*TUPI/2.	23
HOE=-HO*ETA	24
EOH=EO/ETA	25
HO=HO*ETA	26
EOH=EOH*ETA	27
C THE ABOVE TWO LINES CAUSE ETA*H TO BE COMPUTED FOR USE IN RECI.	28
INIT=.FALSE.	29
2 X=PFWL(1)-PSWL(1)	30
Y=PFWL(2)-PSWL(2)	31
Z=PFWL(3)-PSWL(3)	32
R=SQRT(X*X+Y*Y+Z*Z)	33
IF (R.LT..01) GO TO 90	34
KX=X/R	35
KY=Y/R	36
KZ=Z/R	37
PHS=AMOD(TUPI*R, TUPI)	38

	CPHS=CMPLX(0.,-PHS)	39
	CPHS=CEXP(CPHS)	40
	ARO=CPHS*(1./R**3+JAY2PI/R**2)	41
	ATO=.5*(ARO-CPHS*TUPI2/R)	42
	CPO=JPI*ARO*R	43
	ARTO=ARO+ATO	44
	CT=ARO*KX**2-ATO*(1.-KX**2)	45
C	ATO=-.5*CPHS*TUPI2/R	46
C	CPO=JPI*CPHS*JAY2PI/R	47
C	ARTO=ATO	48
C	CT=-ATO*(1.-KX*KX)	49
	ARTOK=ARTO*KX*KY	50
	CPOK=CPO*KZ	51
	E(1)=EO*(JE(1)*CT+JE(2)*ARTOK)+JM(2)*HOE*CPOK	52
	H(1)=HO*(JM(1)*CT+JM(2)*ARTOK)+EOH*JE(2)*CPOK	53
	CT=ARO*KY**2-ATO*(1.-KY**2)	54
C	CT=-ATO*(1.-KY*KY)	55
	E(2)=EO*(JE(1)*ARTOK+JE(2)*CT)-JM(1)*HOE*CPOK	56
	H(2)=HO*(JM(1)*ARTOK+JM(2)*CT)-JE(1)*EOH*CPOK	57
	ARTOK=ARTO*KY*KZ	58
	ARTO=ARTO*KX*KZ	59
	CPOK=CPO*KY	60
	CPO=CPO*KX	61
	E(3)=EO*(JE(1)*ARTO+JE(2)*ARTOK)+HOE*(JM(1)*CPOK	62
	\$-JM(2)*CPO)	63
	H(3)=HO*(JM(1)*ARTO+JM(2)*ARTOK)+EOH*(JE(1)*CPOK	64
	\$-JE(2)*CPO)	65
	RETURN	66
90	WRITE(6,91)	67
91	FORMAT(" **** R.LT..01 WAVELENGTH IN SUBR DIPOLES--STOP****")	68
	STOP	69
	END	70



Table 6-4. Fields Computed by Subroutine DIPOLES Along z-Axis for 4" x 4" Uniform Aperture ( $\lambda=1.18$ ).

1 TEST PROGRAM FOR USING ELEMENTARY SOURCES FOR COMPUTING FRESNEL FIELDS  
 (REF: WALTBY(1965), PP.55-57)  
 AIN= 4.00 INCH M, N= 15 15 LAMBDA= 1.18  
 FIELD IS -10.0 CM AT Z= 24.00 INCHES  
 APERTURE FIELDS TYPE (0.0000, 0.0000) (1.0000, 0.0000) HAP= (0.0000, 0.0000)  
 R, HRC= .07422E+00 .03146E-12 IAX IS= 3 PFML= 0.00 0.00 4.00

N	XYZIN	XYZWL	AMPDB	PHSDEG	EX (HX)	AMPDB	PHSDEG	EY HY	AMPDB	PHSDEG	EZ HZ
1	4.00	3.39	(	-40.0	-180.0	-0.1	-139.2	-40.0	-40.0	177.4	
2	4.33	3.04	(	-0.1	49.9	-40.0	-180.0	-40.0	-40.0	-4.4	
3	4.59	3.09	(	-40.0	-180.0	-0.0	135.3	-40.0	-40.0	92.5	
4	4.09	4.14	(	0.0	-44.6	-40.0	-180.0	-40.0	-40.0	-86.1	
5	5.18	4.39	(	-40.0	-180.0	-0.0	49.9	-40.0	-40.0	10.1	
6	5.48	4.64	(	-0.0	-135.4	-40.0	-180.0	-40.0	-40.0	-168.7	
7	5.77	4.89	(	-40.0	-180.0	-0.1	-36.7	-40.0	-40.0	-72.5	
8	6.07	5.14	(	-0.1	143.4	-40.0	-180.0	-40.0	-40.0	105.2	
9	6.36	5.39	(	-40.0	-180.0	-0.2	-123.1	-40.0	-40.0	-157.1	
10	6.66	5.64	(	-0.2	50.6	-40.0	-180.0	-40.0	-40.0	19.5	
11	6.95	5.89	(	-40.0	-180.0	-0.3	150.1	-40.0	-40.0	118.2	
12	7.25	6.14	(	-0.3	-29.8	-40.0	-180.0	-40.0	-40.0	-69.4	
13	7.54	6.39	(	-40.0	-180.0	-0.4	63.1	-40.0	-40.0	30.8	
			(	-0.4	-110.8	-40.0	-180.0	-40.0	-40.0	-154.4	
			(	-40.0	-180.0	-0.0	-24.1	-40.0	-40.0	-50.7	
			(	-0.0	150.0	-40.0	-180.0	-40.0	-40.0	129.2	
			(	-40.0	-180.0	-0.0	-111.5	-40.0	-40.0	-138.0	
			(	-0.8	64.5	-40.0	-180.0	-40.0	-40.0	38.1	
			(	-40.0	-180.0	-1.0	160.9	-40.0	-40.0	136.4	
			(	-1.0	-19.1	-40.0	-180.0	-40.0	-40.0	-50.0	
			(	-40.0	-180.0	-1.2	73.1	-40.0	-40.0	48.9	
			(	-1.2	-106.9	-40.0	-180.0	-40.0	-40.0	-139.9	
			(	-40.0	-180.0	-1.4	-14.8	-40.0	-40.0	-39.3	
			(	-1.4	165.2	-40.0	-180.0	-40.0	-40.0	133.6	
			(	-40.0	-180.0	-1.6	-102.9	-40.0	-40.0	-131.3	

14	7.84	6.84	(	-1.6	77.1	-43.0	-183.0	-43.0	53.6	39
			(	-40.0	-180.0	-1.8	168.9	-43.0	147.1	40
			(	-1.8	-11.1	-43.0	-183.0	-43.0	-32.2	41
15	8.13	6.89	(	-43.0	-180.0	-2.0	80.6	-43.0	58.0	42
			(	-2.0	-99.4	-40.0	-180.0	-43.0	-121.4	43
16	8.43	7.14	(	-60.0	-180.0	-2.2	-7.8	-40.0	-25.3	44
			(	-2.2	172.2	-40.0	-180.0	-43.0	149.3	45
17	8.72	7.39	(	-43.0	-180.0	-2.4	-96.3	-43.0	-113.5	46
			(	-2.4	83.7	-40.0	-180.0	-43.0	59.3	47
18	9.02	7.54	(	-43.0	-180.0	-2.6	175.1	-40.0	159.8	48
			(	-2.6	-4.9	-40.0	-180.0	-40.0	-26.4	49
19	9.31	7.80	(	-43.0	-180.0	-2.8	86.4	-40.0	70.0	50
			(	-2.8	-93.6	-40.0	-180.0	-43.0	-108.5	51
20	9.61	8.14	(	-43.0	-180.0	-3.0	-2.4	-40.0	-16.4	52
			(	-3.0	177.7	-40.0	-180.0	-40.0	161.1	53
21	9.90	8.39	(	-43.0	-180.0	-3.2	-91.2	-43.0	-135.2	54
			(	-3.2	88.9	-40.0	-180.0	-40.0	71.3	55
22	10.20	8.64	(	-40.0	-180.0	-3.4	179.9	-40.0	164.6	56
			(	-3.4	-0.0	-40.0	-180.0	-40.0	-18.9	57
23	10.49	8.89	(	-40.0	-180.0	-3.6	91.0	-40.0	71.1	58
			(	-3.6	-83.0	-40.0	-180.0	-40.0	-106.5	59
24	10.79	9.14	(	-43.0	-180.0	-3.8	2.0	-40.0	-17.4	60
			(	-3.8	-178.0	-40.0	-180.0	-43.0	166.8	61
25	11.08	9.39	(	-43.0	-180.0	-4.0	-97.0	-40.0	-104.3	62
			(	-4.0	93.0	-43.0	-180.0	-40.0	76.7	63
26	11.38	9.64	(	-40.0	-180.0	-4.1	-176.1	-40.0	168.8	64
			(	-4.1	-3.9	-40.0	-180.0	-40.0	-13.8	65
27	11.67	9.89	(	-40.0	-180.0	-4.3	94.8	-40.0	76.7	66
			(	-4.3	-95.2	-40.0	-180.0	-40.0	-104.2	67
28	11.97	10.14	(	-40.0	-180.0	-4.5	5.6	-40.0	-8.1	68
			(	-4.5	-174.4	-40.0	-180.0	-40.0	168.6	69
29	12.26	10.39	(	-40.0	-180.0	-4.7	-83.6	-40.0	-97.5	70
			(	-4.7	96.4	-40.0	-180.0	-40.0	85.5	71
30	12.56	10.64	(	-40.0	-180.0	-4.8	-172.9	-40.0	172.5	72
			(	-4.8	7.1	-40.0	-180.0	-40.0	-7.5	73
31	12.85	10.89	(	-40.0	-180.0	-5.0	97.8	-40.0	84.8	74
			(	-5.0	-12.1	-40.0	-180.0	-40.0	-96.9	75
32	13.15	11.14	(	-40.0	-180.0	-5.2	8.5	-40.0	-5.4	76

33	13.44	11.31	( -5.2	-171.3	-43.0	-18.0	-43.0	174.2
77								
78								
79								
80								
81								
82								
83								
84								
85								
86								
87								
88								
89								
90								
91								
92								
93								
94								
95								
96								
97								
98								
99								
100								
101								
102								
103								
104								
105								
106								
107								
108								
109								
110								
111								
112								
113								
114								
33	13.44	11.31	( -5.2	-171.3	-43.0	-18.0	-43.0	174.2
77								
78								
79								
80								
81								
82								
83								
84								
85								
86								
87								
88								
89								
90								
91								
92								
93								
94								
95								
96								
97								
98								
99								
100								
101								
102								
103								
104								
105								
106								
107								
108								
109								
110								
111								
112								
113								
114								
33	13.44	11.31	( -5.2	-171.3	-43.0	-18.0	-43.0	174.2
77								
78								
79								
80								
81								
82								
83								
84								
85								
86								
87								
88								
89								
90								
91								
92								
93								
94								
95								
96								
97								
98								
99								
100								
101								
102								
103								
104								
105								
106								
107								
108								
109								
110								
111								
112								
113								
114								

52	19.05	16.14	(	-8.0	-72.3	-40.0	-180.0	-40.0	-40.0	-40.0	-42.0	115
			(	-40.0	-180.0	-8.1	18.3	-40.0	-40.0	-40.0	8.2	116
			(	-8.1	-162.0	-40.0	-160.0	-40.0	-40.0	-40.0	-171.5	117
53	19.34	16.33	(	-40.0	-180.0	-8.2	-71.7	-40.0	-40.0	-40.0	-82.9	118
			(	-8.2	108.3	-40.0	-180.0	-40.0	-40.0	-40.0	98.8	119
54	19.64	16.64	(	-40.0	-180.0	-8.3	-161.4	-40.0	-40.0	-40.0	-172.2	120
			(	-8.3	18.6	-40.0	-180.0	-40.0	-40.0	-40.0	9.1	121
55	19.97	16.83	(	-8.0	-180.0	-8.5	108.9	-40.0	-40.0	-40.0	99.2	122
			(	-8.5	-71.3	-40.0	-180.0	-40.0	-40.0	-40.0	-80.8	123
56	20.23	17.14	(	-40.0	-180.0	-8.6	19.2	-40.0	-40.0	-40.0	11.9	124
			(	-8.6	-160.8	-40.0	-180.0	-40.0	-40.0	-40.0	-170.3	125
57	20.52	17.33	(	-40.0	-180.0	-8.7	-70.5	-40.0	-40.0	-40.0	-80.6	126
			(	-8.7	109.5	-40.0	-180.0	-40.0	-40.0	-40.0	100.7	127
58	20.82	17.64	(	-40.0	-180.0	-8.8	-160.2	-40.0	-40.0	-40.0	-168.4	128
			(	-8.8	19.8	-40.0	-180.0	-40.0	-40.0	-40.0	11.1	129
59	21.11	17.89	(	-40.0	-180.0	-8.9	110.1	-40.0	-40.0	-40.0	103.8	130
			(	-8.9	-60.9	-40.0	-180.0	-40.0	-40.0	-40.0	-78.8	131
60	21.41	18.14	(	-40.0	-180.0	-9.1	20.4	-40.0	-40.0	-40.0	17.4	132
			(	-9.1	-159.0	-40.0	-180.0	-40.0	-40.0	-40.0	-168.5	133
61	21.70	18.33	(	-40.0	-180.0	-9.2	-69.4	-40.0	-40.0	-40.0	-74.7	134
			(	-9.2	110.6	-40.0	-180.0	-40.0	-40.0	-40.0	102.0	135
62	22.00	18.64	(	-40.0	-180.0	-9.3	-159.1	-40.0	-40.0	-40.0	-164.2	136
			(	-9.3	20.9	-40.0	-180.0	-40.0	-40.0	-40.0	12.5	137
63	22.29	18.89	(	-40.0	-180.0	-9.4	111.1	-40.0	-40.0	-40.0	198.5	138
			(	-9.4	-68.9	-40.0	-180.0	-40.0	-40.0	-40.0	-77.1	139
64	22.59	19.14	(	-40.0	-180.0	-9.5	21.4	-40.0	-40.0	-40.0	15.4	140
			(	-9.5	-158.6	-40.0	-180.0	-40.0	-40.0	-40.0	-166.2	141
65	22.88	19.33	(	-40.0	-180.0	-9.6	-68.4	-40.0	-40.0	-40.0	-72.6	142
			(	-9.6	111.5	-40.0	-180.0	-40.0	-40.0	-40.0	104.3	143
66	23.18	19.64	(	-40.0	-180.0	-9.7	-158.2	-40.0	-40.0	-40.0	-164.6	144
			(	-9.7	21.8	-40.0	-180.0	-40.0	-40.0	-40.0	19.4	145
67	23.47	19.89	(	-40.0	-180.0	-9.8	112.0	-40.0	-40.0	-40.0	104.0	146
			(	-9.8	-68.3	-40.0	-180.0	-40.0	-40.0	-40.0	-72.0	147
68	23.77	20.14	(	-40.0	-180.0	-9.9	22.3	-40.0	-40.0	-40.0	14.9	148
			(	-9.9	-157.7	-40.0	-180.0	-40.0	-40.0	-40.0	-162.5	149

Table 6-5. Fields Computed by Subroutine DIPOLES Along x-Axis at z=8 inches.

1 TEST PROGRAM FOR USING ELEMENTARY SOURCES FOR COMPUTING FRESNEL FIELDS  
 (REF: WALTER (1965), PP. 55-57)  
 2 WAVELENGTH = 10.0 CM AT 7 = 24.0 INCHES  
 3 WAVELENGTH = 10.0 CM AT 7 = 24.0 INCHES  
 4 WAVELENGTH = 10.0 CM AT 7 = 24.0 INCHES  
 5 WAVELENGTH = 10.0 CM AT 7 = 24.0 INCHES  
 6 WAVELENGTH = 10.0 CM AT 7 = 24.0 INCHES  
 7 WAVELENGTH = 10.0 CM AT 7 = 24.0 INCHES  
 8 WAVELENGTH = 10.0 CM AT 7 = 24.0 INCHES  
 9 WAVELENGTH = 10.0 CM AT 7 = 24.0 INCHES  
 10 WAVELENGTH = 10.0 CM AT 7 = 24.0 INCHES  
 11 WAVELENGTH = 10.0 CM AT 7 = 24.0 INCHES  
 12 WAVELENGTH = 10.0 CM AT 7 = 24.0 INCHES  
 13 WAVELENGTH = 10.0 CM AT 7 = 24.0 INCHES  
 14 WAVELENGTH = 10.0 CM AT 7 = 24.0 INCHES  
 15 WAVELENGTH = 10.0 CM AT 7 = 24.0 INCHES  
 16 WAVELENGTH = 10.0 CM AT 7 = 24.0 INCHES  
 17 WAVELENGTH = 10.0 CM AT 7 = 24.0 INCHES  
 18 WAVELENGTH = 10.0 CM AT 7 = 24.0 INCHES  
 19 WAVELENGTH = 10.0 CM AT 7 = 24.0 INCHES  
 20 WAVELENGTH = 10.0 CM AT 7 = 24.0 INCHES  
 21 WAVELENGTH = 10.0 CM AT 7 = 24.0 INCHES  
 22 WAVELENGTH = 10.0 CM AT 7 = 24.0 INCHES  
 23 WAVELENGTH = 10.0 CM AT 7 = 24.0 INCHES  
 24 WAVELENGTH = 10.0 CM AT 7 = 24.0 INCHES  
 25 WAVELENGTH = 10.0 CM AT 7 = 24.0 INCHES  
 26 WAVELENGTH = 10.0 CM AT 7 = 24.0 INCHES  
 27 WAVELENGTH = 10.0 CM AT 7 = 24.0 INCHES  
 28 WAVELENGTH = 10.0 CM AT 7 = 24.0 INCHES  
 29 WAVELENGTH = 10.0 CM AT 7 = 24.0 INCHES  
 30 WAVELENGTH = 10.0 CM AT 7 = 24.0 INCHES  
 31 WAVELENGTH = 10.0 CM AT 7 = 24.0 INCHES  
 32 WAVELENGTH = 10.0 CM AT 7 = 24.0 INCHES  
 33 WAVELENGTH = 10.0 CM AT 7 = 24.0 INCHES  
 34 WAVELENGTH = 10.0 CM AT 7 = 24.0 INCHES  
 35 WAVELENGTH = 10.0 CM AT 7 = 24.0 INCHES  
 36 WAVELENGTH = 10.0 CM AT 7 = 24.0 INCHES  
 37 WAVELENGTH = 10.0 CM AT 7 = 24.0 INCHES  
 38 WAVELENGTH = 10.0 CM AT 7 = 24.0 INCHES

N	XVZIN	XYZML	AMPDB	PHSDFG	AMPDB	PHSDFG	AMPDB	PHSDFG	AMPDB	PHSDFG	AMPDB	PHSDFG
1	0.30	0.00	-40.0	-180.0	-1.9	119.5	-40.0	90.3				
2	.30	.25	-1.0	-60.4	-40.0	-180.0	-40.0	-83.0				
3	.30	.50	-40.0	-180.0	-2.1	118.5	-40.0	90.4				
4	.30	.75	-2.1	-61.4	-40.0	-180.0	-40.0	65.7				
5	1.18	1.00	-40.0	-180.0	-2.7	115.0	-40.0	91.9				
6	1.48	1.25	-2.7	-64.2	-40.0	-180.0	-40.0	61.0				
7	1.77	1.50	-40.0	-180.0	-3.7	110.9	-40.0	87.9				
8	2.07	1.75	-3.7	-68.6	-40.0	-180.0	-40.0	54.7				
9	2.36	2.00	-40.0	-180.0	-5.2	104.3	-40.0	86.2				
10	2.66	2.25	-5.2	-74.2	-40.0	-180.0	-40.0	45.1				
11	2.95	2.50	-7.4	-80.2	-7.0	98.0	-40.0	77.5				
12	3.25	2.75	-7.0	-80.2	-9.0	93.0	-40.0	33.2				
13	3.54	3.00	-9.0	-85.4	-11.5	90.2	-40.0	67.2				
			-11.2	-88.6	-13.2	80.0	-40.0	19.3				
			-12.8	-89.9	-14.0	70.0	-40.0	71.7				
			-13.5	-93.1	-13.8	60.0	-40.0	5.0				
			-13.6	-93.1	-13.6	74.9	-40.0	76.9				
			-13.6	-102.7	-14.0	60.0	-40.0	-0.0				
			-13.6	-102.7	-13.8	60.0	-40.0	60.3				
			-13.6	-102.7	-13.6	74.9	-40.0	82.6				
			-13.6	-102.7	-13.6	74.9	-40.0	56.7				
			-13.6	-102.7	-13.4	61.8	-40.0	86.2				
			-13.6	-119.3	-14.0	60.0	-40.0	35.5				
			-13.6	-119.3	-13.5	34.5	-40.0	63.4				
			-13.6	-119.3	-13.5	34.5	-40.0	5.5				

14	3.84	3.25	( -13.9	-141.7	-40.0	-180.0	-24.4	34.6	39
15	4.13	3.50	( -14.5	-180.0	-14.0	10.8	-40.0	7.1	40
16	4.43	3.75	( -15.5	161.5	-14.8	-20.3	-23.5	2.3	41
17	4.72	4.00	( -16.8	129.0	-40.0	-180.0	-23.5	-31.6	42
18	5.02	4.25	( -18.4	95.1	-40.0	-180.0	-23.5	-32.6	43
19	5.31	4.50	( -20.4	60.6	-19.9	-124.9	-40.0	-67.6	44
20	5.61	4.75	( -22.6	26.8	-22.7	-154.5	-40.0	-69.6	45
21	5.90	5.00	( -24.8	-4.7	-40.0	-180.0	-24.1	-109.1	46
22	6.20	5.25	( -26.5	-33.7	-26.9	144.1	-25.3	-108.2	47
23	6.49	5.50	( -27.2	-63.3	-40.0	-180.0	-40.0	-136.0	48
24	6.79	5.75	( -27.1	-97.9	-40.0	-180.0	-27.2	-147.7	49
25	7.08	6.00	( -26.7	-139.0	-24.9	169.5	-40.0	-159.0	50
26	7.38	6.25	( -26.0	-180.0	-40.0	-180.0	-33.7	-173.4	51
27	7.67	6.50	( -26.0	69.9	-40.0	-180.0	-40.0	165.1	52
28	7.97	6.75	( -26.1	13.6	-24.6	-1.9	-31.4	139.6	53
29	8.26	7.00	( -26.0	-180.0	-40.0	-180.0	-40.0	139.6	54
30	8.56	7.25	( -26.4	-44.7	-27.7	119.3	-38.0	123.9	55
31	8.85	7.50	( -26.4	-154.8	-40.0	-180.0	-40.0	64.5	56
32	9.15	7.75	( -27.6	-166.3	-40.0	-180.0	-37.5	124.2	57
			( -27.6	-180.0	-40.0	-180.0	-40.0	56.1	58
			( -27.6	-180.0	-40.0	-180.0	-40.0	97.5	59
			( -27.6	-180.0	-40.0	-180.0	-40.0	15.1	60
			( -27.6	-180.0	-40.0	-180.0	-40.0	53.8	61
			( -27.6	-180.0	-40.0	-180.0	-40.0	-8.7	62
			( -27.6	-180.0	-40.0	-180.0	-29.7	3.3	63
			( -27.6	-180.0	-40.0	-180.0	-40.0	-70.2	64
			( -27.6	-180.0	-40.0	-180.0	-28.6	-50.9	65
			( -27.6	-180.0	-40.0	-180.0	-40.0	-128.1	66
			( -27.6	-180.0	-40.0	-180.0	-27.9	-107.6	67
			( -27.6	-180.0	-40.0	-180.0	-40.0	-167.4	68
			( -27.6	-180.0	-40.0	-180.0	-27.5	-166.2	69
			( -27.6	-180.0	-40.0	-180.0	-40.0	148.5	70
			( -27.6	-180.0	-40.0	-180.0	-27.3	133.5	71
			( -27.6	-180.0	-40.0	-180.0	-40.0	63.8	72
			( -27.6	-180.0	-40.0	-180.0	-27.3	71.8	73
			( -27.6	-180.0	-40.0	-180.0	-40.0	-6.3	74
			( -27.6	-180.0	-40.0	-180.0	-27.5	8.8	75
			( -27.6	-180.0	-40.0	-180.0	-40.0	-76.2	76

33	9.44	H...	(	-24.0	13.4	-70.0	-100.0	-27.0	-55.4	77
			(	-70.0	-160.0	-25.5	-117.2	-40.0	-134.3	78
			(	-28.7	60.7	-40.0	-140.0	-20.2	-120.7	79
34	9.74	N.25	(	-40.0	-180.0	-20.1	174.9	-40.0	172.9	80
			(	-29.5	1.5	-40.0	-140.0	-24.7	173.0	81

Table 6-6. Fields Computed by Subroutine DIPOLES Along x-Axis at z=24 inches.

```

1 TEST PROGRAM FOR USING ELEMENTARY SOURCES FOR COMPUTING FRESNEL FIELDS
2 (REF: WALTER(1965), PP.55-57)
3 WAVE 4.00 BIN= 4.00 M,N= 15 15 LAMBDA= 1.180
4 FIELD IS -10.0 DB AT Z= 24.00 INCHES
APERTURE FIELDS: EAP= (0.0000,0.0000) (1.0000,0.0000) HAP= (0.0000,0.0000)
IPC,HRC= .87422E+01 .27184E-12 IAX ISE= 1 PFWLCT 0.00 0.00 24.00

```

N	XYZIN	XYZWL	AMPDB	PHSDEG	FX	HX	AMPDB	PHSDEG	LY	HY	AMPDB	PHSDEG	EZ	HZ
1	0.00	0.00	-40.0	-180.0	-180.0	-180.0	-10.0	-49.3	-10.0	-49.3	-40.0	-56.7	-40.0	124.4
2	.30	.25	-40.0	-180.0	-180.0	-180.0	-10.0	-49.8	-10.0	-49.8	-40.0	-60.2	-40.0	-60.2
3	.59	.50	-40.0	-180.0	-180.0	-180.0	-10.0	-51.4	-10.0	-51.4	-40.0	-67.5	-40.0	-67.5
4	.89	.75	-40.0	-180.0	-180.0	-180.0	-10.0	-54.0	-10.0	-54.0	-40.0	-69.2	-40.0	-69.2
5	1.18	1.00	-40.0	-180.0	-180.0	-180.0	-10.0	-57.7	-10.0	-57.7	-40.0	-71.9	-40.0	-71.9
6	1.48	1.25	-40.0	-180.0	-180.0	-180.0	-10.0	-62.4	-10.0	-62.4	-40.0	-75.7	-40.0	-75.7
7	1.77	1.50	-40.0	-180.0	-180.0	-180.0	-10.0	-68.2	-10.0	-68.2	-40.0	-80.5	-40.0	-80.5
8	2.07	1.75	-40.0	-180.0	-180.0	-180.0	-11.3	-75.0	-11.3	-75.0	-40.0	-86.5	-40.0	-86.5
9	2.36	2.00	-40.0	-180.0	-180.0	-180.0	-11.7	-80.8	-11.7	-80.8	-40.0	-93.5	-40.0	-93.5
10	2.66	2.25	-40.0	-180.0	-180.0	-180.0	-12.1	-91.6	-12.1	-91.6	-40.0	-101.6	-40.0	-101.6
11	2.95	2.50	-40.0	-180.0	-180.0	-180.0	-12.7	-101.4	-12.7	-101.4	-40.0	-110.8	-40.0	-110.8
12	3.25	2.75	-40.0	-180.0	-180.0	-180.0	-13.2	-112.2	-13.2	-112.2	-40.0	-121.0	-40.0	-121.0
13	3.54	3.00	-40.0	-180.0	-180.0	-180.0	-13.9	-124.0	-13.9	-124.0	-40.0	-132.2	-40.0	-132.2
14			-40.0	-180.0	-180.0	-180.0	-14.6	-136.4	-14.6	-136.4	-40.0	-143.5	-40.0	-143.5
15			-40.0	-180.0	-180.0	-180.0	-15.4	-148.0	-15.4	-148.0	-40.0	-154.9	-40.0	-154.9
16			-40.0	-180.0	-180.0	-180.0	-16.4	-159.0	-16.4	-159.0	-40.0	-166.4	-40.0	-166.4
17			-40.0	-180.0	-180.0	-180.0	-17.4	-170.0	-17.4	-170.0	-40.0	-177.9	-40.0	-177.9
18			-40.0	-180.0	-180.0	-180.0	-18.4	-180.0	-18.4	-180.0	-40.0	-189.5	-40.0	-189.5
19			-40.0	-180.0	-180.0	-180.0	-19.6	-190.0	-19.6	-190.0	-40.0	-201.1	-40.0	-201.1
20			-40.0	-180.0	-180.0	-180.0	-20.9	-200.0	-20.9	-200.0	-40.0	-212.7	-40.0	-212.7
21			-40.0	-180.0	-180.0	-180.0	-22.3	-210.0	-22.3	-210.0	-40.0	-224.3	-40.0	-224.3
22			-40.0	-180.0	-180.0	-180.0	-23.7	-220.0	-23.7	-220.0	-40.0	-235.9	-40.0	-235.9
23			-40.0	-180.0	-180.0	-180.0	-25.2	-230.0	-25.2	-230.0	-40.0	-247.5	-40.0	-247.5
24			-40.0	-180.0	-180.0	-180.0	-26.7	-240.0	-26.7	-240.0	-40.0	-259.1	-40.0	-259.1
25			-40.0	-180.0	-180.0	-180.0	-28.2	-250.0	-28.2	-250.0	-40.0	-270.7	-40.0	-270.7
26			-40.0	-180.0	-180.0	-180.0	-29.7	-260.0	-29.7	-260.0	-40.0	-282.3	-40.0	-282.3
27			-40.0	-180.0	-180.0	-180.0	-31.2	-270.0	-31.2	-270.0	-40.0	-293.9	-40.0	-293.9
28			-40.0	-180.0	-180.0	-180.0	-32.7	-280.0	-32.7	-280.0	-40.0	-305.5	-40.0	-305.5
29			-40.0	-180.0	-180.0	-180.0	-34.2	-290.0	-34.2	-290.0	-40.0	-317.1	-40.0	-317.1
30			-40.0	-180.0	-180.0	-180.0	-35.7	-300.0	-35.7	-300.0	-40.0	-328.7	-40.0	-328.7
31			-40.0	-180.0	-180.0	-180.0	-37.2	-310.0	-37.2	-310.0	-40.0	-340.3	-40.0	-340.3
32			-40.0	-180.0	-180.0	-180.0	-38.7	-320.0	-38.7	-320.0	-40.0	-351.9	-40.0	-351.9
33			-40.0	-180.0	-180.0	-180.0	-40.2	-330.0	-40.2	-330.0	-40.0	-363.5	-40.0	-363.5
34			-40.0	-180.0	-180.0	-180.0	-41.7	-340.0	-41.7	-340.0	-40.0	-375.1	-40.0	-375.1
35			-40.0	-180.0	-180.0	-180.0	-43.2	-350.0	-43.2	-350.0	-40.0	-386.7	-40.0	-386.7
36			-40.0	-180.0	-180.0	-180.0	-44.7	-360.0	-44.7	-360.0	-40.0	-398.3	-40.0	-398.3
37			-40.0	-180.0	-180.0	-180.0	-46.2	-370.0	-46.2	-370.0	-40.0	-409.9	-40.0	-409.9
38			-40.0	-180.0	-180.0	-180.0	-47.7	-380.0	-47.7	-380.0	-40.0	-421.5	-40.0	-421.5



14	3.44	3.25	( -14.3	25.7	-40.0	-14.0	-100.0	-33.7	-144.0	39
15	4.13	3.50	( -14.7	43.8	-40.0	-14.0	-138.7	-40.0	-145.0	40
16	4.43	3.75	( -15.0	30.4	-40.0	-15.5	-150.0	-30.7	-157.9	41
17	4.72	4.00	( -15.0	16.1	-40.0	-15.5	-150.0	-40.0	-158.0	42
18	5.02	4.25	( -17.5	1.0	-40.0	-17.4	-175.9	-31.3	-172.3	43
19	5.31	4.50	( -14.0	-14.7	-40.0	-18.5	-184.3	-40.0	-171.0	44
20	5.01	4.75	( -14.9	-31.0	-40.0	-19.7	-180.0	-31.8	155.9	45
21	5.30	5.00	( -21.3	-47.5	-40.0	-21.1	-131.1	-40.0	134.8	46
22	6.20	5.25	( -22.8	-04.1	-40.0	-22.7	-114.2	-40.0	167.9	47
23	6.49	5.50	( -24.5	-80.2	-40.0	-24.4	-97.9	-35.8	81.0	48
24	6.75	5.75	( -20.4	-94.9	-40.0	-25.4	-82.9	-40.0	81.7	49
25	7.04	6.00	( -28.3	-177.2	-40.0	-30.3	-62.5	-40.0	18.5	50
26	7.30	6.25	( -30.1	-115.9	-40.0	-31.4	-58.4	-40.0	57.1	51
27	7.07	6.50	( -31.1	-121.5	-40.0	-31.2	-53.4	-40.0	90.0	52
28	7.97	6.75	( -31.0	-127.9	-40.0	-30.2	-42.4	-40.0	86.2	53
29	8.26	7.00	( -30.2	-139.2	-40.0	-26.9	-26.3	-40.0	72.6	54
30	8.56	7.25	( -29.1	-156.0	-40.0	-27.6	-4.5	-40.0	48.4	55
31	8.85	7.50	( -28.1	-177.3	-40.0	-26.6	-20.2	-40.0	-33.3	56
32	9.15	7.75	( -27.2	-158.3	-40.0	-26.1	-47.4	-40.0	-8.1	57
33			( -27.2	-180.0	-40.0	-26.1	-47.4	-40.0	-60.1	58
34			( -27.2	-180.0	-40.0	-26.1	-47.4	-40.0	-60.1	59
35			( -27.2	-180.0	-40.0	-26.1	-47.4	-40.0	-60.1	60
36			( -27.2	-180.0	-40.0	-26.1	-47.4	-40.0	-60.1	61
37			( -27.2	-180.0	-40.0	-26.1	-47.4	-40.0	-60.1	62
38			( -27.2	-180.0	-40.0	-26.1	-47.4	-40.0	-60.1	63
39			( -27.2	-180.0	-40.0	-26.1	-47.4	-40.0	-60.1	64
40			( -27.2	-180.0	-40.0	-26.1	-47.4	-40.0	-60.1	65
41			( -27.2	-180.0	-40.0	-26.1	-47.4	-40.0	-60.1	66
42			( -27.2	-180.0	-40.0	-26.1	-47.4	-40.0	-60.1	67
43			( -27.2	-180.0	-40.0	-26.1	-47.4	-40.0	-60.1	68
44			( -27.2	-180.0	-40.0	-26.1	-47.4	-40.0	-60.1	69
45			( -27.2	-180.0	-40.0	-26.1	-47.4	-40.0	-60.1	70
46			( -27.2	-180.0	-40.0	-26.1	-47.4	-40.0	-60.1	71
47			( -27.2	-180.0	-40.0	-26.1	-47.4	-40.0	-60.1	72
48			( -27.2	-180.0	-40.0	-26.1	-47.4	-40.0	-60.1	73
49			( -27.2	-180.0	-40.0	-26.1	-47.4	-40.0	-60.1	74
50			( -27.2	-180.0	-40.0	-26.1	-47.4	-40.0	-60.1	75
51			( -27.2	-180.0	-40.0	-26.1	-47.4	-40.0	-60.1	76
52			( -27.2	-180.0	-40.0	-26.1	-47.4	-40.0	-60.1	77
53			( -27.2	-180.0	-40.0	-26.1	-47.4	-40.0	-60.1	78
54			( -27.2	-180.0	-40.0	-26.1	-47.4	-40.0	-60.1	79
55			( -27.2	-180.0	-40.0	-26.1	-47.4	-40.0	-60.1	80
56			( -27.2	-180.0	-40.0	-26.1	-47.4	-40.0	-60.1	81
57			( -27.2	-180.0	-40.0	-26.1	-47.4	-40.0	-60.1	82
58			( -27.2	-180.0	-40.0	-26.1	-47.4	-40.0	-60.1	83
59			( -27.2	-180.0	-40.0	-26.1	-47.4	-40.0	-60.1	84
60			( -27.2	-180.0	-40.0	-26.1	-47.4	-40.0	-60.1	85
61			( -27.2	-180.0	-40.0	-26.1	-47.4	-40.0	-60.1	86
62			( -27.2	-180.0	-40.0	-26.1	-47.4	-40.0	-60.1	87
63			( -27.2	-180.0	-40.0	-26.1	-47.4	-40.0	-60.1	88
64			( -27.2	-180.0	-40.0	-26.1	-47.4	-40.0	-60.1	89
65			( -27.2	-180.0	-40.0	-26.1	-47.4	-40.0	-60.1	90
66			( -27.2	-180.0	-40.0	-26.1	-47.4	-40.0	-60.1	91
67			( -27.2	-180.0	-40.0	-26.1	-47.4	-40.0	-60.1	92
68			( -27.2	-180.0	-40.0	-26.1	-47.4	-40.0	-60.1	93
69			( -27.2	-180.0	-40.0	-26.1	-47.4	-40.0	-60.1	94
70			( -27.2	-180.0	-40.0	-26.1	-47.4	-40.0	-60.1	95
71			( -27.2	-180.0	-40.0	-26.1	-47.4	-40.0	-60.1	96
72			( -27.2	-180.0	-40.0	-26.1	-47.4	-40.0	-60.1	97
73			( -27.2	-180.0	-40.0	-26.1	-47.4	-40.0	-60.1	98
74			( -27.2	-180.0	-40.0	-26.1	-47.4	-40.0	-60.1	99
75			( -27.2	-180.0	-40.0	-26.1	-47.4	-40.0	-60.1	100
76			( -27.2	-180.0	-40.0	-26.1	-47.4	-40.0	-60.1	101

33	9.44	8.05	(	-26.5	131.3	-40.0	-190.0	-36.0	-38.5
34	9.74	8.25	(	-26.0	102.5	-40.0	-180.0	-35.0	-70.0
35	10.03	8.50	(	-25.6	72.1	-40.0	-180.0	-34.2	-102.5
36	10.33	8.75	(	-25.3	40.4	-40.0	-180.0	-33.5	-135.0
37	10.62	9.00	(	-25.2	7.4	-40.0	-180.0	-33.0	-170.5
38	10.92	9.25	(	-25.1	-26.6	-40.0	-180.0	-32.7	-154.2
39	11.21	9.50	(	-25.2	-61.7	-40.0	-180.0	-32.4	-118.0
40	11.51	9.75	(	-25.3	-97.8	-40.0	-180.0	-32.2	-81.0
41	11.80	10.00	(	-25.4	-134.8	-40.0	-180.0	-32.2	-43.1
42	12.10	10.25	(	-25.7	-172.6	-40.0	-180.0	-32.2	-4.4
43	12.39	10.50	(	-26.0	-148.7	-40.0	-180.0	-32.3	-35.1
44	12.69	10.75	(	-26.4	-109.2	-40.0	-180.0	-32.4	-93.6
45	12.98	11.00	(	-26.9	-68.9	-40.0	-180.0	-32.7	-116.3
46	13.28	11.25	(	-27.4	-27.8	-40.0	-180.0	-40.0	-171.9
47	13.57	11.50	(	-28.0	-13.9	-40.0	-180.0	-40.0	-158.1
48	13.87	11.75	(	-28.6	-56.4	-40.0	-180.0	-40.0	-159.4
49	14.16	12.00	(	-29.3	-90.5	-40.0	-180.0	-40.0	-116.2
50	14.46	12.25	(	-30.1	-143.2	-40.0	-180.0	-40.0	-48.0
51	14.75	12.50	(	-31.0	-172.4	-40.0	-180.0	-40.0	-31.7
77			(	-40.0	-180.0	-40.0	-180.0	-40.0	-68.1
78			(	-40.0	-180.0	-40.0	-180.0	-40.0	-75.0
79			(	-40.0	-180.0	-40.0	-180.0	-40.0	-118.6
80			(	-40.0	-180.0	-40.0	-180.0	-40.0	-102.5
81			(	-40.0	-180.0	-40.0	-180.0	-40.0	-135.0
82			(	-40.0	-180.0	-40.0	-180.0	-40.0	-136.1
83			(	-40.0	-180.0	-40.0	-180.0	-40.0	-169.9
84			(	-40.0	-180.0	-40.0	-180.0	-40.0	-170.5
85			(	-40.0	-180.0	-40.0	-180.0	-40.0	-155.8
86			(	-40.0	-180.0	-40.0	-180.0	-40.0	-154.2
87			(	-40.0	-180.0	-40.0	-180.0	-40.0	-106.3
88			(	-40.0	-180.0	-40.0	-180.0	-40.0	-118.0
89			(	-40.0	-180.0	-40.0	-180.0	-40.0	-82.3
90			(	-40.0	-180.0	-40.0	-180.0	-40.0	-81.0
91			(	-40.0	-180.0	-40.0	-180.0	-40.0	-46.7
92			(	-40.0	-180.0	-40.0	-180.0	-40.0	-43.1
93			(	-40.0	-180.0	-40.0	-180.0	-40.0	-17.0
94			(	-40.0	-180.0	-40.0	-180.0	-40.0	-4.4
95			(	-40.0	-180.0	-40.0	-180.0	-40.0	-40.3
96			(	-40.0	-180.0	-40.0	-180.0	-40.0	-35.1
97			(	-40.0	-180.0	-40.0	-180.0	-40.0	-93.6
98			(	-40.0	-180.0	-40.0	-180.0	-40.0	-75.3
99			(	-40.0	-180.0	-40.0	-180.0	-40.0	-121.7
100			(	-40.0	-180.0	-40.0	-180.0	-40.0	-116.3
101			(	-40.0	-180.0	-40.0	-180.0	-40.0	-171.9
102			(	-40.0	-180.0	-40.0	-180.0	-40.0	-158.1
103			(	-40.0	-180.0	-40.0	-180.0	-40.0	-159.4
104			(	-40.0	-180.0	-40.0	-180.0	-40.0	-116.2
105			(	-40.0	-180.0	-40.0	-180.0	-40.0	-48.0
106			(	-40.0	-180.0	-40.0	-180.0	-40.0	-31.7
107			(	-40.0	-180.0	-40.0	-180.0	-40.0	-17.4
108			(	-40.0	-180.0	-40.0	-180.0	-40.0	-68.1
109			(	-40.0	-180.0	-40.0	-180.0	-40.0	-75.0
110			(	-40.0	-180.0	-40.0	-180.0	-40.0	-118.6
111			(	-40.0	-180.0	-40.0	-180.0	-40.0	-102.5
112			(	-40.0	-180.0	-40.0	-180.0	-40.0	-135.0
113			(	-40.0	-180.0	-40.0	-180.0	-40.0	-136.1
114			(	-40.0	-180.0	-40.0	-180.0	-40.0	-169.9

115

( -32.0 127.4 -40.0 -10.0 -30.6 -63.1 )

Table 6-7. Fields Computed by Subroutine DIPOLES Along x-Axis at z=48 inches.

```

1 TEST PROGRAM FOR USING ELEMENTARY SOURCES FOR COMPUTING FRESNEL FIELDS
  (REF: WALTER(1965), PP.55-57)
  AIN= 4.00 BIN= 4.00 M,N= 15 15 LAMBDA= 1.180
  FIELD IS -10.0 FB AT Z= 24.00 INCHES
  APERTURE FIELDS: EAP= (0.000,0.000) (1.000,0.000) HAP= (0.000,0.0000)
  R0,HR0= .87422E+02 .23188E-02 IAX IS= 1 PFWLC= 0.00 1.00 46.00

```

N	XYZIN	XYZWL	AMPDR	PHSDEG	EX (HX)	AMPDR	PHSDEG	EX HY	AMPDR	PHSDEG	EX HZ
1	0.00	0.00	-42.0	-130.0	-15.9	-152.7	-40.0	-166.1			
2	.30	.25	-15.9	17.3	-40.0	-180.0	-40.0	15.6			
3	.59	.50	-15.9	17.0	-15.9	-163.0	-40.0	-166.5			
4	.89	.75	-15.9	16.2	-40.0	-180.0	-40.0	-171.9			
5	1.18	1.00	-15.9	14.8	-15.9	-163.8	-40.0	-167.5			
6	1.48	1.25	-15.9	13.5	-40.0	-180.0	-40.0	-172.7			
7	1.77	1.50	-15.9	12.9	-15.9	-165.2	-40.0	-170.0			
8	2.07	1.75	-15.9	12.9	-40.0	-180.0	-40.0	-174.1			
9	2.36	2.00	-15.9	12.9	-15.9	-169.5	-40.0	-171.7			
10	2.66	2.25	-15.9	12.9	-40.0	-180.0	-40.0	-176.0			
11	2.95	2.50	-15.9	12.9	-15.9	-169.5	-40.0	-172.8			
12	3.25	2.75	-15.9	12.9	-40.0	-180.0	-40.0	-178.5			
13	3.54	3.00	-15.9	12.9	-15.9	-170.8	-40.0	-174.9			
14			-15.9	12.9	-40.0	-180.0	-40.0	175.9			
15			-15.9	12.9	-15.9	-170.8	-40.0	170.8			
16			-15.9	12.9	-40.0	-180.0	-40.0	171.3			
17			-15.9	12.9	-15.9	-175.2	-40.0	166.1			
18			-15.9	12.9	-40.0	-180.0	-40.0	166.1			
19			-15.9	12.9	-15.9	-170.8	-40.0	166.1			
20			-15.9	12.9	-40.0	-180.0	-40.0	160.0			
21			-15.9	12.9	-15.9	-175.2	-40.0	159.8			
22			-15.9	12.9	-40.0	-180.0	-40.0	155.1			
23			-15.9	12.9	-15.9	-170.8	-40.0	155.1			
24			-15.9	12.9	-40.0	-180.0	-40.0	156.7			
25			-15.9	12.9	-15.9	-175.2	-40.0	156.7			

14	3.44	3.25	( -17.0	-21.1	-43.0	-17.0	-100.0	-39.5	140.8	34
			( -40.0	-180.0	-17.0	191.0	-4.0	148.0		40
			( -17.0	-20.7	-40.0	-140.0	-39.0	142.0		41
15	4.13	3.50	( -40.0	-130.0	-17.0	143.9	-40.0	139.6		42
			( -17.0	-30.1	-40.0	-150.0	-38.5	134.6		43
16	4.43	3.75	( -40.0	-140.0	-17.0	176.0	-40.0	130.9		44
			( -17.0	-43.4	-40.0	-180.0	-30.1	126.6		45
17	4.72	4.00	( -40.0	-180.0	-17.0	127.0	-40.0	120.4		46
			( -17.0	-52.3	-40.0	-180.0	-37.0	118.1		47
18	5.02	4.25	( -40.0	-180.0	-17.0	118.0	-40.0	112.4		48
			( -17.0	-61.3	-40.0	-180.0	-37.5	109.1		49
19	5.31	4.50	( -40.0	-190.0	-15.0	109.1	-40.0	105.2		50
			( -19.0	-70.2	-40.0	-180.0	-37.2	99.5		51
20	5.61	4.75	( -40.0	-190.0	-15.0	99.1	-4.0	47.2		52
			( -19.0	-80.4	-40.0	-180.0	-37.0	39.4		53
21	5.90	5.00	( -40.0	-180.0	-15.0	88.5	-40.0	80.5		54
			( -19.0	-91.3	-40.0	-180.0	-36.9	78.8		55
22	6.20	5.25	( -40.0	-140.0	-18.0	77.5	-40.0	70.7		56
			( -19.0	-102.3	-40.0	-180.0	-30.7	67.0		57
23	6.49	5.50	( -40.0	-180.0	-19.0	65.9	-40.0	63.3		58
			( -19.0	-113.9	-40.0	-180.0	-36.7	55.9		59
24	6.79	5.75	( -40.0	-180.0	-19.0	53.8	-40.0	51.6		60
			( -19.0	-120.0	-40.0	-180.0	-30.6	43.0		61
25	7.08	6.00	( -40.0	-140.0	-19.0	41.1	-40.0	37.7		62
			( -19.0	-138.7	-40.0	-180.0	-30.6	30.0		63
26	7.38	6.25	( -40.0	-180.0	-20.0	28.0	-40.0	22.5		64
			( -20.0	-151.8	-40.0	-180.0	-35.6	17.5		65
27	7.67	6.50	( -40.0	-180.0	-20.0	14.3	-40.0	9.4		66
			( -20.0	-155.4	-40.0	-180.0	-36.7	3.6		67
28	7.97	6.75	( -40.0	-180.0	-21.0	.1	-40.0	1.1		68
			( -21.0	-179.0	-40.0	-180.0	-36.8	-10.7		69
29	8.26	7.00	( -40.0	-180.0	-21.0	-14.0	-40.0	-20.0		70
			( -21.0	-165.7	-40.0	-180.0	-36.9	-25.7		71
30	8.56	7.25	( -40.0	-180.0	-21.0	-29.8	-40.0	-31.4		72
			( -22.0	-150.0	-40.0	-180.0	-37.0	-41.1		73
31	8.85	7.50	( -40.0	-180.0	-22.0	-45.5	-40.0	-42.8		74
			( -22.0	-134.0	-40.0	-180.0	-37.2	-57.0		75
32	9.15	7.75	( -40.0	-180.0	-22.0	-61.0	-40.0	-60.4		76

33	9.44	8.00	( -23.0	119.8	-43.0	-180.0	-37.5	-73.5	77
			-40.0	-180.0	-23.4	-78.3	-40.0	-79.6	78
34	9.74	8.25	( -23.6	102.2	-40.0	-180.0	-37.8	-90.5	79
			-40.0	-180.0	-24.0	-95.4	-40.0	-98.8	80
35	10.03	8.50	( -24.2	85.1	-40.0	-180.0	-38.1	-108.0	81
			-40.0	-180.0	-24.6	-113.0	-40.0	-118.0	82
36	10.33	8.75	( -24.8	67.5	-40.0	-180.0	-38.5	-126.0	83
			-40.0	-180.0	-25.3	-131.1	-40.0	-130.3	84
37	10.62	9.00	( -25.4	49.6	-40.0	-180.0	-38.9	-144.5	85
			-40.0	-180.0	-25.9	-140.5	-40.0	-157.3	86
38	10.92	9.25	( -26.1	31.1	-40.0	-180.0	-39.3	-163.5	87
			-40.0	-180.0	-25.7	-168.4	-40.0	-173.3	88
39	11.21	9.50	( -26.9	12.3	-40.0	-180.0	-39.8	-176.9	89
			-40.0	-180.0	-27.5	-172.3	-40.0	-181.1	90
40	11.51	9.75	( -27.7	-6.9	-40.0	-180.0	-40.0	-186.0	91
			-40.0	-180.0	-28.3	-180.0	-40.0	-195.7	92
41	11.80	10.00	( -28.5	-25.5	-40.0	-180.0	-40.0	-204.4	93
			-40.0	-180.0	-29.2	-180.0	-40.0	-213.4	94
42	12.10	10.25	( -29.4	-46.4	-40.0	-180.0	-40.0	-223.5	95
			-40.0	-180.0	-30.2	-180.0	-40.0	-234.5	96
43	12.39	10.50	( -30.4	-65.5	-40.0	-180.0	-40.0	-246.0	97
			-40.0	-180.0	-31.3	-180.0	-40.0	-258.0	98
44	12.69	10.75	( -31.5	-85.7	-40.0	-180.0	-40.0	-271.1	99
			-40.0	-180.0	-32.4	-180.0	-40.0	-284.8	100
45	12.98	11.00	( -32.6	-107.0	-40.0	-180.0	-40.0	-299.8	101
			-40.0	-180.0	-33.7	-180.0	-40.0	-316.3	102
46	13.28	11.25	( -33.9	-127.2	-40.0	-180.0	-40.0	-333.3	103
			-40.0	-180.0	-35.2	-180.0	-40.0	-351.5	104
47	13.57	11.50	( -35.6	-145.9	-40.0	-180.0	-40.0	-370.6	105
			-40.0	-180.0	-36.6	-180.0	-40.0	-390.6	106
48	13.87	11.75	( -36.9	-165.7	-40.0	-180.0	-40.0	-411.1	107
			-40.0	-180.0	-38.6	-180.0	-40.0	-432.2	108
49	14.16	12.00	( -38.6	-177.1	-40.0	-180.0	-40.0	-454.2	109
			-40.0	-180.0	-40.0	-180.0	-40.0	-477.5	110
50	14.46	12.25	( -40.0	-180.0	-40.0	-180.0	-40.0	-502.0	111
			-40.0	-180.0	-40.0	-180.0	-40.0	-527.5	112
51	14.75	12.50	( -40.0	-180.0	-40.0	-180.0	-40.0	-554.0	113
			-40.0	-180.0	-40.0	-180.0	-40.0	-582.0	114

52	15.05	10.75	( -4.0 )	140.0	-40.0	-1.00	-40.0	-72.0	115
53	15.34	13.00	( -4.0 )	133.5	-40.0	-3.45	-40.0	-77.0	116
54	15.64	15.25	( -4.0 )	124.4	-40.0	-4.40	-40.0	-82.0	117
55	15.93	17.50	( -4.0 )	114.1	-40.0	-5.35	-40.0	-87.0	118
56	16.23	19.75	( -4.0 )	103.8	-40.0	-6.30	-40.0	-92.0	119
57	16.52	22.00	( -4.0 )	93.5	-40.0	-7.25	-40.0	-97.0	120
58	16.82	24.25	( -4.0 )	83.2	-40.0	-8.20	-40.0	-102.0	121
59	17.11	26.50	( -4.0 )	72.9	-40.0	-9.15	-40.0	-107.0	122
60	17.41	28.75	( -4.0 )	62.6	-40.0	-10.10	-40.0	-112.0	123
61	17.70	31.00	( -4.0 )	52.3	-40.0	-11.05	-40.0	-117.0	124
62	18.00	33.25	( -4.0 )	42.0	-40.0	-12.00	-40.0	-122.0	125
63	18.29	35.50	( -4.0 )	31.7	-40.0	-12.95	-40.0	-127.0	126
64	18.59	37.75	( -4.0 )	21.4	-40.0	-13.90	-40.0	-132.0	127
65	18.88	40.00	( -4.0 )	11.1	-40.0	-14.85	-40.0	-137.0	128
66	19.18	42.25	( -4.0 )	0.8	-40.0	-15.80	-40.0	-142.0	129
67	19.47	44.50	( -4.0 )	0.5	-40.0	-16.75	-40.0	-147.0	130
68	19.77	46.75	( -4.0 )	0.2	-40.0	-17.70	-40.0	-152.0	131
69	20.06	49.00	( -4.0 )	0.0	-40.0	-18.65	-40.0	-157.0	132
70	20.36	51.25	( -4.0 )	0.0	-40.0	-19.60	-40.0	-162.0	133
71	20.65	53.50	( -4.0 )	0.0	-40.0	-20.55	-40.0	-167.0	134
72	20.95	55.75	( -4.0 )	0.0	-40.0	-21.50	-40.0	-172.0	135
73	21.24	58.00	( -4.0 )	0.0	-40.0	-22.45	-40.0	-177.0	136
74	21.54	60.25	( -4.0 )	0.0	-40.0	-23.40	-40.0	-182.0	137
75	21.83	62.50	( -4.0 )	0.0	-40.0	-24.35	-40.0	-187.0	138
76	22.13	64.75	( -4.0 )	0.0	-40.0	-25.30	-40.0	-192.0	139
77	22.42	67.00	( -4.0 )	0.0	-40.0	-26.25	-40.0	-197.0	140
78	22.72	69.25	( -4.0 )	0.0	-40.0	-27.20	-40.0	-202.0	141
79	23.01	71.50	( -4.0 )	0.0	-40.0	-28.15	-40.0	-207.0	142
80	23.31	73.75	( -4.0 )	0.0	-40.0	-29.10	-40.0	-212.0	143
81	23.60	76.00	( -4.0 )	0.0	-40.0	-30.05	-40.0	-217.0	144
82	23.90	78.25	( -4.0 )	0.0	-40.0	-31.00	-40.0	-222.0	145
83	24.19	80.50	( -4.0 )	0.0	-40.0	-31.95	-40.0	-227.0	146
84	24.49	82.75	( -4.0 )	0.0	-40.0	-32.90	-40.0	-232.0	147
85	24.78	85.00	( -4.0 )	0.0	-40.0	-33.85	-40.0	-237.0	148
86	25.08	87.25	( -4.0 )	0.0	-40.0	-34.80	-40.0	-242.0	149

## Chapter 7

### SUBROUTINE WALL

7-1. Purpose: To compute the normal transmission ( $T_{\perp}, T_{\parallel}$ ) and reflection coefficients of a N-layer dielectric sheet having thicknesses  $d_n$ , dielectric constants  $\epsilon_{rn}$ , and loss tangents  $\tan\delta_n$  for each layer when a plane wave is incident at angle  $\theta_i$ .

7-2. Usage: CALL WALL (BETA, SINE, D, ER, TD, N, NN, TN1, TN2, RPER, RPAR)

#### 7-3. Arguments

- |            |   |
|------------|---|
| BETA       | - Real input variable = $2\pi/\lambda$ , where $\lambda$ is the free space wavelength.  |
| SINE       | - Real input variable = $\sin \theta_i$ .   |
| D,         | - Real input arrays containing the thickness (cm),  |
| ER,        | - dielectric constant $\epsilon_r$ , and loss tangent $\tan\delta$ of   |
| TD         | each layer.   |
| N          | - Integer input variable equal to the number of layers.   |
| NN         | - Integer input = N+1.  |
| TN1, TN2   | - Complex output variables equal to the normal voltage transmission coefficients for the components of the incident electric field perpendicular to and parallel to the plane of incidence, respectively. |
| RPER, RPAR | - Complex output variables equal to the reflection coefficients $R_{\perp}$ , $R_{\parallel}$ .   |



7-4. Comment and Method

a. Layer 1 is the first layer on the exit side of the panel; layer N is the first layer on the incident side.  $T_{\perp}$ ,  $T_{\parallel}$  have the same value for either side of the panel being the incident side; however,  $R_{\perp}$ ,  $R_{\parallel}$  are different (in phase) for the two cases.

b. The details of the method are presented in Appendix E of Reference 1.

7-5. Program Flow: See Reference 1.

7-6. Test Case: None.

7-7. References

1. G. K. Huddleston, "Radome Analysis Computer Program: Ray Tracing Formulation", Technical Report for JHU/APL, Contract No. 601053, November 1979.

7-8. Program Listing: See following pages.

```

SUBROUTINE WALL(BETA,SINE,D,ER,TD,N,NN,TN1,TN2,RPER,RPAR) 1
C SUBROUTINE WALL COMPUTES THE TRANSMISSION AND REFLECTION 2
C COEFFICIENTS FOR AN N LAYER, PLANE DIELECTRIC PANEL FOR PLANE 3
C WAVE INCIDENT AT SINE(ANGLE) FOR PERPENDICULAR AND 4
C PARALLEL POLARIZATIONS. 5
C PARAMETERS OF THE WALL: N= THE NUMBER OF LAYERS 6
C NN= N+1 REQUIRED TO DIMENSION ARRAYS 7
C D= THICKNESS OF EACH LAYER IN CENTIMETERS 8
C ER= RELATIVE DIELECTRIC CONSTANT OF EACH LAY 9
C TD= THE LOSS TANGENT FOR EACH LAYER 10
C TN1,TN2 ARE THE NORMAL VOLTAGE XMN COEFFICIENTS; TPER,TPAR ARE THE 11
C INSERTION VOLTAGE TRANSMISSION COEFFICIENTS. IT IS IMPORTANT TO 12
C NOTE THAT THE XMN COEFS ARE THE SAME FOR PLANE WAVE INCIDENT FROM 13
C EITHER SIDE OF THE STRATIFIED DIELECTRIC PANEL IMMERSSED IN FREE SPACE; 14
C HOWEVER, THE REFLECTION COEFS ARE NOT. THAT IS, FOR COMPUTING RPER, 15
C RPAR, THE ORDERING OF ER(NN),TD(NN) IS IMPORTANT WITH LAYER 1 BEING 16
C THE FIRST LAYER ON THE EXIT SIDE, LAYER N BEING THE FIRST LAYER ON THE 17
C INCIDENT SIDE. LAYER NN AND LAYER 0 ARE JUST FREE SPACE LAYERS 18
C OF SEMI-INFINITE DEPTH. 19
C E,G,R1,R2, ARE ARRAYS USED IN THE SUBROUTINE HAVING NN DIM"L LIMITS 20
  COMPLEX E(6),G(6),R1(6),R2(6),GG,EE,RR1,RR2,AA1,AA2,X1,X2, 21
  $X3,X4,Y1,Y2,Y3,Y4,U1,U2,U3,U4,V1,V2,V3,V4,P1,P2,P3,P4,Q1,Q2,Q3,Q4 22
  COMPLEX TPER,TPAR,RPER,RPAR,U,V,TN1,TN2 23
  DIMENSION ER(NN),TD(NN),D(N) 24
  ER(NN)=1.0 25
  TD(NN)=0. 26
  DO 50 I=1,NN 27
50 E(I)=CMLPX(ER(I),-ER(I)*TD(I)) 28
  AB=BETA*0.70707070707071 29
C 30
C CALCULATE TOTAL THICKNESS OF WALL IN CM 31
C 32
  DTOTAL=0.0 33
  DO 200 I=1,N 34
200 DTOTAL=DTOTAL+D(I) 35
C S IS THE SINE OF THE ANGLE SQUARED 36
C C IS THE COSINE OF THE ANGLE 37
  S=SINE*SINE 38

```

C=SQRT(1.0-S)	39
AD=ER(1)-S	40
ET=ER(1)*TD(1)	41
SR=SQRT(AD*AD+ET*ET)	42
IF(SR-AD) 76,76,77	43
76 A=0.	44
GO TO 78	45
77 A=AB*SQRT(SR-AD)	46
78 B=AB*SQRT(SR+AD)	47
G(1)=CPLX(A,B)	48
GG=CPLX(0.0,BETA*C)	49
EE=1.0	50
SUM=0.	51
SUM=SUM+D(1)/SQRT(AD)	52
RR1=(G(1)-GG)/(G(1)+GG)	53
RR2=(EE*G(1)-E(1)*GG)/(EE*G(1)+E(1)*GG)	54
DO 84 I=1,N	55
II=I+1	56
AD=ER(II)-S	57
ET=ER(II)*TD(II)	58
IF (I-N) 176,177,177	59
176 SUM=SUM+D(II)/SQRT(AD)	60
177 CONTINUE	61
SR=SQRT(AD*AD+ET*ET)	62
IF(SR-AD) 79,79,80	63
79 A=0.	64
GO TO 81	65
80 A=AB*SQRT(SR-AD)	66
81 B=AB*SQRT(SR+AD)	67
G(II)=CPLX(A,B)	68
R1(I)=(G(II)-G(I))/(G(II)+G(I))	69
84 R2(I)=(E(I)*G(II)-E(II)*G(I))/(E(I)*G(II)+E(II)*G(I))	70
SUM=S*SUM	71
AA1=1.0-RR1	72
AA2=1.0-RR2	73
DO 85 I=1,N	74
AA1=AA1*(1.0-R1(I))	75
85 AA2=AA2*(1.0-R2(I))	76

	AA1=1.0/ AA1	77
	AA2=1.0/ AA2	78
	U=-G(1)*D(1)	79
	V=G(1)*D(1)	80
	X1=CEXP(U)	81
	X4=CEXP(V)	82
	X2=-RR1*X4	83
	X3=-RR1*X1	84
	Y1=X1	85
	Y4=X4	86
	Y2=-RR2*Y4	87
	Y3=-RR2*Y1	88
	DO 105 I=2, NN	89
	IF (I-NN) 95, 90, 1	90
90	U1=1.0	91
	U2=-R1(N)	92
	U3=-R1(N)	93
	U4=1.0	94
	V1=1.0	95
	V2=-R2(N)	96
	V3=-R2(N)	97
	V4=1.0	98
	GO TO 100	99
95	II=I-1	100
	U=-G(I)*D(I)	101
	V=G(I)*D(I)	102
	U1=CEXP(U)	103
	U4=CEXP(V)	104
	U2=-R1(II)*U4	105
	U3=-R1(II)*U1	106
	V1=U1	107
	V4=U4	108
	V2=-R2(II)*V4	109
	V3=-R2(II)*V1	110
100	P1=X1*U1+X2*U3	111
	P2=X1*U2+X2*U4	112
	P3=X3*U1+X4*U3	113
	P4=X3*U2+X4*U4	114

	Q1=Y1*V1+Y2*V3	115
	Q2=Y1*V2+Y2*V4	116
	Q3=Y3*V1+Y4*V3	117
	Q4=Y3*V2+Y4*V4	118
	X1=P1	119
	X2=P2	120
	X3=P3	121
	X4=P4	122
	Y1=Q1	123
	Y2=Q2	124
	Y3=Q3	125
105	Y4=Q4	126
	RPER=-X3/X4	127
C	TN1,TN2 ARE NORMAL VOLTAGE XMN COEFFICIENTS.	128
	RPAR=-Y3/Y4	129
	TN1=(X1+X2*RPER)*AA1	130
	U=CMPLX(0.0,-SUM*BETA)	131
	U=CEXP(U)	132
C	TPER,TPAR HERE ARE VOLTAGE XMN COEFFICIENTS AT EXIT POINT OF RAY.	133
	TPER=TN1*U	134
	TN2=(Y1+Y2*RPAR)*AA2	135
	TPAR=TN2*U	136
C	MODIFY TRANSMISSION COEFFICIENTS FOR INSERTION	137
	U=CMPLX(0.0,BETA*DTOTAL*C)	138
	U=CEXP(U)	139
	TPER=TN1*U	140
	TPAR=TN2*U	141
1	CONTINUE	142
300	RETURN	143
	END	144

## Chapter 8

### SUBROUTINE CAXCB

8-1. Purpose: To compute the complex vector cross product  $\underline{C} = \underline{A} \times \underline{B}$ , where  $\underline{A}$  and  $\underline{B}$  are a complex vectors expressed in rectangular coordinates.

8-2. Usage: CALL CAXCB (A, B, C)

8-3. Arguments

- A - Complex input array containing the rectangular components of the vector  $\underline{A} = \hat{x} A_x + \hat{y} A_y + \hat{z} A_z$ ; i.e., A ( $A_x, A_y, A_z$ ).
- B - Complex input array B ( $B_x, B_y, B_z$ ) representing the vector  $\underline{B}$ .
- C - Complex output array C ( $C_x, C_y, C_z$ ) representing the vector  $\underline{C} = \underline{A} \times \underline{B}$ .

8-4. Comment and Method: None

8-5. Program Flow: See listing below.

8-6. Test Case: None.

8-7. References: None.

8-8. Program Listing: See following page.

```

SUBROUTINE CAXCB(A,B,C)
COMPLEX A(3),B(3),C(3)
C SUBR CAXCB COMPUTES THE VECTOR CROSS PRODUCT C=AXB OF
C TWO COMPLEX VECTORS A AND B
C(1)=A(2)*B(3)-A(3)*B(2)
C(2)=A(3)*B(1)-A(1)*B(3)
C(3)=A(1)*B(2)-A(2)*B(1)
RETURN
END
```

1  
2  
3  
4  
5  
6  
7  
8  
9

**DATE**  
**ILME**